

Maria Louise Bekkelund

Techno-economic assessment of direct air capture powered by nuclear energy

Master's thesis in Energy and Environmental Engineering

Supervisor: Jacob Joseph Lamb

Co-supervisor: Schalk Cloete

January 2024

Maria Louise Bekkelund

Techno-economic assessment of direct air capture powered by nuclear energy

Master's thesis in Energy and Environmental Engineering
Supervisor: Jacob Joseph Lamb
Co-supervisor: Schalk Cloete
January 2024

Norwegian University of Science and Technology
Faculty of Engineering
Department of Energy and Process Engineering



Abstract

As the urgency to achieve net zero emissions (NZE) by 2050 intensifies, several initiatives are looking into technologies that remove accumulated CO₂ from the atmosphere. Direct air capture (DAC) has received increased attention as an option to mitigate climate change. DAC requires a large amount of heat, and an exciting pathway is to utilize the large amount of waste heat produced from nuclear energy for DAC. In addition, synthetic fuels have been recognized as a pivotal element in transitioning toward carbon neutrality in the global transportation sector by 2050. Green methanol, a class of synthetic fuels, can be produced by low-carbon electricity, green hydrogen (H₂), and recycled CO₂, lowering the CO₂ footprint of methanol compared to conventional methanol produced from fossil fuels.

This thesis compares two plants intended to be constructed in the mid-century that use nuclear power for DAC purposes: the reference plant, which utilizes a third-generation nuclear reactor for CO₂ capture, and the advanced plant, which employs a fourth-generation nuclear reactor, using excess electricity after DAC for H₂ production by a proton exchange membrane electrolyzer combined with DAC CO₂ for green methanol production. The DAC process is based on Climeworks technology for solid sorbent DAC utilizing heat at 100 °C. First, a comprehensive technical simulation of both plants was conducted in UniSim Design R492 before an in-depth economic assessment assuming a 40-year lifetime, including an uncertainty quantification, was conducted with the standardized economic assessment tool.

The technological analysis found that the CO₂ capture capacity for the reference plant was 14 MtCO₂/y and 14.4 MtCO₂/y for the advanced plant. The advanced plant used 9.5% of the captured CO₂ for methanol production. The plant produced 2 735 tMeOH/d, and the efficiency of the methanol synthesis was 54.3%. This work found that the reference plant is marginally more economically favorable to build than the advanced plant. The levelized cost of CO₂ (LCOC) for the reference plant was 98.3 \$/ton and 104.9 \$/ton for the advanced plant. This increase was due to capital expenditures linked to a larger nuclear plant, a fourth-generation nuclear reactor, and additional methanol synthesis costs, not fully recuperated by the assumed methanol sales price of 400 \$/ton. These plants could become economically profitable if a CO₂ tax of 100 \$/ton or more is largely enforced globally, as assumed in the announced pledges and NZE scenario.

The uncertainty quantification showed that in 58.8% of the 1000 instances examined, the reference plant would be cheaper to produce than the advanced plant. The median and 90% confidence interval for the reference and advanced plants were 100.5 (76.1-141.3) \$/ton and 109 (72.9-161.9) \$/ton, respectively. DAC unit cost and expenditures related to the nuclear reactors were found to be the two main uncertainty factors of the respective plants.

The numbers for the LCOC ranging from slightly under to slightly above 100 \$/ton for the reference and advanced plant are attractively low for DAC technology. Reaching these costs would need extensive innovation across the DAC value chain. A rapid scale-up and commercializing of DAC and fourth-generation nuclear reactors are needed to determine and drive costs down. Lastly, more research is needed to investigate the blend of methanol into petrol and diesel, facilitating a smoother transition towards adopting pure methanol as a fuel in the future.

Sammendrag

Med økende søkelys på å nå netto null-utslipp (NZE) innen 2050 retter flere oppmerksomheten mot teknologier som reduserer mengden akkumulert CO₂ i atmosfæren, slik som direct air capture (DAC). DAC er en energikrevende prosess, som krever store mengder varme. Et innovativt alternativ er å utnytte den store mengden spillvarme fra kjernekraftverk til å drive DAC prosessen. For å nå de ambisiøse klimamålene er også syntetiske drivstoff anerkjent som en viktig bidragsyter i overgangen mot karbonnøytralitet i den globale transportsektoren innen 2050. Metanol er en type syntetisk drivstoff som kan produseres med elektrisitet fra energikilder med lave CO₂ utslipp, grønt hydrogen (H₂) og resirkulert CO₂, som reduserer CO₂-fotavtrykket til metanol sammenliknet med konvensjonell metanolproduksjon basert på fossile brensler.

Denne masteroppgaven sammenligner to anlegg som er planlagt å bygges på midten av århundret og bruker kjernekraft til DAC: referanseanlegget, som bruker en tredje generasjons kjernekraftreaktor for CO₂-fangst, og det avanserte anlegget, som bruker en fjerde generasjons kjernekraftreaktor og overskuddselektrisitet etter DAC for H₂-produksjon ved hjelp av en proton utveksling membran elektrolysecelle kombinert med CO₂ fra DAC for produksjon av grønn metanol. DAC-prosessen er basert på Climeworks-teknologi for faststoffabsorberende DAC og bruker varme ved 100 °C. Først ble det gjennomført en teknisk simulering av begge anleggene i UniSim Design R492 før en grundig økonomisk vurdering med en forventet levetid på 40 år for anleggene, og en usikkerhetskvantifisering ble utført med et standardisert økonomisk analyseverktøy.

Den teknologiske analysen viste at CO₂-fangsten for referanseanlegget var 14 MtCO₂/år, og 14.4 MtCO₂/år for det avanserte anlegget. Det avanserte anlegget brukte 9.5% av fanget CO₂ til metanolproduksjon. Anlegget produserte 2 735 tMeOH/dag og metanolproduksjonen oppnådde en virkningsgrad på 54.3%. Denne studien fant at referanseanlegget er marginalt mer økonomisk gunstig å bygge enn det avanserte anlegget. Leveliced cost of CO₂ (LCOC) for referanseanlegget var 98.3 \$/tonn og 104.9 \$/tonn for det avanserte anlegget. Denne økningen skyldes større kapitalutgifter knyttet til et større kjernekraftanlegg, en fjerde generasjons kjernekraftreaktor og ekstra kostnader knyttet til metanol syntese, som ikke ble fullstendig dekket av den antatte salgsprisen for metanol på 400 \$/tonn. Disse anleggene kan bli økonomisk lønnsomme hvis en CO₂-avgift på 100 \$/tonn eller mer blir implementert globalt, som antatt i NZE scenarioet.

I 58.8% av de 1000 tilfellene som ble undersøkt i usikkerhetskvantifiseringen, ville referanseanlegget være billigere å produsere enn det avanserte anlegget. Medianen og 90% konfidensintervallet for referanse og det avanserte anlegget var henholdsvis 100.5 (76.1-141.3) \$/tonn og 109 (72.9-161.9) \$/tonn. DAC-enhetens kostnad og utgifter knyttet til kjernekraftreaktorene ble identifisert som de to viktigste usikkerhetsfaktorene for de respektive anleggene.

Tallene for LCOC, som varierer fra litt under til litt over 100 \$/tonn for henholdsvis referanseanlegget og det avanserte anlegget, er tiltalende lave for DAC-teknologien. Å oppnå de relativt lave kostnadene vil kreve omfattende innovasjon gjennom hele verdikjeden for DAC. En rask oppskalering og kommersialisering av DAC og fjerde generasjons kjernekraftreaktorer er nødvendig for å fastslå og redusere kostnadene. Til slutt er ytterligere forskning nødvendig for å undersøke blandingen av metanol i bensin og diesel, og dermed legge til rette for en god overgang til å bruke ren metanol i fremtiden.

Preface


This thesis represents the work performed to complete the master's degree in Energy and Environment at the Norwegian University of Science and Technology (NTNU). This project was carried out during the autumn of 2023 as well as January 2024. The work was conducted under the guidance of Jacob J. Lamb, belonging to the Department of Energy and Process Engineering at NTNU. The co-supervisor at SINTEF Industry was Schalk Cloete. I would also like to thank Carlos Arnaiz del Pozo for guidance in UniSim and for providing his models from previous work. I am grateful for the opportunity to work with Lamb, Cloete, and Arnaiz del Pozo on this exciting and contemporary project.

The project delves into the technical and economic aspects of utilizing the electricity and heat from nuclear power plants for direct air capture. Furthermore, an advanced nuclear reactor has been used to increase electricity production for electrolytic hydrogen production, subsequently used in green methanol synthesis.

I wish to express sincere gratitude to my supervisors for the remarkable effort and unwavering support extended throughout the course of this thesis. Schalk's comprehensive knowledge of chemical processes and techno-economic projects has been invaluable for this work. Jacob Lamb has been very helpful with the set-up and finalization of the thesis and has encouraged when problems have occurred. Ultimately, my appreciation goes to family and friends who have shown unwavering support in completing this academic journey.

Norwegian University of Science and Technology
Trondheim, January 2024

Maria Louise Bekkelund

A handwritten signature in black ink that reads "Maria L. Bekkelund". The signature is written in a cursive, slightly slanted style.

List of Figures

1.1	Atmospheric CO ₂ concentration and annual CO ₂ emission [2]. The figure has been modified.	1
2.1	P-T diagram showing different phases for a fluid [16]. The figure has been modified.	5
2.2	T-S diagram and component flowsheet of an ideal Rankine cycle [21]. The figure has been modified.	6
2.3	T-S diagram and component flowsheet of an ideal Rankine reheat cycle [21]. The figure has been modified.	7
2.4	The capital cost breakdown in categories [24]. The figure has been modified.	8
2.5	Historical and future energy production from nuclear power plants to reach NZE by 2050 [7]. The figure has been modified.	9
2.6	Simplified illustration of a nuclear power plant [32]. The figure has been modified.	10
2.7	TOC and construction times for some recent nuclear projects [7]. The figure has been modified.	14
2.8	Simplified figure of S-DAC [11]. The figure has been modified.	16
2.9	Simplified figure of L-DAC [11]. The figure has been modified.	17
2.10	Pathways for CO ₂ utilization [64].	20
2.11	Production of grey, blue and green hydrogen [68].	23
2.12	Simplified illustration of PEM electrolyzer [70].	24
2.13	Levelized cost of hydrogen for different energy sources [7].	26
2.14	Future utilization of hydrogen in different industries for APS an NZE by 2050 [3]. The figure has been modified.	27
2.15	Energy density for different energy sources [78]. The figure has been modified.	28
2.16	Feedstocks of methanol synthesis [9].	29
2.17	Traditional MeOH plant [76].	30
2.18	Different pathways for methanol production [9].	31
3.1	Graphical overview for the methodology of the technical and economical assessment.	34
3.2	Simplified illustration of the reference plant with a nuclear plant, DAC, and CO ₂ compression.	35
3.3	Simplified illustration of the advanced plant, with DAC, CO ₂ compression, electrolysis, syngas production and green methanol production.	35
3.4	Simplified flowsheet of the reference nuclear-powered DAC plant.	37
3.5	Simplified flowsheet of the advanced nuclear-powered DAC plant.	38
3.6	Simplified flowsheet of the cooling water cycle.	40
3.7	Simplified flowsheet of CO ₂ compression with cooling.	41
3.8	Flowsheet of the modified PEM model.	42
3.9	Simplified flowsheet of synthetic gas production for methanol synthesis.	44
3.10	Simplified flowsheet of the methanol synthesis.	47
4.1	Total overnight cost expressed as k\$/tonCO ₂ for the reference and advanced plant.	57

4.2	Fixed and variable operational and maintenance (FOM & VOM) cost as cost contributor for each ton CO ₂ produced for the reference and advanced plant.	59
4.3	LCOC for the reference and advanced plant.	60
4.4	The change in LCOC across half of the parameters uncertainty range.	62
4.5	LCOC for all 1000 points in the uncertainty quantification for the reference and advanced plant.	65
4.6	A representation of the 1000 cases in the UQ. For a negative x-value, the LCOC for the advanced plant will be lower than the reference plant. For a positive x-value, the LCOC for the reference plant will be lower than for the advanced plant.	66
4.7	The correlation between MeOH sale price and advanced nuclear reactor factor to make the advanced plant break even with the reference plant. Factor 1 corresponds to 1000 \$/kW _h	67
4.8	Future projections for DAC scale-up capacities to reach NZE by 2050, and projected CO ₂ prices for the APS and NZE scenario [6, 62].	70
B.1	Levelized cost for DAC with and without carbon tax for different regions for years 2030 and 2050 [6].	II
C.1	Total overnight cost for nuclear generating technologies [44].	III
E.1	Advanced nuclear plant with CWT.	VI
E.2	Advanced nuclear plant with DAC.	VI
E.3	Reference nuclear plant with CWT.	VII
E.4	Reference nuclear plant with DAC.	VII
E.5	A flowsheet comprising all the simulated sub-processes represented as a sub-flowsheet, including the nuclear power plant, CO ₂ compression, PEM electrolyzer, syngas production, and methanol synthesis.	VIII
E.6	Flowsheet of the syngas production.	IX
E.7	Flowsheet of CO ₂ compression.	X
E.8	Flowsheet of the PEM electrolyzer model.	X
E.9	Flowsheet of the methanol synthesis.	XI
E.10	A plot of the methanol mole fraction as a function of reactor length.	XII

List of Tables

2.1	Generation III and generation IV nuclear reactors [37, 40]	12
2.2	Total overnight cost for nuclear energy [44]	14
2.3	Predicted energy consumption for the S-DAC in future scenarios [5]	18
2.4	TRL for DAC [60]	18
2.5	Specific capital cost for the S-DAC unit [5]	19
2.6	13 of the 27 DAC plants operation worldwide [6]	21
2.7	Key performance indicators of electrolysis technologies [69, 70]	23
3.1	Basic process modelling assumptions	36
3.2	Process modelling assumptions for the reference nuclear-powered DAC plant	37
3.3	Process modelling assumptions for the advanced nuclear-powered DAC plant	38
3.4	DAC key calculation assumptions	39
3.5	Cooling water cycle modelling assumptions for the reference plant	39
3.6	Cooling water cycle modeling assumptions for the advanced plant	40
3.7	Compression of CO ₂ modeling assumptions	41
3.8	Parameters for the PEM cell found in literature for Nafion membranes [12]	42
3.9	PEM model modeling assumptions	43
3.10	Syngas production modeling assumptions	44
3.11	Reactor modeling assumptions	45
3.12	Methanol synthesis modeling assumptions	46
3.13	Target basis for the economic assessment	48
3.14	Cash flow analysis assumptions	49
3.15	Scaling parameter, reference capacity and -cost, and scaling exponent for different components calculating the BEC following the scaling approach	50
3.16	Component, cost and cost reduction assumptions for the PEM electrolyzer [12]	52
3.17	Values chosen for the uncertainty quantification	53
4.1	Energy breakdown and plant performance for reference plant and advanced plant	55
4.2	Heat demand and production of waste heat to distillation column	56
A.1	The parameters and calculations of the sorbent [94]	I
D.1	Justification for the uncertainty quantification	IV
D.2	Justification for the uncertainty quantification	V

Nomenclature

Acronyms

ACF	Annual Cash Flow
APS	Announced Pledges Scenario
BEC	Bare Erected Cost
BWR	Boiling Water Reactor
CaCO₃	Limestone
Ca(OH)₂	Calcium Hydroxide
CAPEX	Capital Expenditures
CCS	Carbon Capture and Storage
CDR	Carbon Dioxide Removal
CEPCI	Chemical Engineering Plant Cost Index
CF	Capacity Factor
CH₃OH	Methanol
CO₂eq.	CO ₂ Equivalent
COP28	Conference of the Parties 28th meeting
CRI	Carbon Recycling International
CS	Carbon Steel
CSTR	Continuous Stirred Tank Reactor
DAC	Direct Air Capture
e⁻	Electrons
FOM	Fixed Operating and Maintaining
GFR	Gas-cooled Fast Reactor
H⁺	Proton
H₂	Hydrogen
HE	Heat Exchanger
H-PT	High Pressure Turbine
IEA	International Energy Agency
I-PT	Intermediate Pressure Turbine
IRENA	International Renewable Energy Agency
K₂CO₃	Potassium Carbonate
KOH	Potassium Hydroxide
LCOC	Levelized Cost Of CO ₂
LCOE	Levelized Cost Of Electricity
LCOM	Levelized Cost Of Methanol
LCOP	Levelized Cost Of Product
L-DAC	Liquid DAC
LFR	Lead-cooled Fast Reactor
LHV	Lower Heating Value

L-PT	Low Pressure Turbine
MeOH	Methanol
MI	Methanol Institute
MSR	Molten Salt Reactor
N₂	Nitrogen
NET	Negative Emission Technologies
NPV	Net Present Value
NZE	Net Zero Emission
O₂	Oxygen
O&M	Operating and Maintaining
OPEX	Operational Expenditures
PPM	Parts Per Million
PtL	Power to Liquid
PWR	Pressurized water reactor
SCWR	Supercritical-Cooled-Water-Reactor
S-DAC	Solid DAC
SEA	Standardized Economic Assessment
SFR	Sodium-cooled Fast Reactor
SOE	Solid Oxide Electrolyzer
SS	Stainless Steel
STEPS	Stated Policies Scenario
Syngas	Synthetic Gas
TOC	Total Overnight Cost
TPC	Total Plant Cost
TRL	Technology Readiness Level
UQ	Uncertainty Quantification
VHTR	Very-High Temperature Reactor
VOM	Variable Operating and Maintaining
WH	Waste Heat
WGS	Water Gas Shift

Symbols

C	Cost for scaling approach
C_0	Reference cost
E	Activation energy
e	Train exponent
F	Faraday's constant
f	Unit exponent
F_L	Factor for material and labor
H	Enthalpy
I	Interest rate
j	Current
j_0	Exchange current density
kWh_e	Kilowatt hour of electricity
kWh_h	Kilowatt hour of heat
n	Number
P	Power
P_e	Net rated power
Q_r	Reactor heat
Q_w	Waste heat
R	Gas constant
R_{ion}	Ionic resistance
R^2	Coefficient of determination
S	Entropy
S_1	Reference scale capacity
S_0	Reference capacity
T	Temperature
U	Internal energy
V_{act}	Activation voltage
V_{cell}	Cell voltage
V_{oc}	Open-circuit voltage
V_{ohm}	Ohmic voltage
V_{rev}	Reversible voltage
W	Work
α	Charge transfer coefficient
Δ	Delta
η	Efficiency

Contents

List of Figures	iv
List of Tables	vi
List of Abbreviations	vii
1 Introduction	1
1.1 Motivation	1
1.2 Researchers Objective	2
1.3 Outline of the Thesis	3
2 Theory	4
2.1 IEA’s Climate Scenarios for Different Future Pathways	4
2.2 Thermodynamics	4
2.2.1 First and Second Law of Thermodynamics	4
2.2.2 Supercritical Conditions	5
2.2.3 Ideal Rankine Cycle	5
2.2.4 Ideal Rankine Reheat Cycle	6
2.3 Economics	7
2.3.1 Capital Expenditure	7
2.3.2 Operational Expenditure	8
2.3.3 Net Present Value	8
2.4 Nuclear Energy	9
2.4.1 Nuclear Power Plants	9
2.4.2 Nuclear Fuel Cycle	10
2.4.3 Nuclear Reactors	11
2.4.4 Cooling Water Tower	12
2.4.5 Capacity Factor	13
2.4.6 Efficiency	13
2.4.7 Cost	13
2.4.8 Emission	14
2.4.9 Social Aspect	15
2.4.10 Nuclear Power Future and Outlook	15
2.5 Direct Air Capture	15
2.5.1 Solid DAC	16
2.5.2 Liquid DAC	16
2.5.3 Energy Usage	17
2.5.4 Technology Readiness Level	18
2.5.5 Cost	19
2.5.6 CO ₂ Storage and Utilization	20
2.5.7 Commercial Pathways to DAC	20
2.5.8 Nuclear Power Plants Coupled with DAC	22
2.6 Hydrogen Production	22

2.6.1	Water Electrolysis	23
2.6.2	PEM Electrolysis	24
2.6.3	Efficiency	26
2.6.4	Cost	26
2.7	Synthetic Fuels	27
2.7.1	Power to Liquid	28
2.7.2	Methanol	28
2.7.3	Cost	29
2.8	Methanol Synthesis	29
2.8.1	Green Methanol	30
2.8.2	Green Methanol Synthesis	31
2.8.3	Efficiency	32
2.8.4	Cost	32
2.8.5	Demonstration and Commercial Green Methanol Projects	33
3	Method	34
3.1	Technical Assessment	36
3.1.1	UniSim Design R492	36
3.1.2	Reference Nuclear Power Plant	36
3.1.3	Advanced Nuclear Power Plant	38
3.1.4	Direct Air Capture	39
3.1.5	Nuclear Power Plant with CWT	39
3.1.6	CO ₂ Compression	40
3.1.7	PEM Electrolysis Model	41
3.1.8	Synthetic Gas Production	43
3.1.9	Methanol Synthesis	45
3.1.10	Optimization Tool	46
3.2	Economical Assessment	48
3.2.1	SEA Tool	48
3.2.2	Reference Nuclear Power Plant	51
3.2.3	Advanced Nuclear Power Plant	52
3.2.4	Uncertainty Quantification	53
4	Results and Discussion	55
4.1	Energy Distribution and Environmental Performance	55
4.2	Capital Expenditures	57
4.3	Operational Expenditures	58
4.4	Levelized Cost of CO ₂	60
4.5	Uncertainty Quantification	61
4.5.1	Influencing Parameters of the LCOC	61
4.5.2	Comparison of LCOC	64
4.5.3	Advanced Nuclear Reactor and Methanol Cost Sensitivity	66
4.6	Future Outlook: Green Methanol from Nuclear Power Plants	68

5 Conclusion	76
5.1 Future Work	77
A DAC Sorbent Calculations	I
B Future Levelized Cost of DAC With and Without Carbon Tax	II
C Total Overnight Cost for Nuclear Generating Technologies	III
D Justification for the Uncertainty Quantification	IV
E UniSim Flowsheets	VI

1 Introduction

On the 28th meeting of the Conference of the Parties (COP28), President Sultan Ahmed Al-Jaber said in December 2023: *Together we have confronted realities and we have set the world in the right direction.* For the first time, the deal calls on all countries to transition away from fossil fuels, emphasizing the critical need to reduce global warming [1]. Global warming is caused by greenhouse gases (GHG), mainly through the presence of accumulated CO₂ in the atmosphere from burning fossil fuels. The CO₂ concentration in the atmosphere has rapidly increased from 280 parts per million (PPM) preindustrial times to 422 PPM in 2022 as a result of the annual increase of CO₂ emission illustrated in Figure 1.1 [2]. The Paris Agreement, adopted by 196 parties at the United Nations Climate Change Conference, aims to mitigate climate change, keeping the temperature rise below 2 °C. Preferably, the warming would be limited to 1.5 °C above preindustrial levels, which would need global GHG emissions to peak before 2025, decline by 43% by 2030, and be net zero by 2050 [3].

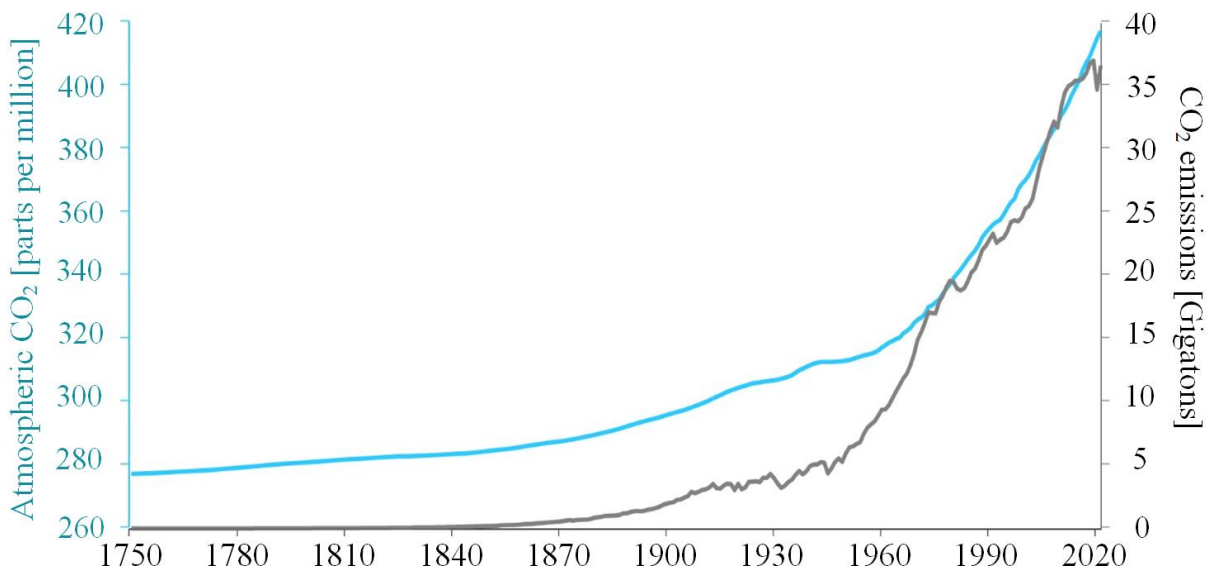


Figure 1.1: Atmospheric CO₂ concentration and annual CO₂ emission [2]. The figure has been modified.

1.1 Motivation

Early climate policy focused on gradually reducing emissions, but the CO₂ concentration rose rapidly. Today, large-scale carbon removal is recognized as a crucial path to combat global warming [4]. To reach the goal of net zero emissions (NZE) by 2050, negative emissions technologies (NET) are needed [5]. The recognition that direct air capture (DAC) has the potential to mitigate climate change is proliferating. Still, a major boost is needed in DAC deployment to meet NZE goals. The International Energy Agency (IEA) has stated that to limit the long-term increase in average global temperatures, DAC rapidly needs an upscale to reach a capture of 90 MtCO₂/y in 2030 and 980 MtCO₂/y in 2050. For comparison, today's global CO₂ capture from DAC is approximately 0.1 MtCO₂/y [6].

DAC needs large amounts of heat and can be powered from multiple energy sources. Nuclear energy can power DAC and is a source of low-carbon electricity that can contribute to securely and rapidly reaching the NZE by 2050. This combination is considered a good fit, utilizing the significant share of waste heat generated by nuclear power plants. Even though nuclear power plants have technical, economic, and social challenges to overcome and some nations already have distanced themselves from nuclear energy, rising climate challenges and the emerging energy crisis could offer initiatives to take a fresh look at the possible advantages of nuclear energy.[7]

Growing climate change concerns drive interest in alternative energy carriers to fossil fuels. The energy demand is rapidly increasing, and a large portion of fuel is needed to meet this demand. Today, a large share of these are fossil fuels, such as oil, gas, and coal. Low-emissions hydrogen-based liquid fuels, such as methanol, offer an alternative to oil [8]. Methanol can be used in some internal combustion engines and is compatible with some of the existing distribution infrastructure [9]. Several industries, such as the maritime sector, have shown a growing interest in methanol as fuel. Driven by recent emissions regulations for the maritime industry set by the International Maritime Organization, Det Norske Veritas reports that more than 20 large ships fueled by methanol are ordered or under operation [9].

The transportation sector stands at the forefront of global challenges, where its significant contribution to GHG emissions and air pollution has become an urgent matter demanding immediate attention. Green methanol with recycled CO₂ could reduce the emissions by up to 95% compared to gasoline and diesel [9]. One of the promising pathways is to produce green methanol from renewable hydrogen (H₂) and recycled CO₂. Several initiatives have investigated green methanol production from renewables such as solar and wind power, providing electricity for CO₂ capture and H₂ production. The IEA has identified nuclear power as an exiting source of electrolytic hydrogen production [10]. In addition, several initiatives explore the utilization of DAC coupled with nuclear power plants [11]. However, after a thorough literature study, studies investigating green methanol production from nuclear power have not been found.

1.2 Researchers Objective

This thesis aims to cover the knowledge gap of green methanol production from a nuclear power plant, conducting an in-depth techno-economic assessment, progressing from a nuclear power plant integrated with DAC to a more advanced facility with an advanced nuclear reactor, DAC, hydrogen, and methanol production. The plants were designed for DAC to perform CO₂ removal on a megaton scale, being self-sufficient with electricity and heat. The plants were assumed to be constructed in the mid-century. The two plants will be referred to further in the thesis as the reference plant and the advanced plant, and a comprehensive description follows below.

- **Reference Plant:** Nuclear power plant with a third-generation nuclear reactor linked to a DAC unit.
- **Advanced Plant:** Nuclear power plant with a fourth-generation reactor linked to a DAC unit. Surplus electricity is used to produce H₂ from electrolysis, which is mixed with CO₂ downstream, forming synthetic gas that is fed into a methanol production plant.

A consistent, bottom-up analysis has been carried out to determine the levelized cost of CO₂ (LCOC) for both plants. The technological analysis builds the intended plants, aiming to utilize heat and electricity from the nuclear power plant seamlessly, removing the need to import energy. The UniSim model for the green methanol synthesis and the proton exchange membrane (PEM) electrolyser was provided by Arnaiz del Pozo et al. [12, 13]. The economic analysis included an estimation of the capital and operational expenditures and an uncertainty quantification investigating the main influencing parameters. The core aspects included in this work are listed below.

1. Develop the model of the two plants in UniSim Design R492 for the technical analysis. Modify the size of the plants provided for the hydrogen and methanol production.
2. Utilize heat and electricity from the nuclear power plants and the PEM electrolyser to support the activities downstream in the process.
3. Make a complete flowsheet comprising all of the different parts of the plant for seamless heat and electricity integration.
4. Conduct an in-depth economic analysis for both plants.
5. Carry out a comprehensive uncertainty quantification to evaluate the influence of key parameters.

1.3 Outline of the Thesis

To effectively discuss and interpret the results, a thorough theoretical foundation is required. Chapter 2 will provide background information on the fundamental thermodynamic and economic relationships, as well as the aspects related to nuclear power, DAC, hydrogen production, synthetic fuels, and methanol production. The technical and economic assessment methodology will be presented in Sections 3.1 and 3.2, respectively. Finally, the results and discussion are provided in Chapter 4, and the conclusion is presented in Chapter 5.

This master thesis is a continuous work from the project thesis, and some paragraphs in the introduction and theory are reused. The reference nuclear plant was modeled in the project thesis, but has been modified to fit the perspective introduced in the more comprehensive master thesis.

2 Theory

In this chapter, the theoretical foundation will be presented. Firstly, the pathways for different climate scenarios will be described. Then, a brief introduction to the thermodynamical and economic terms will be provided, followed by a description of nuclear energy, DAC, electrolysis, and methanol production in terms of technology, operation, and cost.

2.1 IEA's Climate Scenarios for Different Future Pathways

The IEA uses an integrated global energy and climate model framework to generate detailed long-term climate scenarios. The company has carefully developed three scenarios investigating sector-by-sector and region-by-region, providing the whole picture. The three scenarios include the Stated Policies Scenario (STEPS), the Announced Pledges Scenario (APS), and the NZE. These projections have been used for the technical and economic assessment and will be discussed in Chapter 4.[14]

The STEPS is developed to show the climate trajectory for today's climate policy. The APS illustrates the degree to which announced climate ambitions and targets can contribute to the desired emission reductions to reach NZE by 2050. The most optimistic approach is the NZE by 2050, which shows a pathway for the global energy sector that can reach net zero CO₂ emissions by 2050. A CO₂ tax is predicted to be emerging both for the APS and NZE scenario.[14]

2.2 Thermodynamics

Thermodynamical relations are crucial as they form the foundation for equipment used worldwide in everyday life, including heat engines, power plants, and chemical reactions [15]. The following sections will briefly introduce thermodynamical aspects important for energy conservation, nuclear power plants, and power plants operating at and above supercritical levels.

2.2.1 First and Second Law of Thermodynamics

The first law of thermodynamics is an expression of the conservation of energy, stating that energy can neither be created nor destroyed. The law states that the change in internal energy in a system, ΔU , equals the net heat transferred into the system, Q , including the net work, W , done on the system. The formula is presented in equation 2.1.[15]

$$\Delta U = Q + W \tag{2.1}$$

The second law of thermodynamics addresses the direction when a spontaneous process unfolds. Several processes occur spontaneously in one direction but are only irreversible for a given set of conditions. In terms of entropy, the law states that every energy transfer that takes place will increase the entropy of the universe and reduce the share of usable energy that could be utilized to do work. In other words, any process, such as a chemical reaction or set of connected reactions, will proceed in a direction that increases the overall entropy of the universe.[15]

2.2.2 Supercritical Conditions

For a given temperature and pressure, a pure substance may be found in a solid, liquid, or vapor phase. When one or both of those properties change, the substance may change from one phase to another [16]. The different phases are illustrated in Figure 2.1. The critical point is located where the vaporization line ends, at the critical pressure, P_C , and the critical temperature, T_C , respectively. If $T > T_C$ or $P > P_C$ the substance enters the supercritical state, called a supercritical fluid. At this stage, no distinct liquid or gas exists. Supercritical properties vary for different substances. Water reaches supercritical states above 220 bar and 373 °C. Engines operating at supercritical steam could reach efficiencies up to 46-47% with state-of-the-art technology [17].

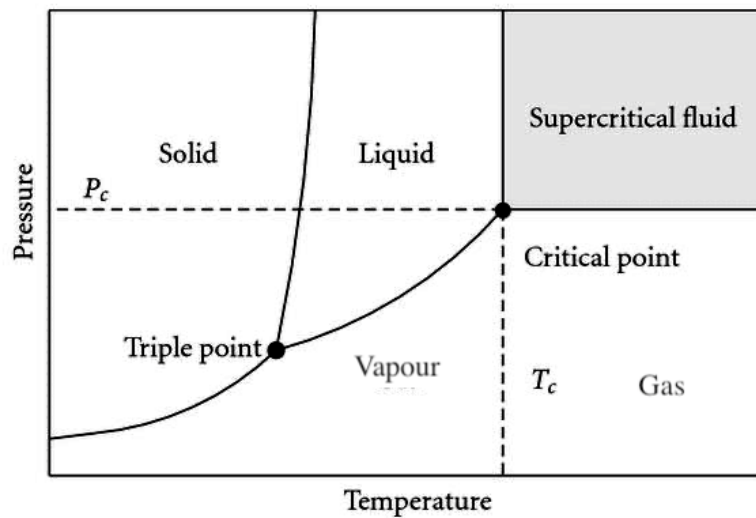


Figure 2.1: P-T diagram showing different phases for a fluid [16]. The figure has been modified.

The boiler could reach ultra-supercritical conditions if the pressure increases to 300 bars or above. Ultra-supercritical steam turbines working above 300 bar and 600 °C are one of the most promising technologies today, especially for thermal power generation, such as nuclear plants [18]. The ultra-supercritical steam power plants could reach efficiencies up to 50% based on lower heating value (LHV) [17]. This power cycle is typically modeled as the Rankine cycle with an ultra-supercritical boiler, described further in the next section.

2.2.3 Ideal Rankine Cycle

The Rankine cycle is an idealized thermodynamic cycle that converts heat into mechanical work from a constant-pressure heat source. The process, named after John Macquorn Rankine, is one of the most utilized thermodynamical cycles to produce electricity worldwide [19]. Several substances can be utilized as the working fluid. However, the most used fluid is water (steam) mainly due to its well thermodynamic properties, non-toxicity, and low cost [20]. The Rankine cycle consists of four main components: a pump, a condenser, a turbine, and an evaporator. The vapor generator is usually illustrated as a boiler, with the primary objective of obtaining super-heated steam [21].

The ideal Rankine cycle comprises the four reversible processes described below and can be seen in Figure 2.2 [21].

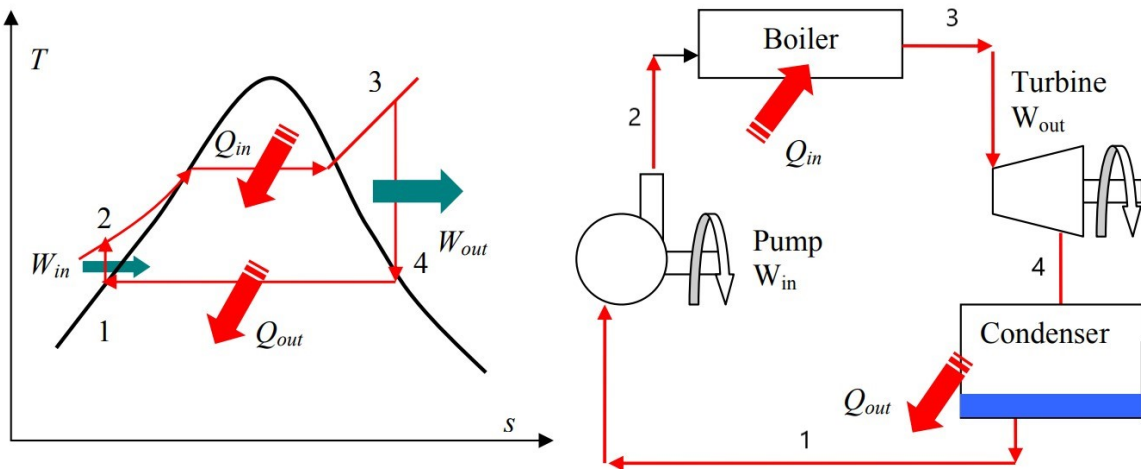


Figure 2.2: T-S diagram and component flowsheet of an ideal Rankine cycle [21]. The figure has been modified.

- **1-2: Isentropic compression** - Water enters the pump as saturated liquid and is compressed isentropically to the operating pressure of the boiler.
- **2-3: Heat addition** - The compressed fluid is heated in the boiler to the final temperature, and leaves the boiler as super-heated vapour.
- **3-4: Isentropic expansion** - Super-heated vapour enters the turbine and expand isentropically.
- **4-1: Heat rejection** - The vapor cools down in the condenser - returning to a liquid phase. The waste heat is transferred to the atmosphere or a large body of water.

Typical thermal power plants have relatively low efficiencies ranging from 30% for average plants and up to 45% and ever 60% for state-of-the-art solutions [22]. The energy efficiency, η , of the Rankine cycle is written using net work output, W_{net} , and the total heat input, Q_{in} , from the boiler derived in equation 2.2.

$$\eta = \frac{W_{net}}{Q_{in}} \quad (2.2)$$

2.2.4 Ideal Rankine Reheat Cycle

The ideal Rankine cycle can improve efficiency by reducing the presence of moisture in the steam during the final stage of expansion. Implementing a two-stage turbine with reheating in between can reduce the amount of moisture, hence increasing the efficiency of the cycle. In the

first high-pressure stage, the steam expands isentropically and is then sent back to the boiler at an intermediate pressure to be reheated at constant pressure. Further, in the low-pressure stage, the steam is isentropically expanded to the condenser pressure. The fluid is then condensed and pressurized back to the original pressure.[21]

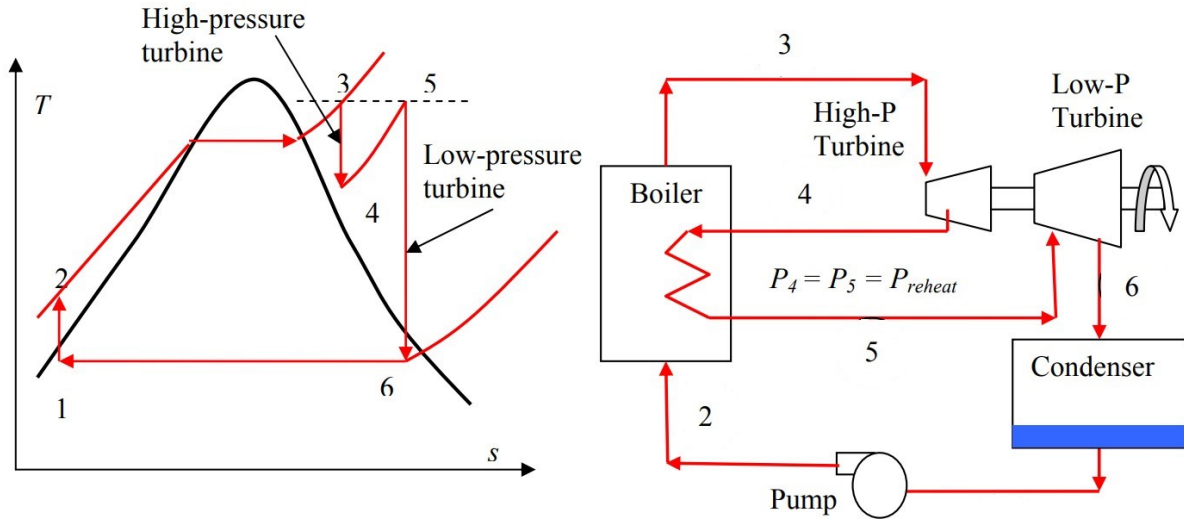


Figure 2.3: T-S diagram and component flowsheet of an ideal Rankine reheat cycle [21]. The figure has been modified.

Implementing one stage of reheating could raise the efficiency of the plant with 4-5% [21]. Two stages of reheating could gain the efficiency of the plant with 8%, more than two stages of reheat is not considered economically beneficial for most power plants [23].

2.3 Economics

Economics plays a vital role in the construction of any given power plant, especially for capital-intensive plants that require a large amount of up-front cash. The economic aspect influences the project's feasibility, long-term sustainability, and plant payback time. The essential economic expressions and performance factors will be described below.

2.3.1 Capital Expenditure

Capital expenditures (CAPEX) account for the cost related to the facility's construction and installation of the plant's components, development, enhancement, or expansion. When the CAPEX is calculated, it is commonly divided into minor categories, as presented in Figure 2.4. The bare erected cost (BEC) includes the cost of the process equipment, infrastructure, and expenditures for the installation. The total plant cost (TPC) includes the contingency to cover uncertainties with equipment indicated by a technology readiness level (TRL) indicator and unexpected costs. Total overnight costs (TOC) comprise the owner's cost, which includes fees, financing, land cost, and permits. The TOC is important as the figure indicates the financial commitment associated with the project. The last step is the total capital requirement (TCR), which represents an aggregation of the CAPEX cost, including escalation and interest.[24]

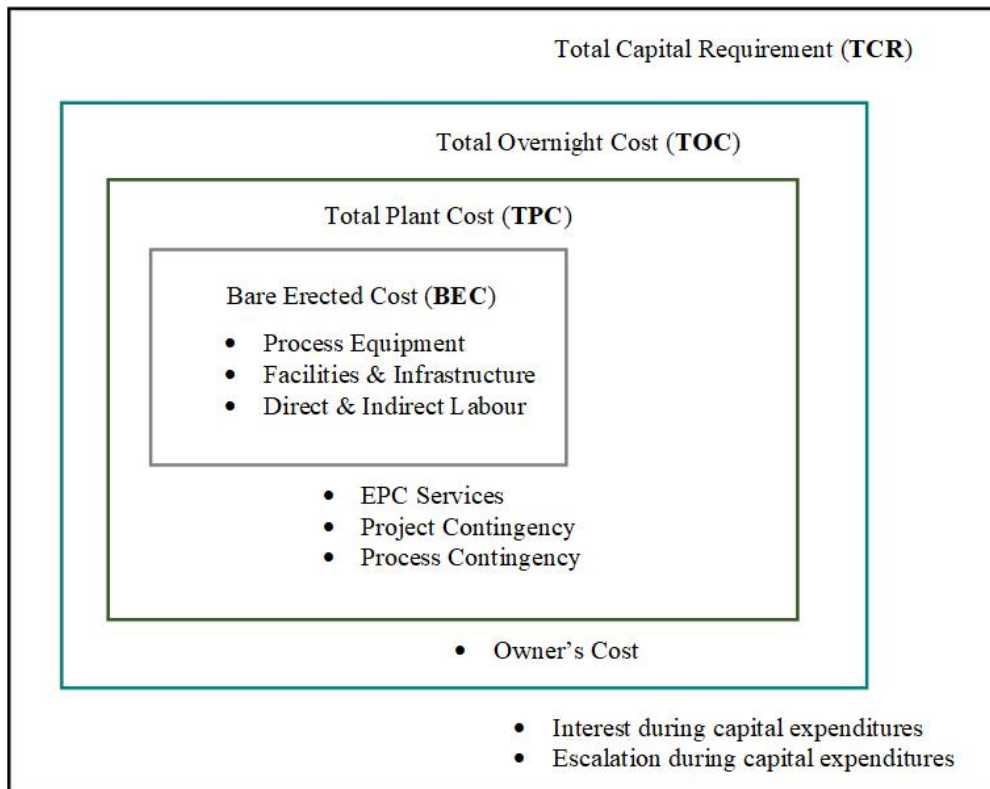


Figure 2.4: The capital cost breakdown in categories [24]. The figure has been modified.

2.3.2 Operational Expenditure

Operational Expenditures (OPEX) are ongoing business, product, or system costs. These costs include employee payroll, raw materials, maintenance, day-to-day expenditures, utility consumption, insurance, and general and administrative expenses. In general, companies are pursuing a reduction of OPEX without impacting the functionality of the ongoing production or the quality of products or services. However, effective and proper management of the OPEX is required to ensure a sustainable and environmentally safe operation. If the OPEX were reduced irresponsibly, the company could suffer long-term consequences or, in the worst case, accidents caused by a lack of maintenance or surveillance.[25]

2.3.3 Net Present Value

The levelized cost of product (LCOP) is defined as the price the product needs to be sold at to achieve a net present value (NPV) at zero at the end of the facility's lifetime. The NPV is calculated by adding the annual cash flow (ACF) for the plant's construction and operational phase. The equation for the NPV is shown in equation 2.3, where ACF_t is annual cash flow, i is the discount rate, and t is time.[24]

$$NPV = \sum_{t=0}^n \frac{ACF_t}{(1+i)^t} \quad (2.3)$$

2.4 Nuclear Energy

Physicists Lise Meitner and Otto Frisch made a startling discovery in 1938 that would immediately revolutionize nuclear physics. They discovered that a uranium nucleus had split in two, today known as the fission process. Fission can occur spontaneously, but most commonly by inducing an external influence by bombarding the nuclei with gamma radiation, neutrons, or other particles [26]. Large amounts of energy are released when the nucleus core, comprising protons and neutrons, is split into two atoms. In addition, 2-3 neutrons are typically formed in the process, bombarding other atoms and sustaining a chain reaction. The most common nuclear fuel is uranium (typically the U-235 isotope). Both fission and fusion are the two main nuclear reactions, where fission releases energy while fusion can either release or consume energy. The latter have been investigated for power plant purposes but still have to prove an energy gain commercially [27].

2.4.1 Nuclear Power Plants

Nuclear power is a low-emission source of electricity that produces around 10% of the global electricity generation from around 440 nuclear reactors. Nuclear has been recognized as an essential source of energy that can complement renewable power in reducing emissions in the power sector. In addition, nuclear energy is a stable and reliable energy source recently identified as an option for producing low-emission heat and hydrogen [28]. In 2022, nuclear capacity additions grew with nearly 8 GW_e installed capacity, corresponding to 40% growth from the growth the previous year. IEA has identified nuclear energy as an important energy source to reach the goal of NZE in 2050, as presented in Figure 2.5 [7].

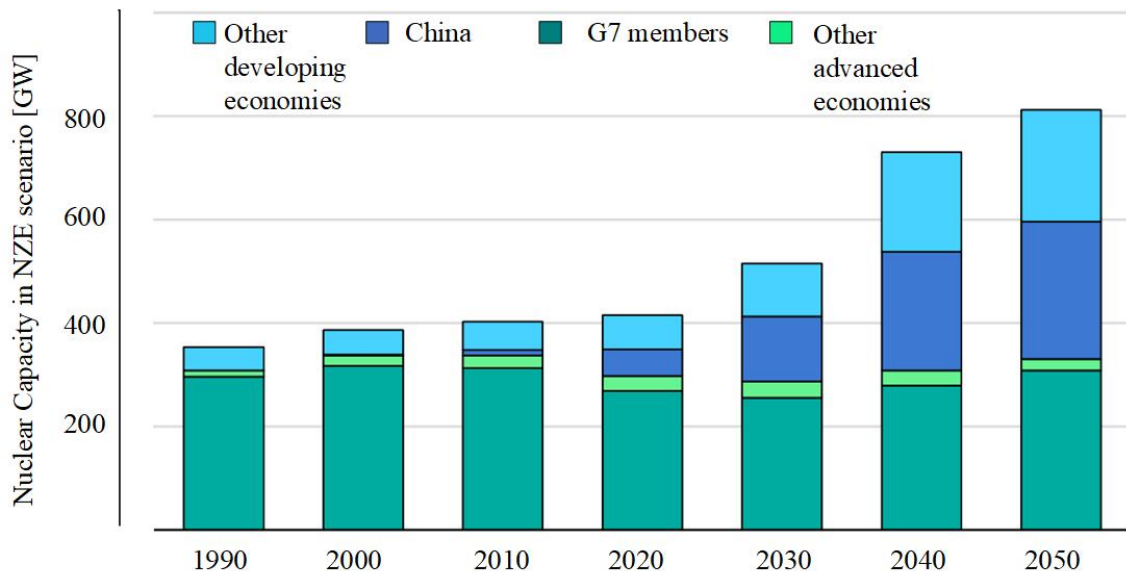


Figure 2.5: Historical and future energy production from nuclear power plants to reach NZE by 2050 [7]. The figure has been modified.

The development of nuclear plants has come a long way since the first commercialized nuclear plant began operation in the 1950s [28]. Today, the average production from a nuclear plant

is around 1 GW_e , less for smaller plants and up towards $1.8\text{-}2 \text{ GW}_e$ for larger, more advanced plants. Also, small modular reactors have received increased interest in the last years, producing up to 300 MW_e per unit [29]. The expected lifetime of a nuclear reactor varies between 20-40 years. However, upgraded and recently built plants can last up to 60 years [27, 30, 31]. An illustration of a typical nuclear power plant is presented in Figure 2.6 [32].

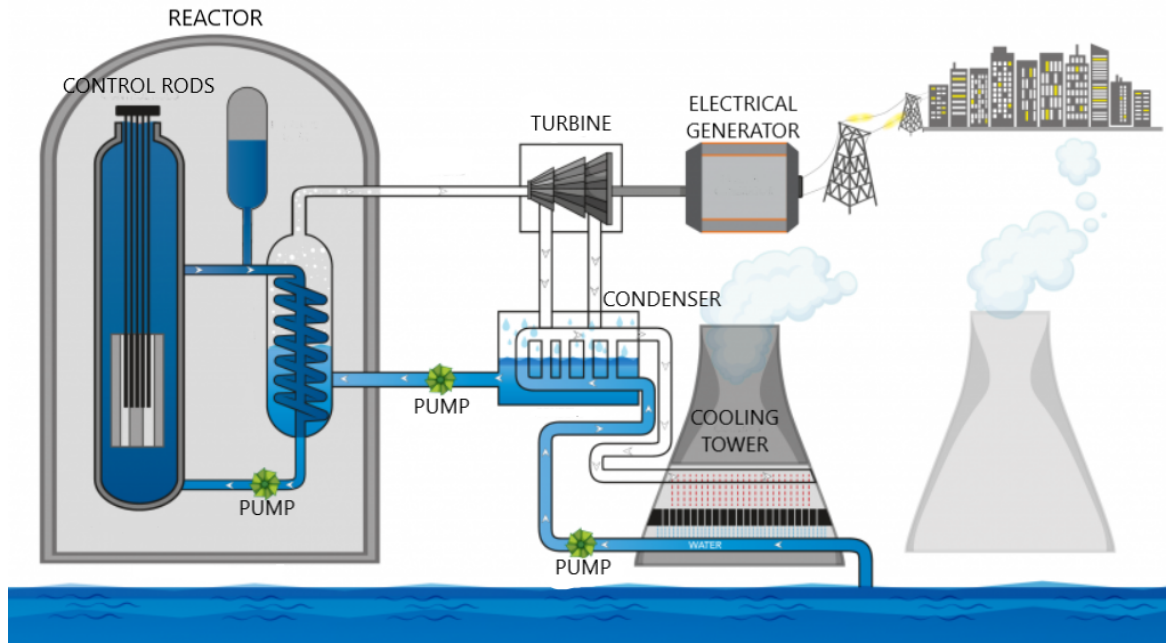


Figure 2.6: Simplified illustration of a nuclear power plant [32]. The figure has been modified.

2.4.2 Nuclear Fuel Cycle

The nuclear fuel cycle comprises several steps, such as: mining, milling, enrichment, and waste disposal. Enrichment is the step in the process that increases the U-235 isotope, where an enrichment between 0.7-5% is most common. There are economically recoverable uranium deposits in the western US, Australia, Central Asia, Africa, South America, Canada, and Russia. The process of preparing uranium for nuclear reactors can be time-consuming and cost-intensive. The discovered uranium existing now can provide nuclear power in the future for approximately 1000 years more [33]. Radioactive nuclear waste poses a long-term hazard to life on Earth. Despite natural decay, the waste needs substantial treatment and disposal, which is time-demanding and cost-intensive [27].

Today, uranium is the only fuel that is supplied to nuclear reactors. However, thorium is seen as a promising fuel in some nuclear reactors, such as the CANDU reactor. The World Nuclear Association reports that thorium is three times more abundant than uranium in the Earth's crust [34]. Plutonium is also investigated as a fuel for nuclear fast breeder reactors. The fissile isotope Pu-239 is produced and consumed in the reactor, holding large amounts of U-238 [27, 33].

2.4.3 Nuclear Reactors

The nuclear reactor is considered the heart of the nuclear power plant. The main job of the reactor is to house and control the fission reaction. The nuclear fuel inside the reactor consists of small ceramic pellets stacked together into sealed metal tubes, known as the fuel rods. Normally, 200 of these fuel rods are bundled together inside the reactor. To control the fission reaction, control rods can be applied in the reactor core to reduce the reaction rate and withdrawn to increase it.[35]

Inside the most used reactors, the fuel rods are immersed in water, acting as a coolant and moderator. The role of the moderator is to decelerate the neutrons generated during fission to sustain the chain reaction. At the same time, the coolant receives and transports heat to other parts of the nuclear plant. Water is converted into steam, which spins a turbine to create electricity [35]. The reactors mainly used in nuclear power plants today are the pressurized water reactor (PWR) and boiling water reactor (BWR). An overview of the reactor types can be found in Table 2.1. A heterogeneous arrangement is implemented in most modern reactors, meaning the fuel is isolated from the coolant. On the other hand, a homogeneous mixture is a mix of fuel and coolant or fuel and moderator. About one-third of the reactor core (40-90 assemblies) is replaced with new fuel every 12-24 months [33].

One of the main concerns with nuclear reactors is that the nuclear reaction will accelerate out of control, causing overheating and a reactor meltdown. This happened in Fukushima when the emergency cooling water system failed, exposing the environment to radiation. After this accident in 2011, there have been multiple initiatives to strengthen the security of nuclear reactors. The International Atomic Energy Agency has several “Safety Guides” related to safety restrictions for nuclear design. An Economic Co-operation and Development Nuclear Energy Agency study in 2010 pointed out that the theoretical frequency of considerable release of radioactivity from a severe nuclear accident is reduced by a factor of 1600 between the first reactors (called Generation I) and the reactors being built today (Generation III and IV).[36]

Generation IV Reactors

In 2000, a forum comprising 13 countries where nuclear power is significant or on the rise was invited to a joint development working on the next generation of nuclear technology [37]. The fourth-generation designs aspire to elevate efficiencies, optimize fuel consumption, minimize waste production, and meet strict safety standards. The Generation IV International Forum chose six reactor technologies to develop and aims for commercial deployment in 2030. The technologies selected for further research and development were the gas-cooled fast reactor (GFR), the lead-cooled fast reactor (LFR), the molten salt reactor (MSR), the sodium-cooled fast reactor (SFR), the supercritical-water-cooled reactor (SCWR) and the very high-temperature reactor (VHTR). As seen in Table 2.1, several of the fourth-generation reactors operate with non-water fluids. This allows some technologies to operate at low pressures [38, 39]. SCWR will be described in further detail since the advanced reactor’s design is based on this reactor.

The SCWR operates at a very high pressure above the thermodynamic critical point of water. The supercritical water drives the steam turbine. Since the system is based on the well-known BWR and conventional fossil-fired power plants operating at supercritical water, it can readily be developed. A reactor operating at ultra-supercritical levels can achieve up to 50% efficiency. These reactors operate at pressure levels of 300 bar or more. Over 400 such ultra-supercritical coal-fired plants are operating worldwide.[37, 40]

Table 2.1: Generation III and generation IV nuclear reactors [37, 40]

Reactor type	Number	Temperature	Working fluid	Nuclear fuel
Gen. III nuclear reactors				
PWR	307	290-330 °C	water	3% U-235
BWR	60	286 °C	water	2.5% U-235
Heavy water (CANDU)	48	300-400 °C	heavy water	0.7% U-235
Gen. IV nuclear reactors				
SWCR		510-625 °C	water	U-235
GCFR	-	850 °C	helium	U-238+
LFR		480-570 °C	lead or Pb-Bi	U-238+
MSR	-	700-800 °C	fluoride salts	UF in salt
SFR	-	500-550 °C	sodium	U-238
VHTR	-	900-1000 °C	helium	U-235

A new technology currently being developed for nuclear reactors comprises the breeder reactor, which is a nuclear reactor that produces more fissile material than it consumes. There are two categories of breeder reactors, fast breeder and thermal breeder reactors that consume U-238 and Th-232 as fuel. Developing these reactors could influence the future of nuclear fuel as a viable technology that drastically reduces nuclear fuel consumption.[41]

2.4.4 Cooling Water Tower

The electrical power generated by the consumption of any fuel implies the release of large amounts of waste heat. While fossil-fueled plants can release heat via the flue gas, nuclear units must release waste heat via condensing cooling water. The cooling water tower (CWT) is a large heat exchanger, with airflow provided by mechanical blowers or natural convection, and aims to reject waste heat to the atmosphere. If the power plant is located near a lake or river, the water resources can transport waste heat, removing the need for a CWT. This solution is mostly used for smaller power plants.[27]

The waste heat from nuclear power plants represents a significant amount and can be found using equation 2.4, where Q_w , is the waste heat and Q_r , is the reactor heat, P_e is the electrical power respectively.[27]

$$Q_w = Q_r - P_e \quad (2.4)$$

2.4.5 Capacity Factor

An important parameter describing the performance of a power reactor is the capacity factor (CF). The CF is defined as the ratio of electric energy produced in a given time interval, P , divided by what could have been produced at net rated power, P_e , during the same period, T . Equation 2.5 shows the method for calculating the capacity factor.[27]

$$CF = \int_T^0 \frac{P(t)dt}{(P_e T)} \quad (2.5)$$

The main reasons for the nuclear plant not having full production throughout the year are maintenance and refueling. The median CF has risen from 59% in the period 1974-1976 to 90% in 2001-2012 in the United States [33]. Data collected by the IEA in the US shows that in 2021, Nuclear Power Plants had an average CF of 92.7%. For other widely used energy sources, such as natural gas and coal, the CF was 54.4% and 49.3%, respectively. Renewable sources like wind and solar energy had a yearly average of 34.6% and 24.6% [42].

2.4.6 Efficiency

The efficiency for a nuclear plant, η , is determined by the amount of electric power produced, ΔW , divided by the heat put into the system, Q_{in} , shown in equation 2.6. Typically, nuclear power plants have an efficiency of 33%, meaning that 3000 MW_h of thermal heat is required to produce 1000 MW_e of electricity. Based on this efficiency, about twice the energy is wasted as it is converted to electrical energy.[27]

$$\eta = \frac{\Delta W}{Q_{in}} = \frac{W_{turbine} - W_{pump}}{Q_{reactor}} \quad (2.6)$$

2.4.7 Cost

The largest share of the cost of nuclear energy is mainly from the up-front capital cost. The cost share is due to the complexity, strict requirements, and safety measures for nuclear reactors, material production, and manufacturing. The capital cost accounts for at least 60% of their levelized cost of electricity (LCOE). LCOE is the total cost to build and operate the power plant over its lifetime divided by the total electricity produced in that period.[43]

The total cost for nuclear power plants varies depending on several factors, such as knowledge and routines, type of reactor, material, and fuel cost. In addition, there are significant variations in the cost of nuclear power plants for different nations. A collaboration between the IEA and the Nuclear Energy Agency did a series of studies on electricity generating costs. Some key insights show that the cost of electricity from new nuclear power plants remains stable. The same report presented the TOC for nuclear-generating technologies for different regions in the world and can be found in Table 2.2. The whole table can be found in Appendix C, providing information on net capacity and reactor type [44]. The cost of nuclear energy has been projected to be lowered in the future [45].

Table 2.2: Total overnight cost for nuclear energy [44]

Country	Japan	France	Russia	Slovakia	China	India
TOC [\$/kW _e]	4013	3963	2271	6920	2500	2778

A nuclear plant OPEX includes fuel costs, operation and maintenance (O&M) costs, and treatment and disposal of nuclear fuel waste. The price of fuel varies with many factors but is stated in literature to lay in the range of 0.27-2.77 \$/GJ [45–47].

Recent nuclear power plants, especially in Europe and the U.S, have tended to exceed budget and time estimates. Two reactors in the state of Georgia were projected to cost around 4 300 \$/kW_e on a TOC basis. However, the newest estimate is close to reaching 9 000 \$/kW_e. Additionally, the construction period was extended from four to nine years. Korea, which was earlier shown to stay within nuclear projects’ financial constraints and project timelines, has had delays and cost overruns on its latest projects. IEA has collected data for the TOC and duration of some recent nuclear projects, illustrated in Figure 2.7.[7]

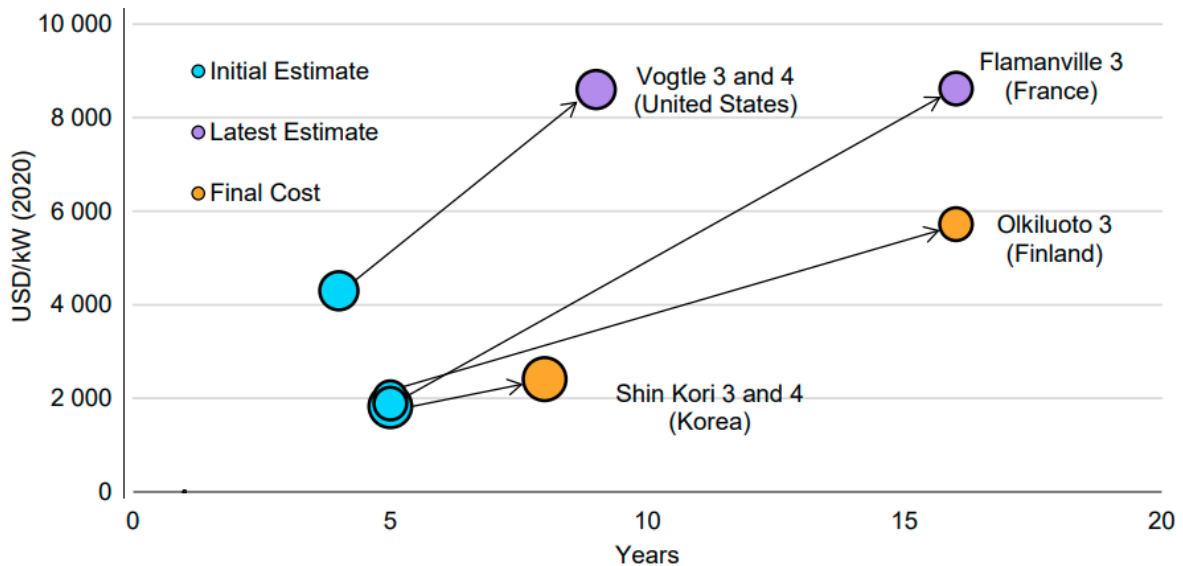


Figure 2.7: TOC and construction times for some recent nuclear projects [7]. The figure has been modified.

2.4.8 Emission

Nuclear energy is considered a low-carbon energy source. This energy source can produce electricity with zero emissions since most of the emissions arise at the upstream stages of a nuclear plant. The energy consumption related to the fuel cycle described earlier is considerably high. Large amounts of concrete and metals are also required, mainly for the reactor and the large cooling tower(s). If the energy needed to manufacture, create materials, and provide fuel to the power plant is based upon fossil fuels, the emission related to burning those fuels would be associated with nuclear emissions, increasing the carbon footprint of nuclear energy.[26]

A life cycle analysis by Weisner analyses the emissions related to different energy sources in terms of CO₂ equivalents (CO₂eq). Weisner investigated a nuclear plant with a light-water reactor, including all emissions in the upstream process, production phase, and downstream activity, including decommissioning and waste management, and found the emissions to range from 2.8-24 gCO₂eq./kWh_e. Renewables such as solar and onshore wind were reported with 50-73 gCO₂eq./kWh_e and 8-30 gCO₂eq./kWh_e respectively. In contrast, cumulative emission for coal plants ranges between 750-1250 gCO₂eq./kWh_e. [48]

2.4.9 Social Aspect

The benefits of nuclear energy have always been accompanied by its respective risks. Critics raise issues related to safety, nuclear weapons, and the comprehensive management of nuclear waste. Nuclear energy disasters have received much attention around the world, resulting in great resistance among people and several anti-nuclear organizations. Throughout the years, there have been reported over 100 nuclear accidents, where there have been two significant disasters, Chernobyl (then Soviet Union, now Ukraine) in 1986 and Fukushima (Japan) in 2011 [31]. The social perception of nuclear energy determines whether the energy policy or the nuclear technology can be successfully implemented within the nation [49].

2.4.10 Nuclear Power Future and Outlook

Nuclear power capacity is increasing steadily worldwide, with about 60 reactors under construction and plans for 110 more [50]. However, nuclear power faces a future with crucial challenges to overcome. Due to political and social aspects regarding nuclear power, some nations have begun to shut down nuclear reactors. Germany decided to phase out nuclear power, resulting in the shutdown of all 17 units (as of 2011). The last three reactors stopped production in 2023 [51].

The global energy landscape is facing uncertainties, forcing nations to explore additional energy sources to lower the reliability of imported energy. Nuclear energy is one option seen by several nations to make their respective energy supply more reliable and stable. Finland has recently built new plants with the largest reactor in Europe producing 1.6 GW_e. They also compiled a survey showing that 70% of the Finns favor nuclear energy, a significant increase from 30 years ago [52]. Sweden has also found a new interest in nuclear power, regardless of the Swedish government's decision to phase out nuclear power in 1980. In June 2023, Sweden replaced the goal of "100% renewable electricity by 2040" with "100% fossil-free electricity by 2040", empowering the government to proceed with new plans for nuclear plants [53].

2.5 Direct Air Capture

There are several technological pathways available for carbon dioxide removal (CDR) on the market today. The leading industrial technologies are industrial separation, pre- and post-combustion, oxyfuel combustion, chemical looping combustion, and DAC systems. The Global CCS Institutes report for 2022 states that the CO₂ capture capacity for carbon capture and storage (CCS) facilities (including operational and developing plants) has grown to 244 MtCO₂/year,

corresponding to a growth of 44% from 2021 [54]. DAC is recognized as one of the most promising pathways to reach NZE by 2050. DAC technologies extract CO_2 from the atmosphere for storage and/or utilization. There are two main pathways for DAC, solid DAC (S-DAC) and liquid DAC (L-DAC). According to the IEAs numbers for July 2030, 27 DAC plants were operating worldwide, capturing approximately $0.01 \text{ MtCO}_2/\text{yr}$. There are emerging initiatives for DAC deployment, and there are currently plans for 130 new DAC facilities [6, 55].

2.5.1 Solid DAC

S-DAC operates with a solid adsorbent undergoing a cycling process of absorption/desorption. In the absorption step, ambient air enters the S-DAC unit, and CO_2 is chemically bound to the sorbent. The chemical adsorption of CO_2 is an exothermic reaction of a sorbent with the CO_2 present in the inlet stream at ambient temperatures. The absorption process is preferably conducted at low partial pressure with an amine or carbonate solution.[56]

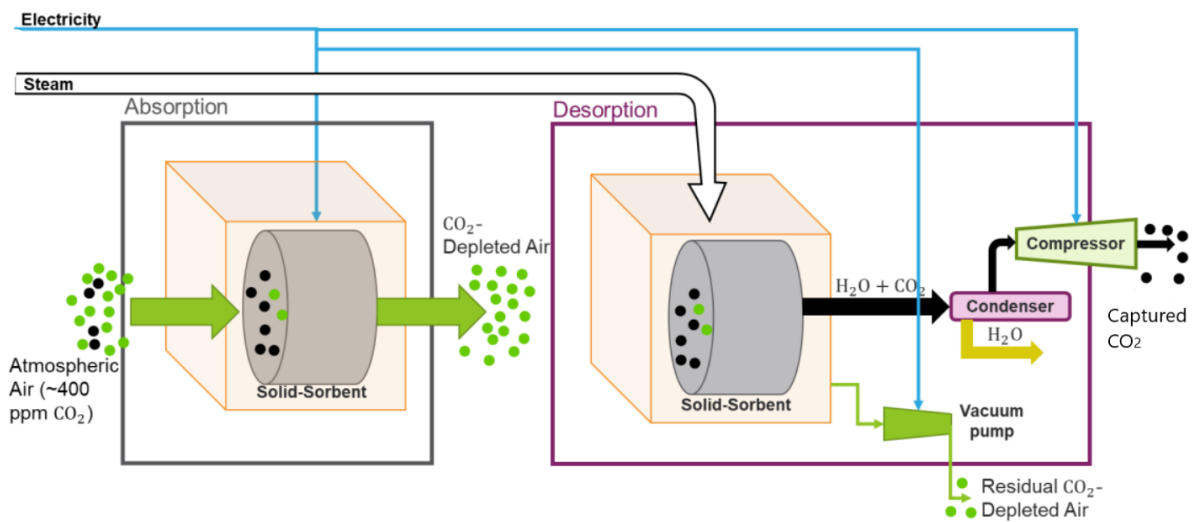


Figure 2.8: Simplified figure of S-DAC [11]. The figure has been modified.

When the sorbent is fully saturated, the CO_2 is released in the desorption step. This step goes through a temperature-vacuum swing process, and CO_2 is released at low pressures under the supply of medium-temperature heat. The DAC unit is then cooled to ambient temperatures to undergo a new cycle of CO_2 capture. The S-DAC process is illustrated in Figure 2.8.[6, 11]

In a literature review conducted by Fashihi et al. the pressure out from the vacuum pressure drop process ranges between 0.2 bar to 1.4 bar, varying with what type of sorbent is used. Temperature also ranges $85\text{-}450 \text{ }^\circ\text{C}$ but typically within the range of $70\text{-}120 \text{ }^\circ\text{C}$. The CO_2 captured from the S-DAC process obtains a high purity of more than 99%.[5, 57]

2.5.2 Liquid DAC

The most common L-DAC technology relies on a basic solution, typically potassium hydroxide (KOH) to capture CO_2 . The regeneration of the solvent goes through a series of operations that typically need temperatures between $300 \text{ }^\circ\text{C}$ and $900 \text{ }^\circ\text{C}$, where $900 \text{ }^\circ\text{C}$ is most utilized. L-DAC

is based on two closed chemical loops, the contactor loop and the calciner loop, as seen in Figure 2.9.[5, 11]

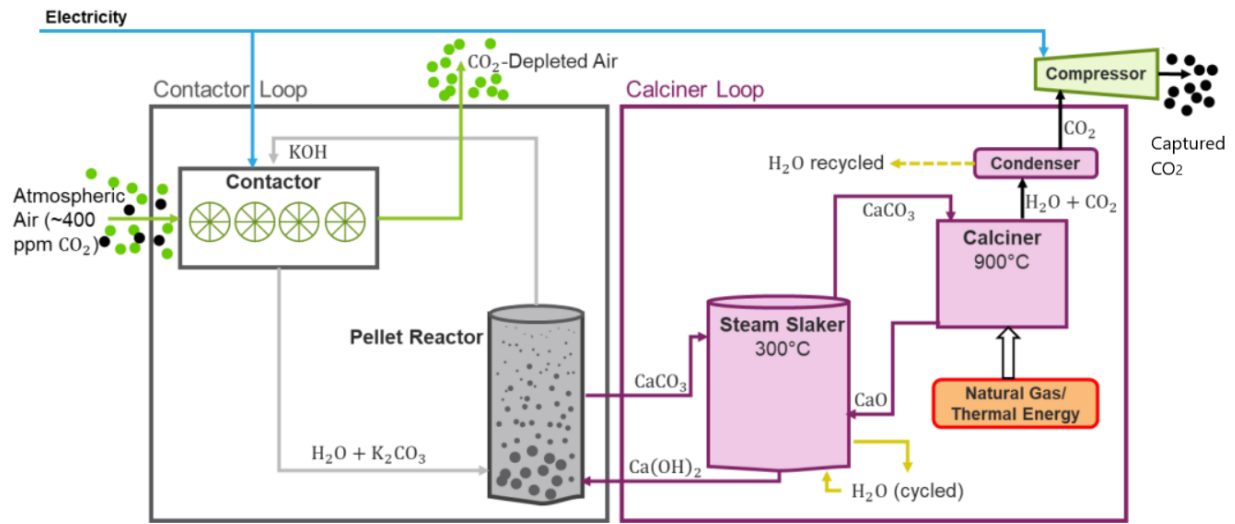
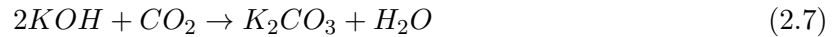
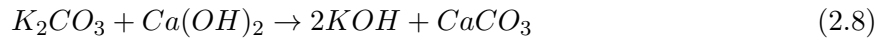


Figure 2.9: Simplified figure of L-DAC [11]. The figure has been modified.

In the first loop, ambient air is forced through a contactor with KOH. The KOH reacts with the CO₂ and forms potassium carbonate (K₂CO₃) solution, as shown in equation 2.7.[5, 11]



KOH is recovered in a pellet reactor where K₂CO₃ reacts with calcium dehydroxide (Ca(OH)₂) to form limestone (CaCO₃), as shown in equation 2.8.[11]



CO₂ is recovered from CaCO₃ in a calciner at high temperatures, purified, and compressed for storage or utilization. The Ca(OH)₂ returns to its original state in contact with steam in the slaker.[5, 11]

2.5.3 Energy Usage

Today, DAC has the highest energy consumption of any carbon capture method. This is due to the much more dilute CO₂ concentration in ambient air than for other CDR methods that remove CO₂ from a point source [55]. A general rule for the most common DAC technologies is that the energy consumption typically is around 80% thermal energy and 20% electrical energy. Fashihi et Al. found the energy demand to range between 77-440 kWh_e and 1485-2780 kWh_h per tonne CO₂ captured for liquid DAC. For S-DAC, the energy demand ranges between 150-1420 kWh_e and 1170-2083 kWh_h per tonne CO₂ captured. The large amount of energy required to elevate the temperature for L-DAC often requires a higher thermal energy demand. The same paper investigated S-DAC in future scenarios, looking at a conservative and optimistic future for DAC. According to both scenarios for S-DAC development, energy demand is expected to be

significantly reduced in the coming decades. The conservative energy consumption development is seen in Table 2.3.[5]

Table 2.3: Predicted energy consumption for the S-DAC in future scenarios [5]

Year	2020	2030	2040	2050
Heat energy demand [MJ/kgCO ₂]	6.30	5.40	4.63	3.97
Electricity energy demand [MJ/kgCO ₂]	0.90	0.81	0.73	0.66

Another study on energy usage of DAC technologies was carried out by An et al. This review demonstrates that the work equivalent regeneration energy demand (supported by either the electric grid or fossil fuel combustion) ranges from 0.5–18.75 MJ/kgCO₂ for solid sorbent DAC systems and 0.62–17.28 MJ/kgCO₂ for liquid solvent DAC systems [58]. Ozkan et al. found that the energy required for L-DAC was 6.57–9.9 MJ/kgCO₂ and 3.5–6.6 MJ/kgCO₂ for S-DAC.[59]

2.5.4 Technology Readiness Level

TRL estimates the maturity of technologies within a defined scale. This scale goes from TRL 1, where the basic principles are defined, to TRL 9, meaning that the technology is commercially available. A thorough explanation of each step can be found in Table 2.4.

Table 2.4: TRL for DAC [60]

TRL Level	Definition and indication of scale	DAC status in 2023
TRL 1 - concept	Basic principle observed and reported	-
TRL 2 - formulation	Analytical or experimental proof of concept	-
TRL 3 - proof of concept	Component and/or system validation in lab	-
TRL 4 - lab prototype	Lab-scale demonstrated in a relevant environment	-
TRL 5 - lab scale system	Pilot-scale demonstrated in a relevant environment	-
TRL 6 - pilot system	Prototype demonstrated in an operational environment at precommercial scale	L-DAC Climeworks 1 t/d pilot
TRL 7 - demonstration system	Complete system demonstrated and qualified in plant environment	Enzyme solvent 30 t/d system
TRL 8 - preeconomical system	Complete system demonstrated and qualified in plant environment	S-DAC Climeworks Iceland 4000 t/d
TRL 9 - commercial system	Complete system operated at expected conditions	-

According to the EIA, DAC is currently at stage TRL 6, the level where the prototype has been tested in the way it will be deployed. Because the technology is still at a relatively low level, it has considerable potential for improvements and cost and energy reduction [6]. However, some of the operational plants have been given a higher TRL due to the commercial deployment of the respective plant. A summary of the plants receiving a higher TRL can be seen in Table 2.4. This overview is based on Rackley et al. literature review published in 2023 [60].

2.5.5 Cost

DAC is one of the most expensive routes for CO₂ capture. Today, DAC is not demonstrated at a large scale (>1 MtCO₂/year), and its related cost is highly uncertain. The cost of DAC found in the literature ranges from 100 \$/ton to 1000 \$/ton. A recent study by the IEA Greenhouse Gas R&D Program estimates that the cost for CO₂ removal with DAC would be between 200-700 \$/ton.[6]

Table 2.5: Specific capital cost for the S-DAC unit [5]

Year	2020	2030	2040	2050
Cost DAC unit [\$/tCO ₂ ·yr]	803	372	261	219

The largest share of cost is related to the capital cost for DAC. However, since it is early days for DAC with a relatively low TRL level, the price is expected to be reduced greatly. Price will be driven down by scaling up manufacturing capacity from hundreds to millions of DAC modules. However, this is far ahead on a time scale [61]. Fasihi et al. found that the prices for S-DAC will be reduced until 2050, and the results from their analysis can be found in Table 2.5. Even though these results were obtained in a conservative scenario, the price is predicted to already be halved by the end of the decade [5].

DAC’s O&M cost is less than the capital cost but is still high. The primary cost attribute for the O&M cost comes from the heat and electricity energy consumption. The cost varies significantly due to the type and cost of the energy supplied [6]. Also, a share of the cost is related to the sorbent material needed in DAC. Currently, multiple initiatives are carrying out research for different sorbent materials. There is a need for chemical engineering innovation dedicated to sorbent manufacturing to create a good-fit sorbent that could be commercialized for mass-producing. Gigascale S-DAC deployment requires up to 5 Mt of sorbent production according to a recent life cycle assessment for S-DAC facilities [61].

The implementation of a carbon tax could reduce the cost of DAC. The IEA conducted a study for different regions and found that with a carbon tax, the levelized cost of DAC could fall well below 100 \$/ton. For DAC to make a markable impact in the carbon removal pathway, it must reach Gt scale of CO₂ removal at 100 \$/ton [6]. The complete study for the different regions with and without carbon taxes can be found in Appendix B. It is hard to predict the influence of the CO₂ tax in the future. The “World Energy Outlook” finds the predicted price of CO₂ emitted from electricity generation, industry, and energy production to increase significantly. The price is assumed to rise to 40-135 \$/tCO₂ in 2030 and reach over 200 \$/tCO₂ in 2050 in the NZE scenario [62].

2.5.6 CO₂ Storage and Utilization

The Intergovernmental Panel on Climate Change sixth assessment report has recognized CO₂ utilization as a key mitigation technology to avoid and reduce fossil carbon emissions while sustaining a vital supply chain [4]. As the world moves toward a less carbon-dependent society, some sectors are hard to abate, and the CO₂ footprint could be lowered using recycled CO₂ [63]. An overview of the different ways to utilize CO₂ is illustrated in Figure 2.10. The IEA finds the future scale of CO₂ to be uncertain. However, a high-level screening of different pathways for CO₂ utilization shows that using CO₂ to produce fuels has the largest potential to have a meaningful impact due to the vast market size, and will be described further in Section 2.7 [64].

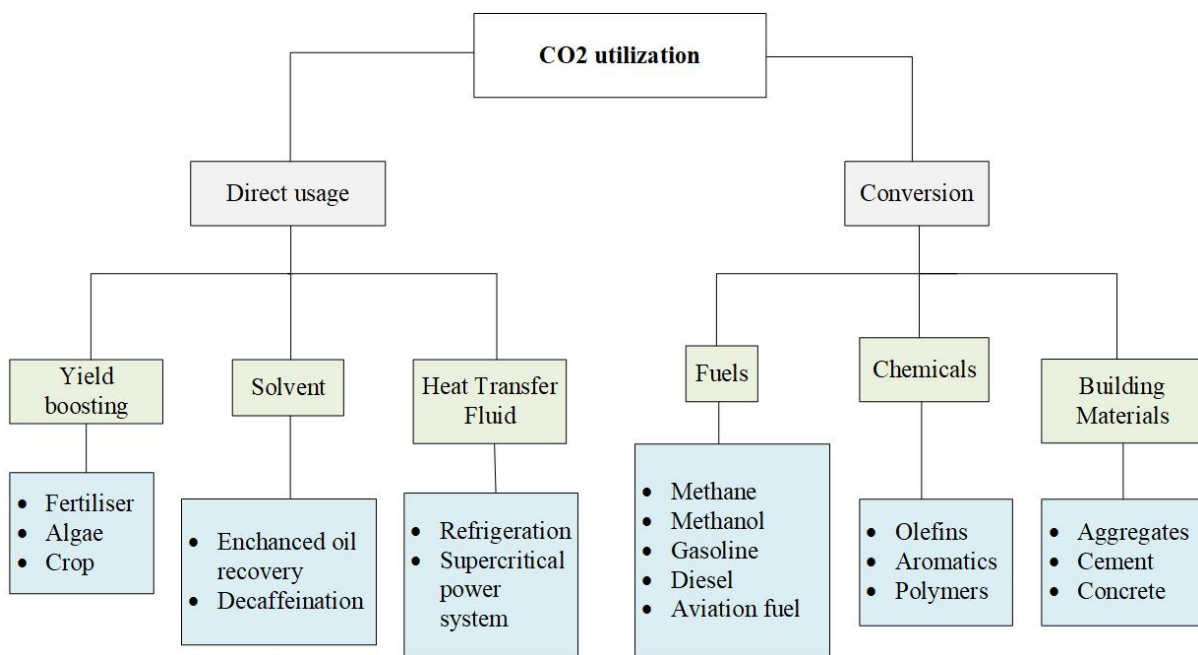


Figure 2.10: Pathways for CO₂ utilization [64].

Large amounts of captured CO₂ can be transported in a dense phase (supercritical form at pressure and temperature above 74 bar and 31 °C, respectively) by pipelines or by refrigerating CO₂ to a liquid phase for shipping, truck, or rail transport. Storage and injections of CO₂ into geological formations require a high CO₂ pressure (100-300 bar). This step increases the operating cost due to the higher energy needed for the compression step. The energy provided must have a low carbon footprint to avoid positive net emission of CO₂. Both storage and selling the CO₂ for further usage would require some sort of compression. Compression with a multi-stage inter-cooled process is a well-known approach that is widely used in industrial applications.[65]

2.5.7 Commercial Pathways to DAC

Today, Carbon Engineering, Climeworks, and Global Thermostat are leading the commercialization of DAC technology. The IEA reported a number of 27 commercial DAC plants worldwide

in July 2023 [55]. Some of the plants that were operational in 2022 are presented in Table 2.6, showing that Climeworks has the most operating plants by 2022. Other smaller companies are developing and commercializing their technology (TRL <6) for industrial purposes [6].

Table 2.6: 13 of the 27 DAC plants operation worldwide [6]

Company	Country	CO₂ storage or usage	Start-up year	Capture capacity (tCO₂/y)
Global Thermostat	United States	Unknown	2010	500
Global Thermostat	United States	Unknown	2013	1 000
Climeworks	Germany	Use	2015	1
Carbon Eng.	Canada	Use	2015	Up to 365
Climeworks	Switzerland	Use	2016	50
Climeworks	Switzerland	Use	2017	900
Climeworks	Iceland	Storage	2017	50
Climeworks	Switzerland	Use	2018	600
Climeworks	Italy	Use	2018	150
Climeworks	Germany	Use	2019	3
Climeworks	Germany	Use	2019	50
Climeworks	Germany	Use	2020	50
Climeworks	Iceland	Storage	2021	4 000

Carbon Engineering

Carbon Engineering, a Canadian company founded in 2009, is the first commercial company to use the L-DAC technology. The company is privately owned and funded by commitments or investments from private operators. In 2015, they constructed their first pilot-scale DAC plant and are building the world’s largest DAC plant, scheduled for operation in 2024. Carbon Engineering has initiated an air-to-fuel plant that is supposed to become operational in 2026, combining DAC with hydrogen production to produce near carbon-neutral synthetic fuel.[6, 11]

Climeworks

Climeworks was founded in 2009 in Switzerland, and by 2013, they had developed the first working prototype of their S-DAC technology. Climeworks applies a filter made of special cellulose fiber, supported by amines in solid form, and has a regeneration temperature of 100 °C. Six years later, they started providing their technology and offered carbon removal to customers. Climeworks has set a climate goal to remove 225 MtCO₂ from the atmosphere by 2025 [6]. The company has announced the construction of its largest plant, Mammoth (capture capacity up to 36,000 tCO₂/year), which should become operational by 2024. By 2030, Climeworks estimates the cost of their technology will decline to around 300 \$/ton, and be around 200 \$/ton in the middle of the next decade [11].

Global Thermostat

Global Thermostat is located in the U.S and was founded in 2010. Their technology is based on S-DAC with an amino-polymer adsorbent. The regeneration process occurs at temperatures between 85-95 C°. Currently, they have two pilot plants with the capacity to capture a total of approximately 1500 tCO₂/year. They have delivered DAC units to a pilot plant in Chile with a capacity of 2000 tCO₂/year to produce synthetic gasoline. This plant has yet to start production [6]. In 2021, the U.S. Department of Energy granted funding for Global Thermostat’s work to develop the design for an S-DAC plant in Colorado with an annual capacity of 100 000 tCO₂ [11].

2.5.8 Nuclear Power Plants Coupled with DAC

Studies have recently been carried out to investigate the possibility of linking nuclear power to DAC technology. In the report “Assessment of Nuclear Energy to Support Negative Emission Technologies”, both S-DAC and L-DAC are found to be compatible with nuclear power plants. Nuclear power can provide electricity for the DAC air fans, CO₂ compression, and other electrical equipment. For the S-DAC, nuclear power can provide the heat needed in the desorption step in several ways using different reactor technologies. For L-DAC the heat from nuclear power plants can be used to sustain some of the calcination heat in the calciner. Since this step requires temperatures around 900 °C, there will be a need for some additional heating for the regeneration.[11]

Several nations and companies are investigating nuclear power plants combined with DAC technology. Constellation Energy, the largest nuclear power operator in the U.S, announced in 2022 that they won a grant to determine the feasibility of combining a nuclear plant in northern Illinois with Carbon Engineering’s DAC technology. The study aims to capture 250 000 tCO₂/y from the air, with a total funding of 3.1 M\$. Another project team from Battelle Memorial Institute will conduct a study to deploy an S-DAC system delivered by AirCapture LLC with a nuclear power plant in Columbia, Alabama. The project received total funding of 3.3 M\$.[66]

2.6 Hydrogen Production

The agreement signed on the COP28 had several points emphasizing the role of hydrogen in meeting global energy needs [67]. Hydrogen is a high-density energy source that can tackle various critical energy challenges, and can be produced from energy generated by several energy sources, such as nuclear energy. Hydrogen energy is a secondary energy source, and there are three main ways to produce hydrogen today. The first way is by steam reforming, where methane is reacted with steam to produce hydrogen. Second, hydrogen production by biological processes involves the usage of microorganisms to produce hydrogen from organic material. The third option is electrolysis, where electricity is applied to split H₂O into hydrogen and oxygen. Water electrolysis will be described in detail since this thesis emphasizes the use of a PEM electrolyzer. An overview of hydrogen produced from fossil fuels (grey hydrogen), fossil fuels with CCS (blue hydrogen), and renewable energy (green hydrogen) is illustrated in Figure 2.11.[68]

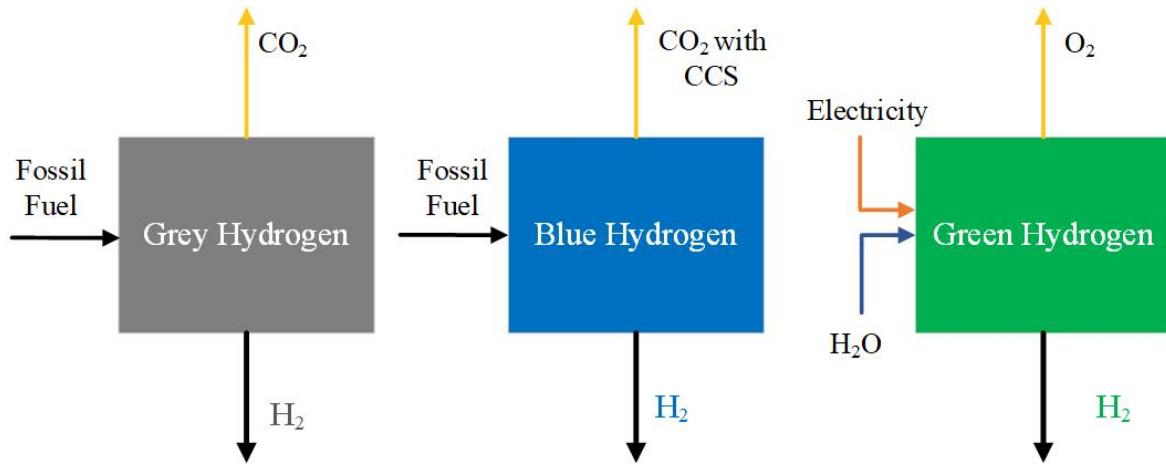


Figure 2.11: Production of grey, blue and green hydrogen [68].

2.6.1 Water Electrolysis

Water electrolysis is a process in which electricity splits water into hydrogen (H_2) and oxygen (O_2). There are three leading technologies for water electrolysis: alkaline electrolyzer, PEM electrolyzer, and solid oxide electrolyzer (SOE). The principle is the same for the three technologies. Water is fed into an electrochemical cell where hydrogen evolves at the negative electrode (cathode) and oxygen forms at the positive electrode (anode) when an electrical potential is applied. Alkaline electrolysis is the most commercially viable technology with TRL at 9 and currently yields H_2 at the lowest cost. PEM is considered a good alternative in terms of cell voltage, high current densities, high temperature, and pressures, resulting in higher efficiencies. SOE operates at very high temperatures, but the technology is still being developed and is not commercially available [69]. An overview of key performance indicators for electrolysis technologies can be seen in Table 2.7. Regarding sustainability and environmental impact, PEM water electrolysis has been considered the most promising technique for hydrogen production from renewable energy sources.[70]

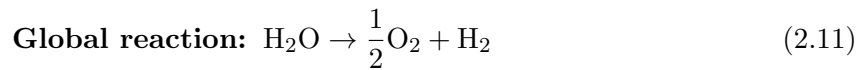
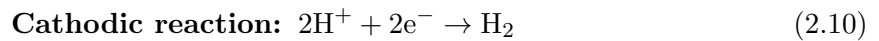
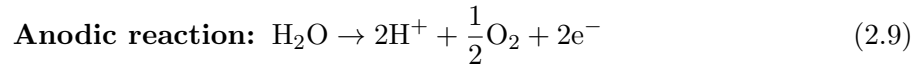
Table 2.7: Key performance indicators of electrolysis technologies [69, 70]

	Alkaline	PEM	SOE	Unit
Temperature	60-90	50-80	600-10000	°C
Pressure	1.05-30	10-200	1-25	bar
Electricity consumption	4.5-6.6	4.2-6.6	3.7-3.9	kWh/m ³ H ₂
Capital cost	800-1500	900-2200	>2000	euro/kW
TRL	9	5-7	3-5	-

Due to the economic aspect, only 4% of hydrogen supplied to industrial processes is produced from water splitting [70]. However, hydrogen from electrolysis, mainly produced from renewable and nuclear sources, is considered to play a significant role in the NZE scenario [71]. Numbers presented by the IEA indicate that the production from electrolyzers in 2023 is expected to be 2 884 MW, equaling a 19% rise from the year before. To be on track for the NZE by 2050, the global capacity from electrolysis should reach 560 000 MW in 2030 [72].

2.6.2 PEM Electrolysis

In the PEM water electrolyzer, the cathode and anode are separated by a membrane called Nafion, with a thickness below 0.2 mm. At the anode, water is oxidized to oxygen (O_2), creating electrons (e^-) and protons (H^+). The protons are transported across the membrane to the cathode side, where the protons react with electrons to produce hydrogen. The electrons are transported through the external power circuit, creating a cell voltage, which is the driving force for the electrolysis cell. A simplified illustration of a PEM electrolyzer can be seen in Figure 2.12. The anode, cathode, and overall reactions are presented below.[70]



The catalyst at the anode is typically iridium, which can withstand a corrosive environment due to high overpotentials. The cathode has a platinum-based catalyst. The PEM electrolyzer has a high proton conductivity, high efficiency (large range reported in the literature from 50% up to 90%), and high-pressure operations. In addition, gaseous products have a high purity, which requires less after-treatment. The technology is currently benefiting from research and development in order to significantly accelerate the massive scale-up needed to reach NZE capacities.[70]

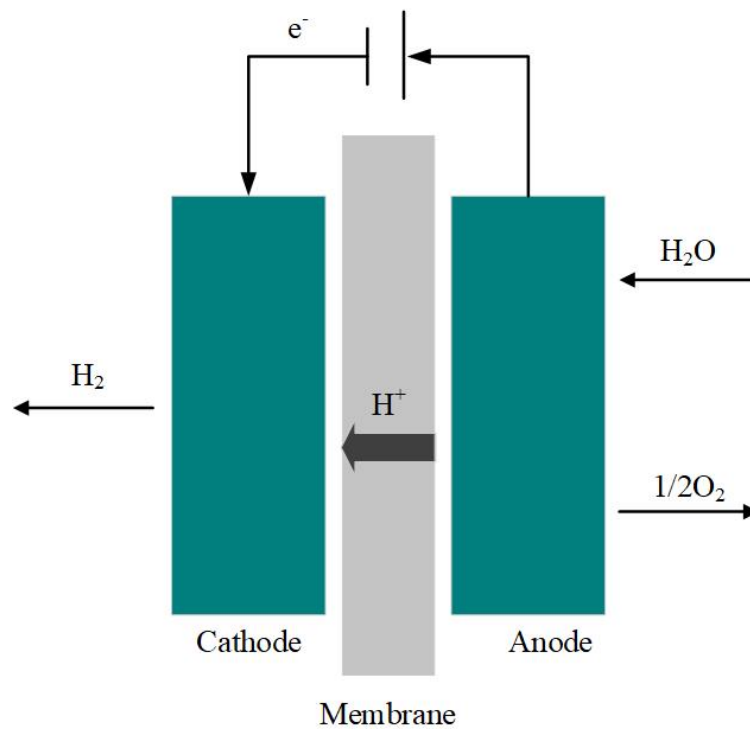


Figure 2.12: Simplified illustration of PEM electrolyzer [70].

To further develop the performance and raise the efficiency of the PEM electrolyzer in terms of activation over-potentials and electrode kinetics, the operating temperatures can be elevated above 100 °C. This technology is attractive for higher hydrogen production efficiency since higher temperature operation of the electrolyzer increases the ionic conductivity and decreases the activation over-potential of the anode and cathode. This could lower the overall voltage of the cell needed for splitting water. When the cell's temperature is elevated, the Gibbs free energy decreases, resulting in less electricity needed for water splitting [73]. Some of the equations used in the development of the PEM cell used in this thesis are described below.

The reversible voltage for a PEM cell, V_{rev} , also called the open circuit voltage, is based on the Nernst equation and is presented in equation 2.12. Where H is enthalpy, T is temperature, S is entropy, R is the gas constant, F is the Faradays constant, and P is partial pressure.[12]

$$V_{rev} = \frac{\Delta H - T\Delta S + RT\ln\left(P_{H_2}P_{O_2}^{1/2}\right)}{2F} \quad (2.12)$$

The PEM cell voltage, V_{cell} , can be predicted by adding the overpotentials occurring in the cell to the open circuit voltage, V_{oc} . These voltage losses are defined as the electrode's activation energy losses, $V_{act,anode}$ and $V_{act,cathode}$, ohmic losses, V_{ohm} and concentration losses, V_{cons} . The expression for the cell's voltage is derived in equation 2.13.[12]

$$V_{cell} = V_{oc} + V_{act,anode} + V_{act,cathode} + V_{ohm} + V_{cons} \quad (2.13)$$

The correlation between current, j, and voltage, V, in an electrochemical system, is described in equation 2.14 and is used to determine the voltage losses due to activation overpotentials. α is the charge transfer coefficient, n_e is the number of electrons, j_0 is the exchange current density, and T and R are explained above.[12]

$$j = j_0 \left(\exp\left(\frac{\alpha n_e F V_{act}}{RT}\right) + \exp\left(-\frac{(1-\alpha)n_e F V_{act}}{RT}\right) \right) \quad (2.14)$$

The ohmic loss, V_{ohm} , is derived from ohms law and is presented in equation 2.15. The loss is mainly due to the ionic resistance, R_{ion} of the membrane.[12]

$$V_{ohm} = R_{ion} \cdot j \quad (2.15)$$

The concentration overpotential, V_c , comes from the concentration polarization due to the applied electric current. The losses can be ignored when the current density drops under 1.6 A/cm² [12]. This loss will not be described further since the PEM electrolyzer included in this work operates below 1.6 A/cm².

2.6.3 Efficiency

The efficiency, η , of an electrolyzer can be calculated based on the LHV of H_2 , the mass flow of hydrogen, \dot{m}_{H_2} , and the electricity supplied to the PEM stack, W_{PEM} , and is derived below.[70]

$$\eta = \frac{LHV_{H_2} \cdot \dot{m}_{H_2}}{W_{PEM}} \quad (2.16)$$

2.6.4 Cost

One of the major challenges in hydrogen production is its respective cost. The cost for different hydrogen production pathways differs widely. Today, the cheapest option is to produce hydrogen from fossil fuels. Depending on the gas price, the levelized costs of grey hydrogen typically ranges from 0.5-1.7 \$/kg. The levelized cost of blue hydrogen, increases the production cost by 1-2 \$/kg. Producing green hydrogen from low-carbon electricity with electrolysis elevates costs ranging between 3-8 \$/kg [9]. The high price is mainly due to the cost of electricity and the electrolyzer module [10]. Another costly aspect of hydrogen is the need for more infrastructure for distribution and storage. The most common way of transporting hydrogen is in gaseous form, needing costly specialized equipment to ensure safety [68].

The cost of green hydrogen has the potential to be substantially reduced through technological innovation and increased deployment. The potential to reduce cost is highlighted in the NZE scenario. The cost for green hydrogen have the potential to reach levels of 1.3-3.5 \$/kg, where the lowest values would be obtained in regions with abundant renewable resources.[10]

The potential connection between nuclear power and hydrogen production was discussed already in 1973 [27]. The IEA has investigated the competitiveness of hydrogen produced by electrolysis from nuclear power plants with other hydrogen production sources. The study points out that nuclear-powered hydrogen production has a long way to go to achieve the same cost estimations as renewables and fossil fuels with CCU. Figure 2.13 illustrates that nuclear investment costs need to fall below 2000 \$/kW_e and the gas and coal prices to remain above 12 \$/mmBtu and 125 \$/tonne for nuclear to become competitive [7].

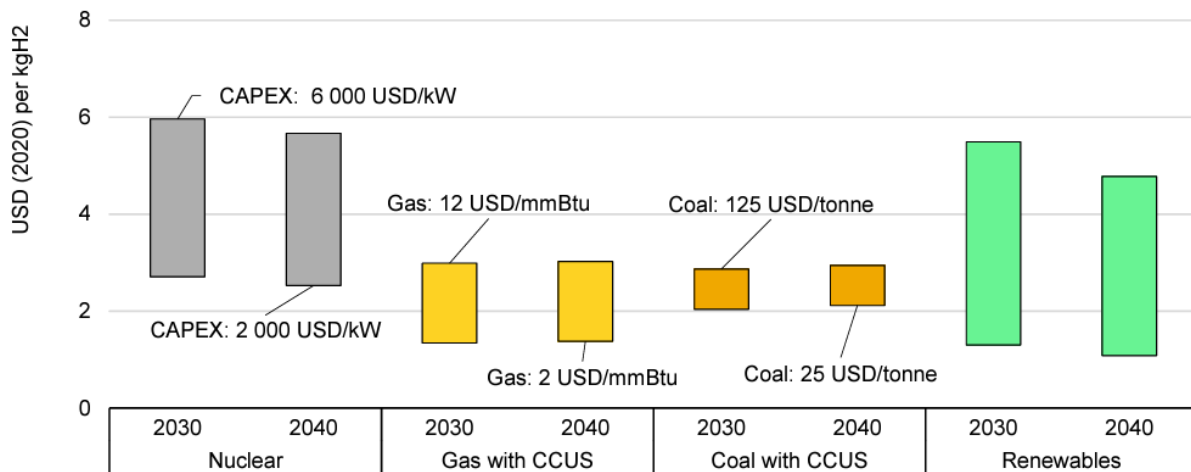


Figure 2.13: Levelized cost of hydrogen for different energy sources [7].

2.7 Synthetic Fuels

Synthetic fuels are considered as a good fit for CO₂ and H₂ utilization. Achieving the goal of NZE by 2050 requires low-emission fuels in the energy sectors where electricity is neither easy nor economically feasible. These sectors are typically long-distance transportation, including trucks, aviation, and shipping. Several synthetic fuels can be integrated into some of the existing infrastructure and some of the engines that currently run on fossil fuels. Synthetic fuels can also replace fossil fuels in other applications, such as electricity generation and heating.[3]

Synthetic fuels are chemically designed, aiming to have the same physical and chemical properties as fossil fuels. Synthetic fuels can be produced from renewable or non-renewable sources. E-fuels are a class of synthetic fuels produced with electricity from renewable/low-carbon energy. The typical feedstock used for chemical conversion to e-fuels is biomass, CO₂, and water. Hydrogen-based fuels are a group within e-fuels recognized as a pathway for CO₂ reduction. Hydrogen is the most abundant element in the universe. When burned, it produces heat and water as byproducts, meaning no harmful greenhouse gases or other pollutants. Using fuels created from captured CO₂ from the atmosphere can offset the CO₂ emissions associated with the end-usage of the fuel.[3, 68]

Today, low-emission fuels account for 1% of the global energy demand. This share is projected to rise, and the total need for liquid biofuels and hydrogen-based fuels as transportation fuels achieving NZE by 2050 are 14% and 28%, respectively. Significant efforts are needed before synthetic fuels can be developed on a commercially large scale. Figure 2.14 shows the distribution of hydrogen produced in different industries for the APS and NZE scenarios. The production of synthetic fuels is emerging in the NZE scenario. For the APS, the production of synthetic fuels will be seen as a minor pathway for hydrogen utilization [3]. There exist multiple synthetic fuels, but the most promising are methanol, liquefied natural gas (LNG), and ammonia [68].

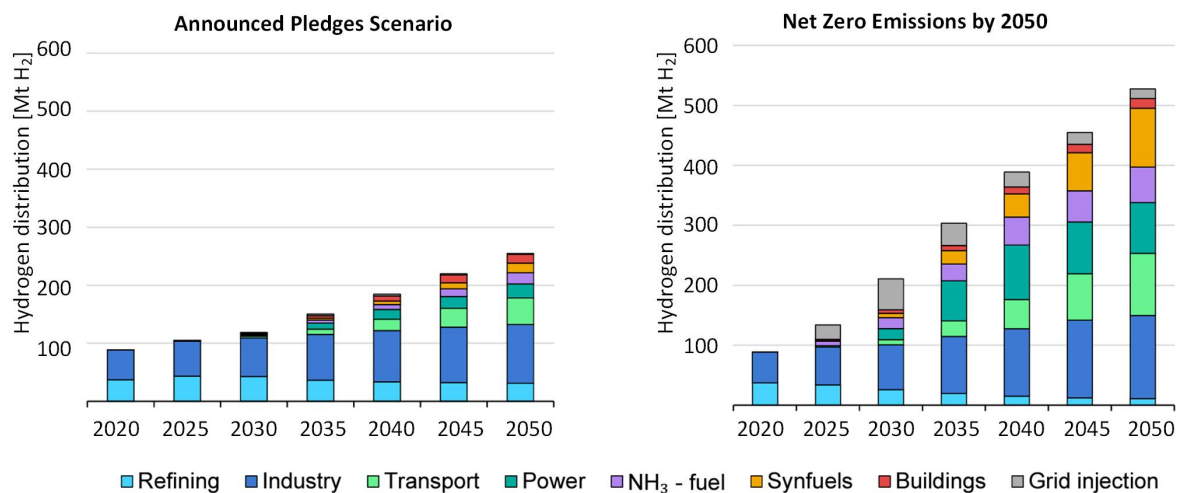


Figure 2.14: Future utilization of hydrogen in different industries for APS and NZE by 2050 [3]. The figure has been modified.

2.7.1 Power to Liquid

The process of transforming synthetic fuels into liquids from electricity is known as Power to Liquid (PtL). The major difference between PtL fuels and conventional synthetic fuels is the source of the starting material. PtL is produced from renewable electricity, meaning no additional CO₂ emissions during their production, making them favorable compared to traditional fossil fuels. Today, several types of PtL fuels are developed and tested. This thesis has chosen methanol as the pathway for H₂ and CO₂ utilization and will be described further in detail in the next sections.[68]

The commercial adoption of e-fuels is still in its early stages. However, the number of companies and organizations implementing e-fuels is rising. Norsk e-Fuel is a Norwegian company aiming to produce e-fuels based on the PtL technology, planning on having its first commercialized facility in production by 2026 in Mosjøen. They have stated that their technology will utilize renewable energy, water, biogenic CO₂, and CO₂ from DAC. The aviation company "Norwegian" has announced a collaboration with Norsk e-Fuel, contributing with over 50 MNOK with plans to buy around 20% of their future need for renewable fuel from the company.[74, 75]

2.7.2 Methanol

Methanol (MeOH), also called wood spirit, is an organic compound with the chemical formula, CH₃OH. Methanol serves a broad specter of applications, mainly serving the chemical industry as a base material for a wide range of chemical products. It is also used as a fuel or fuel additive. It is the simplest alcohol with the highest hydrogen content and lowest carbon content compared to other liquid fuels [76]. At atmospheric pressure, methanol is a flammable liquid between -93 °C and 65 °C. Methanol is considered a good fit for hydrogen utilization and has low toxicity and low-chain-alcohols [77].

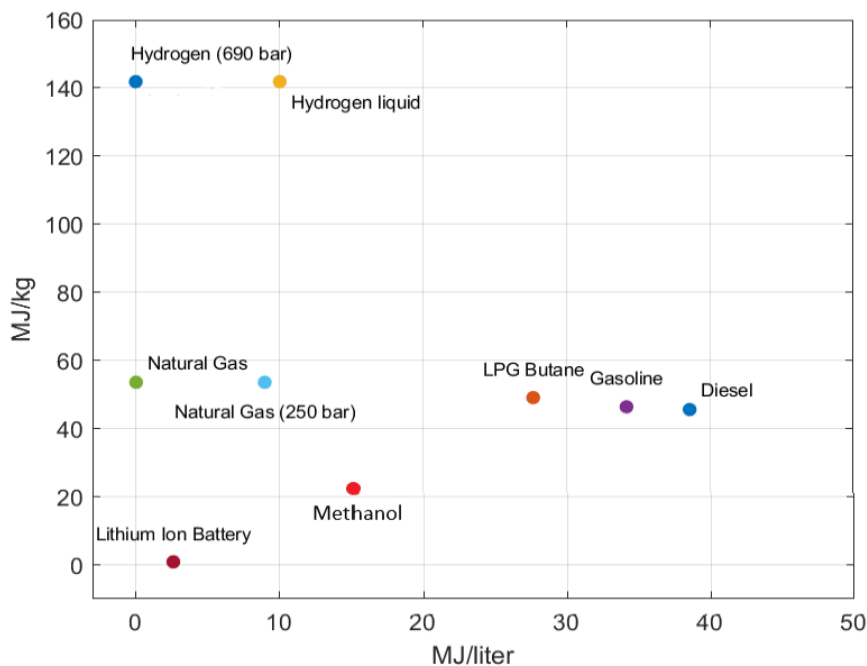


Figure 2.15: Energy density for different energy sources [78]. The figure has been modified.

Methanol has been seen as suitable for a wide range of shipping applications, including cruise ships, inland waterway bulk transport vessels, short-sea container ships, ferries, short-sea tankers, deep-sea container vessels, and general cargo vessels. In addition, methanol has a higher energy content compared to other shipping fuels such as hydrogen, LNG, and ammonia. However, the gravimetric and volumetric energy densities of methanol have less than half the energy density compared to diesel [77, 79]. Figure 2.15 shows the gravimetric energy density (MJ/kg) and the volumetric energy density (MJ/L) of methanol and other commonly used fuels.

2.7.3 Cost

Synthetic fuels are currently costly, and significant efforts are needed before synthetic fuels can be commercialized and mass-produced in order to compete with fossil-based fuels. One of the main reasons for the high cost is due to renewable electricity being expensive. Also, many countries that rely on fossil fuels will require a cost increase in new infrastructure employing synthetic fuels. As a result of increased initiatives and investments in renewable energy, synthetic fuel prices are expected to drop within the following decades [68]. Martin et al. developed a holistic cost model applied to Norway to investigate the levelized costs of renewable fuels. E-fuels were the type of synthetic fuel that was expected to decrease the most until 2050, with 41% to 68% depending on what type of electricity was provided for hydrogen production and the cost of CO₂ [80].

2.8 Methanol Synthesis

Methanol synthesis is a well-known process and is utilized for methanol production worldwide. Methanol can be produced from multiple feedstocks containing carbon, such as natural gas, biomass, coal, and CO₂ [9, 68]. The majority of methanol is produced from natural gas (around 65%), followed by coal (around 35%). As seen in Figure 2.16, methanol produced from biomass and renewable sources is below 1%. The production and use of methanol results in about 165 MtCO₂/y, or about 0.3% of the world's total carbon emissions, according to a report by the International Methanol Producers and Consumers Association published in 2022 [81].

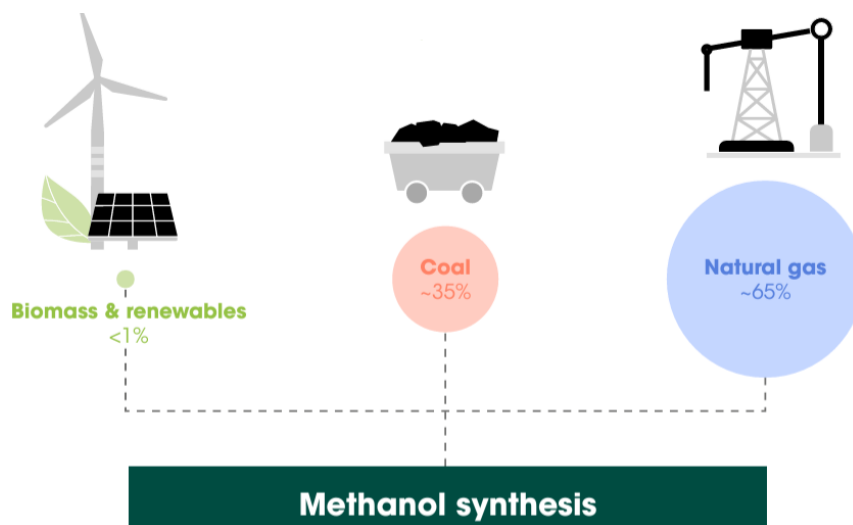


Figure 2.16: Feedstocks of methanol synthesis [9].

The traditional route for industrial methanol production comprises three steps. The first step is producing synthesis gas (syngas) at the desired pressure and temperature to fit the synthesis loop. Then, the syngas is converted into methanol in the reactor. The reaction is exothermic, and cooling systems remove the heat to prevent the reaction from escalating [68]. In the final step, methanol is purified in the distillation column. The steps are illustrated in the simplified flowsheet of the methanol production in Figure 2.17 [76]. The conversion of syngas into crude methanol takes place at pressure ranges from 50-100 bar and temperature between 200-300 °C. The high temperature and pressures increase the reaction rate and the yield of methanol. A catalyst, typically Cu/ZnO/Al₂O₃, is present in methanol production to enhance methanol quality. The syngas mixture consists of H₂, CO, and CO₂ and is mainly produced by steam reforming and auto-thermal reforming [9, 76].

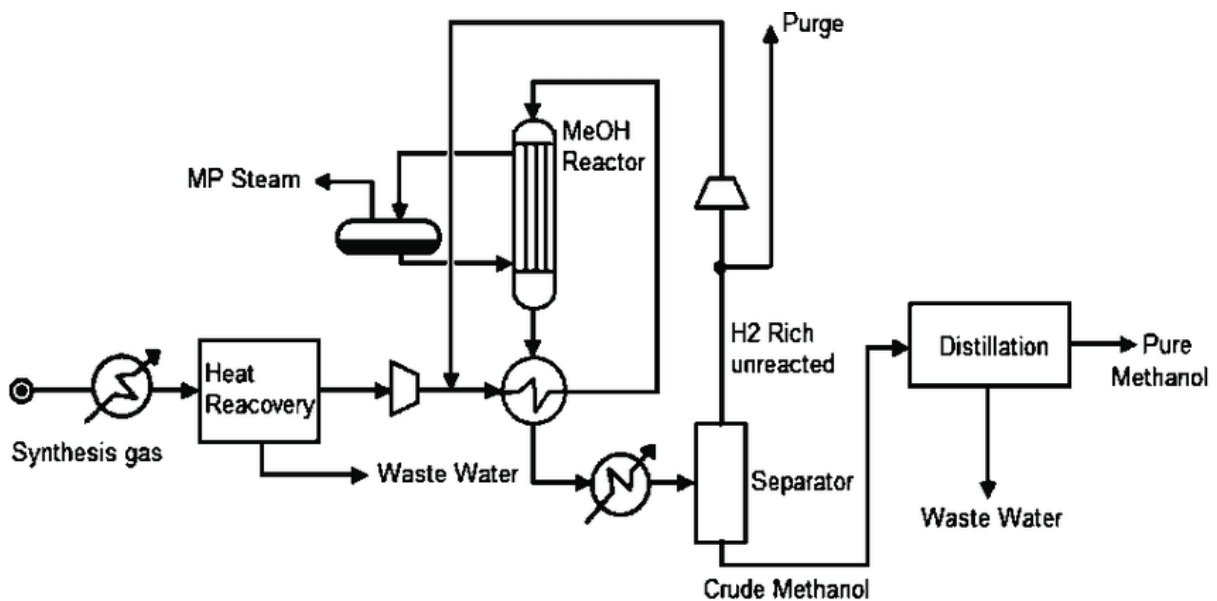


Figure 2.17: Traditional MeOH plant [76].

2.8.1 Green Methanol

Green methanol, also called renewable methanol, is produced with low or zero CO₂ emissions related to the process. Green methanol can be divided into two categories: bio-methanol, which is produced from sustainable biomass, and e-methanol, which is produced from CO₂, and renewable hydrogen. The technology for e-methanol synthesis is almost identical to the conventional methanol synthesis, which is a mature technology with a TRL of 8-9 [9]. CO₂ is recognized as a promising feedstock for methanol production because it is inexpensive, abundant, non-toxic, and relatively safe to use. Furthermore, CO₂ can easily be stored, transported, and fed into existing syngas conversion plants without comprehensive adjustments [77]. CO₂-derived methanol can provide climate benefits, but the use of low-carbon energy for their production is critical. Studies show that, in a best-case scenario, emissions can be reduced by 74% to 93% for green methanol compared to other conventional methanol production routes [64]. Currently, there are few commercialized green methanol production plants. However, many initiatives and

projects are planned to begin operation in the next few years [82]. An illustration of different pathways for the production of grey, blue, and green methanol can be seen in Figure 2.18 [9].

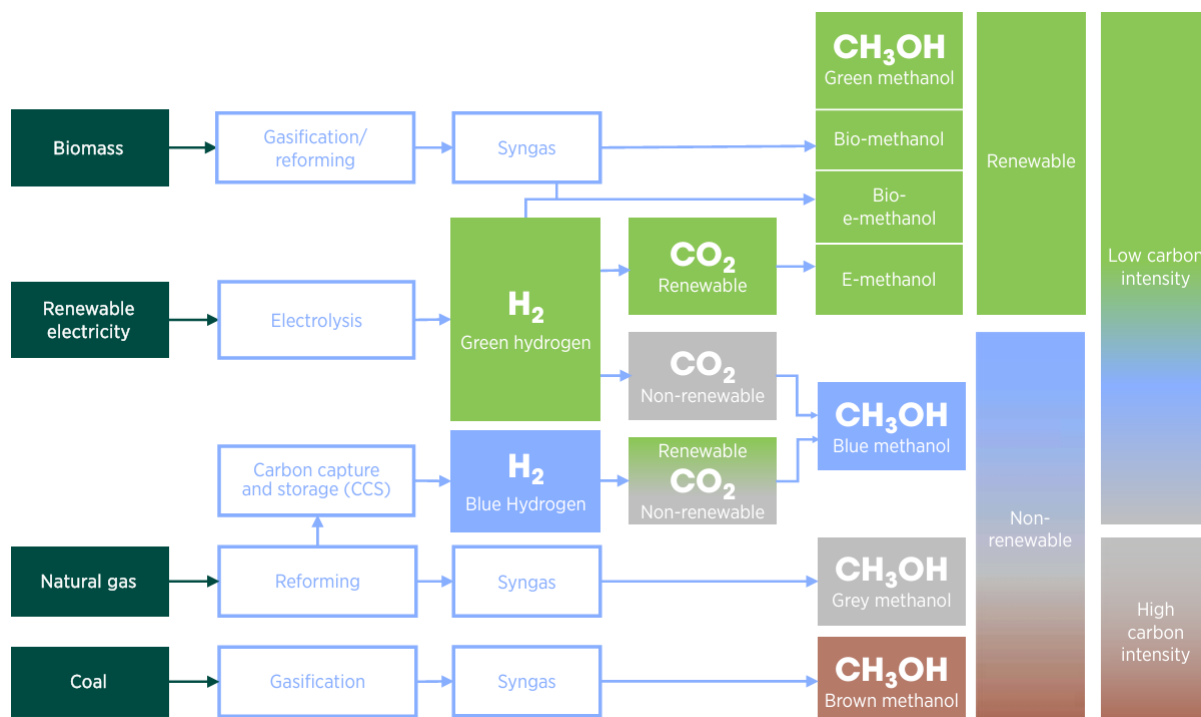


Figure 2.18: Different pathways for methanol production [9].

The Methanol Institute (MI) has made projections that the production of renewable methanol will become more prominent in the coming years, tracing over 80 renewable methanol projects around the world. Based on current operating plants and announced plants, the running sum of capacity for e-methanol and bio-methanol will rise from approximately 0.4 MtMeOH/y to slightly above 8 MtMeOH/y in 2027. With economic initiatives and substitutions, as well as advancements in technology, the global capacity is expected to rise from between 5 000-10 000 MtMeOH/y to 50 000-250 000 MtMeOH/yr.[82]

2.8.2 Green Methanol Synthesis

There are two ways to convert CO_2 to methanol. One pathway is conducting a two-step process where CO_2 is reduced to carbon monoxide (CO) and then reacts with H_2 to make methanol. The chemical reaction of the two-step process is shown in equation 2.17. The second pathway is directly hydrogenating CO_2 over a heterogeneous catalyst in a one-step process. The chemical reaction or direct hydrogenation can be seen in equation 2.18. Both technologies can use CO_2 from different sources, such as point source capture and DAC. The CO_2 required to produce the syngas needs to be relatively pure and may need some sort of purification before the methanol synthesis. DAC is favorable in this way due to the purity of CO_2 as described in Section 2.5.1. Of the two bespoke approaches, reacting hydrogen produced by electrolysis of water with CO_2 in a direct hydrogenation is the pathway closest to the market.[9, 68]



For syngas with a high CO/CO₂ ratio, optimal operation and maximal conversion for the synthesis loop are achieved by feeding the reactants as close to the stoichiometric ratio of 2 as possible. This is defined in equation 2.19.[12, 83, 84]

$$M = \frac{H_2 - \text{CO}_2}{\text{CO} - \text{CO}_2} \approx 2 \quad (2.19)$$

To reduce the ratio shown in equation 2.19, the water gas shift (WGS) reaction can be employed, shown in equation 2.20. This typically increases the concentration of H₂ and reduces the amount of CO by reforming the mixture with steam. If the ratio needs to be increased, the reversed-WGS reaction could be utilized to convert CO₂ into CO.[68]



2.8.3 Efficiency

The efficiency, η , of a methanol plant producing green methanol is derived in equation 2.21. Where \dot{m}_{MeOH} , is the mass flow of methanol, LHV_{MeOH} is the LHV for methanol. W_{total} is the total of electricity put into the production of syngas and the methanol synthesis process.

$$\eta = \frac{\dot{m}_{\text{MeOH}} \cdot \text{LHV}_{\text{MeOH}}}{W_{\text{total}}} \quad (2.21)$$

2.8.4 Cost

The traditional route of methanol production has one of the lowest costs compared to other fuels. A report made by the International Renewable Energy Agency (IRENA) in cooperation with the MI found that methanol production from fossil fuels ranges between 100-250 \$/ton. Assuming CO₂ obtained from DAC at price levels of 300-600 \$/ton, this would result in an e-methanol production cost of 1 200-2 400 \$/ton. If renewable electricity prices decrease as expected, the e-methanol cost could drop to 250-630 \$/ton.[9]

A detailed study carried out by the EIA indicated a near-term e-methanol production cost ranging from 750-1300 \$/ton. Future projections show that the cost is expected to drop to 346-441 \$/ton. This fall is mainly due to the decrease in electricity price that accounts for 40-70% of the production cost. Political aspects in the light of the new European policies can also be seen as a contribution to lowering the price.[83]

2.8.5 Demonstration and Commercial Green Methanol Projects

The CO₂ hydrogenation technology has successfully been demonstrated for the e-methanol production plant in George Olah Renewable Methanol Plant in Iceland. The plant is owned by Carbon Recycling International (CRI) and has been operating since 2012, producing 4 000 tMeOH/year. The plant uses 5 500 tonnes of recycled CO₂ each year for MeOH production [83]. Moreover, a new commercial-scale plant in China (Henan province), based on the CRI technology, was commissioned at the end of 2022. The facility has a capacity of capturing 160 000 tCO₂/y, which results in a production of 110 000 tMeOH/y. CRI is currently developing another plant in China that is expected to begin operation before 2024.[85]

A project in Norway (Finnfjord) is planned to produce 80 000 tMeOH/y of e-methanol. The plant is one of the largest producers of ferrosilicon in Europe. This industry generates a significant amount of CO₂, and CCS is planned to be employed for the flue gas emitted from the plant to mitigate emissions. Hydrogen is indicated to be produced through electrolysis. “Innovation Norway” has decided to support the new facility with 100 MNOK.[81, 86]

Spain is currently investigating the establishment of large-scale green methanol production plants. At the COP28 the two companies, Cepsa and C2X announced that they are joining forces to create the largest green methanol plant in Europa. The plant will first aim to produce 300 000 tMeOH/year. Up until 2027, the production will be ramped up to 1 MtMeOH/year. In the third construction phase, the production will be increased up to 2 MtMeOH/year in 2030.[81]

3 Method

A techno-economic study was carried out to make an in-depth analysis of the performance of the reference and advanced plant, providing a fair foundation for comparison. UniSim Design R492 was used for the technical assessment and the standardized economic assessment (SEA) tool for the economic evaluation. The mentioned programs will be presented in section 3.1.1 and 3.2.1, respectively. A graphical overview of the methodology applied in the work of this thesis is illustrated in Figure 3.1.

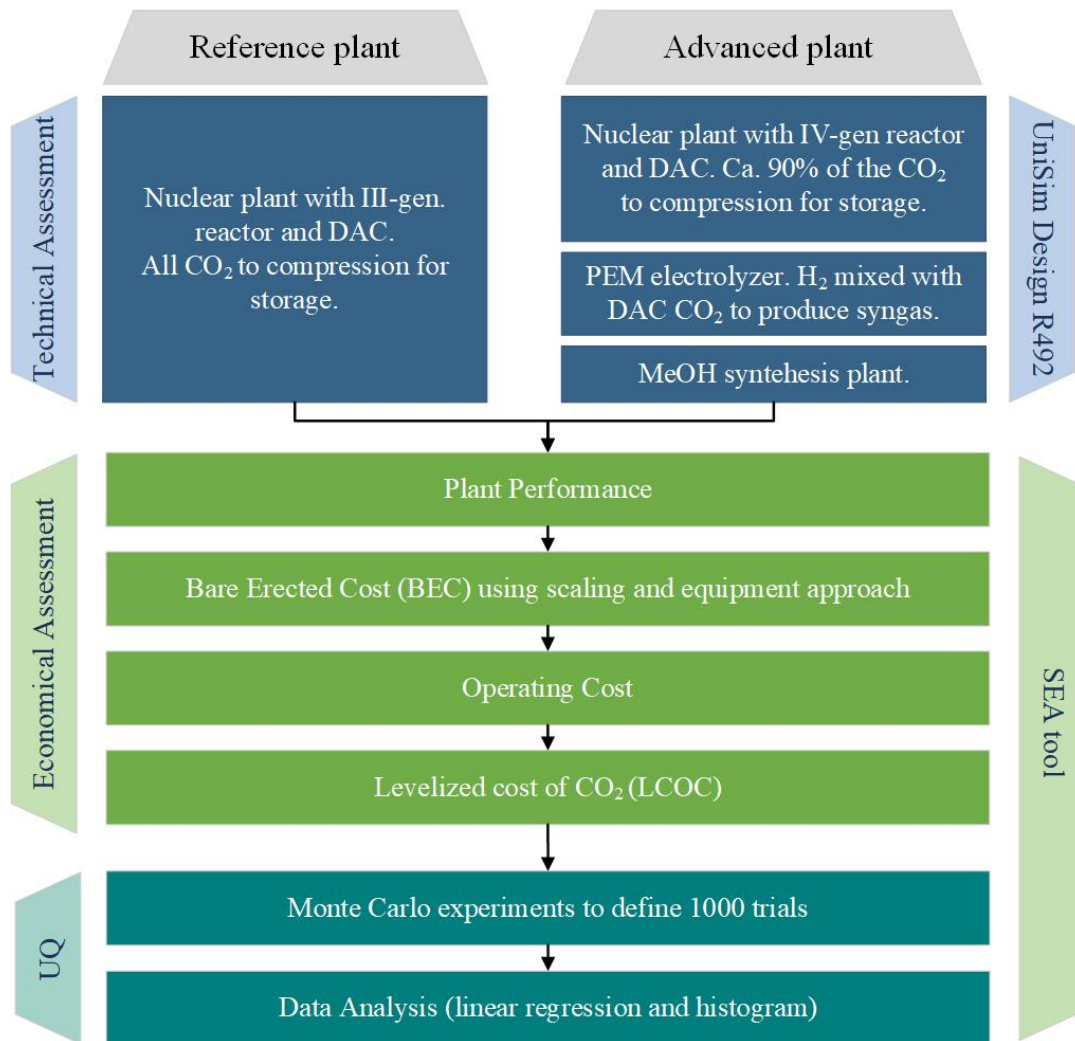


Figure 3.1: Graphical overview for the methodology of the technical and economical assessment.

The technical part of the work includes the model developed by Arnaiz del Pozo for the PEM electrolyzer cell and the methanol synthesis model [12, 13]. The electrolyzer model uses a Scilab code connected with a CAPE-OPEN license to determine the working properties of the PEM model and the hydrogen production capacity. The work has combined all the different activities into one flowsheet to optimize heat and electrical integration. The nuclear power plants have been modeled as a Rankine-reheat cycle. Some changes were made to the PEM model and the methanol synthesis to fit the plants under investigation in this thesis. The changes will be described in detail in the following sections.

The reference plant used a third-generation pressurized water reactor, operating at 300 °C and 85 bar. The plant was designed to be self-sufficient with electricity for DAC and CO₂ compression. Waste heat at 100 °C was used for DAC. The plant aimed to sell CO₂ that was assumed to be stored in boreholes in the ground at 75 bar on-site. Figure 3.2 shows a simplified illustration of the reference plant.

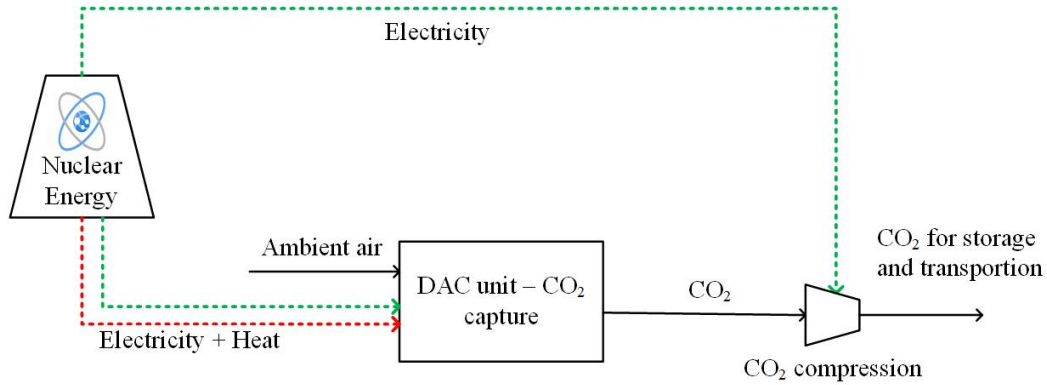


Figure 3.2: Simplified illustration of the reference plant with a nuclear plant, DAC, and CO₂ compression.

The advanced plant employs a fourth-generation pressurized water reactor operating at ultra-supercritical conditions, at 600 °C and 300 bar. The plant was designed to have a significant surplus of electricity for water electrolysis after DAC and CO₂ compression. The DAC process and CO₂ storage are the same as for the reference plant. The plant combined CO₂ from DAC and hydrogen in a direct hydrogenation for methanol production in a methanol synthesis plant. The methanol was assumed to be stored in tanks at the facility, sized to store methanol produced for up to a week. The simplified model of the advanced plant is illustrated in Figure 3.3.

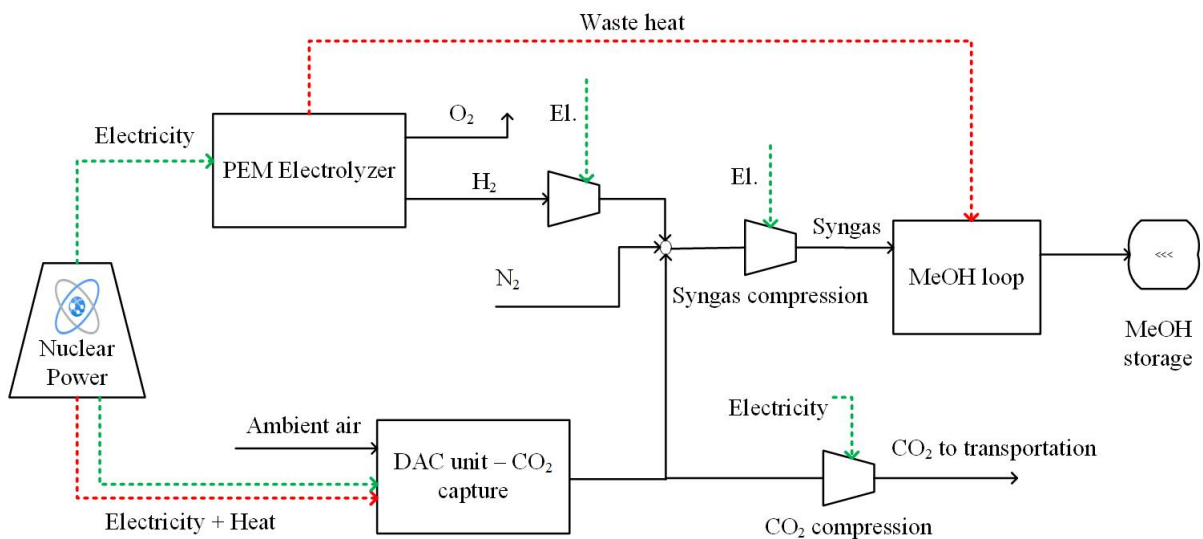


Figure 3.3: Simplified illustration of the advanced plant, with DAC, CO₂ compression, electrolysis, syngas production and green methanol production.

3.1 Technical Assessment

The technical assessment aimed to build the proposed plants that will serve as input parameters for the economic analysis. The following sections describe the methodology for constructing each part of the reference and advanced plant. The main assumptions for the components reoccurring throughout the simulation are described in Table 3.1. The thermodynamic fluid package (FP) was different for the various parts of the plant. The FP was determined based on the operating fluids and the FD thermodynamical properties suited for each part of the plant [87]. ASME Steam was used for the nuclear plant and all water streams in heat exchangers (HE) for cooling purposes. Peng Robinson was employed for the PEM model, syngas production, and CO₂ compression. Lastly, the methanol synthesis model had SRK as FD [12, 13].

Table 3.1: Basic process modelling assumptions

Item	Value	Units
ΔP HE gas	2	%
ΔP HE liquid	0.6	bar
Cooling water inlet	15	°C
Cooling water outlet	25	°C
Cooling water pressure inlet	1.8	bar
ΔP cooling water pump	0.6	bar
Pump adiabatic efficiencies	85	%
Turbine adiabatic efficiencies	85	%

The presented flowsheets in the following sections are produced in Visio. The original UniSim flowsheets can be found in Appendix E.

3.1.1 UniSim Design R492

The technical assessment was carried out in UniSim Design R492. The software allows users to design the intended model and simulate complex calculations in a steady-state environment. In addition, UniSim provides a detailed breakdown of the energy performance and sizing of the plant's equipment [88]. Some crucial UniSim features were used to construct the complex model where every component was connected for the different sub-flowsheets. The use of set, recycle, adjust, and spreadsheet functions has been widely used in the simulation work, allowing for simple mathematical and logical relations within UniSim. The "Logical Unit Operation" guide describes each feature in detail [89].

3.1.2 Reference Nuclear Power Plant

The reference nuclear plant was designed with a third-generation pressurized water reactor. The plant operated with two turbines with a reheat stage, which employs the principle described in Section 2.2.4 for the two-stage Rankine cycle with reheat. The CWT that removes heat from a large nuclear power plant was replaced with the DAC unit. The UniSim simulation simplifies the DAC unit to a black box. This box rejects heat at a temperature of approximately 100 °C,

which corresponds to the heat needed for the chosen DAC technology. The plant’s turbines were designed only to produce enough electricity to cover the electricity consumption of the DAC process and the CO₂ compression stage. The flowsheet of the reference nuclear-powered DAC plant can be seen in Figure 3.4.

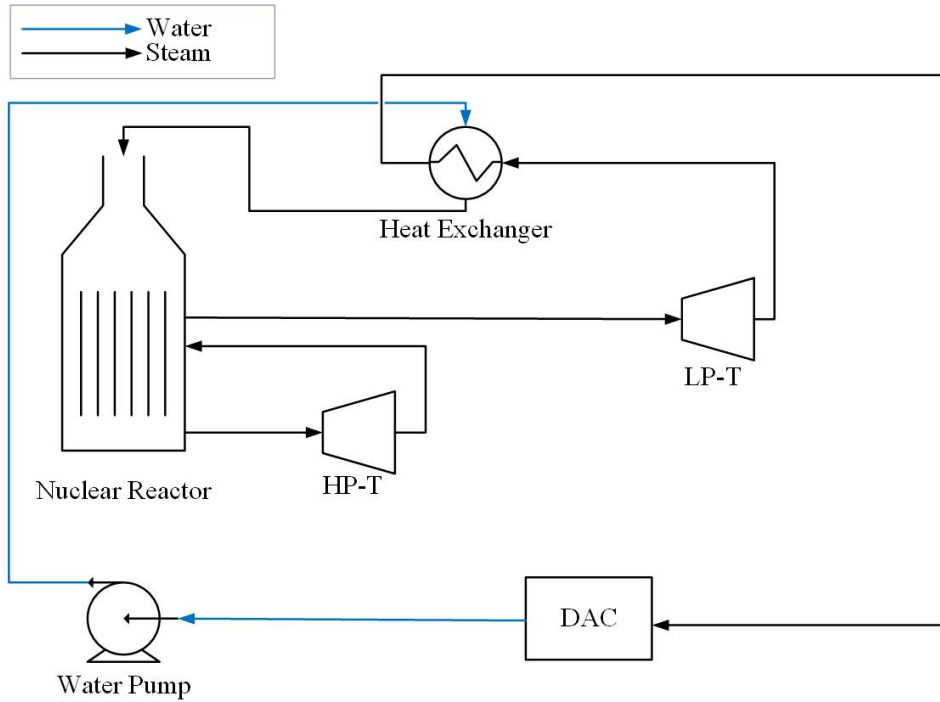


Figure 3.4: Simplified flowsheet of the reference nuclear-powered DAC plant.

H₂O, serving as the working fluid, was heated up to 300 °C and pressurized to 85 bar. The first expansion in the high-pressure turbine (HP-T) reduced the pressure to 35 bar. The H₂O stream was returned to the reactor and reheated to 300 °C. The nuclear reactor and reheater were simplified to two separate heaters in UniSim. The pressure out of the low-pressure turbine (LP-T) was set to 3.9 bar. The stream out of the last turbine holds a significant amount of energy, and an HE was implemented to recorporate the heat. The H₂O stream was further channeled into the DAC unit and rejected heat for regeneration of the sorbent, following the methodology of S-DAC described in Section 2.5.1. The water was pressurized with a pump back into 85 bar before entering the HE for pre-heating. Ultimately, the water enters the nuclear reactor again to undergo another cycle. The main modeling assumptions are described in Table 3.2.

Table 3.2: Process modelling assumptions for the reference nuclear-powered DAC plant

Item	Value	Units
Reactor temperature	300	°C
Reactor pressure	85	bar
Pressure out of HP turbine	35	bar
Pressure out of LP turbine	3.9	bar
Temperature out of DAC unit	99	°C

3.1.3 Advanced Nuclear Power Plant

The advanced nuclear plant was modeled with a fourth-generation pressurized water nuclear reactor. The plant had three turbines: an HP-T, an intermediate pressure turbine (IP-T), and an LP-T. After the expansion of the steam in each turbine, the steam was channeled back into the nuclear reactor to elevate the temperature back to the reactor’s operational temperature, as seen in Figure 3.5. The steam out of the last turbine follows the same principle of recorporation in a HE and DAC heat rejection methodology described above for the reference plant.

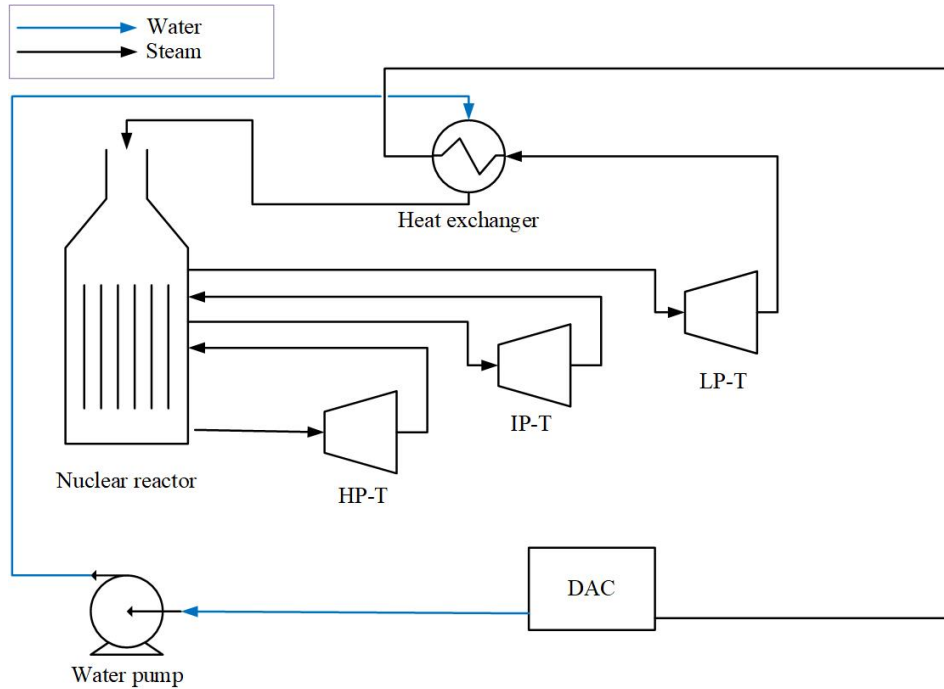


Figure 3.5: Simplified flowsheet of the advanced nuclear-powered DAC plant.

Water was heated up to 600 °C and pressurized with a pump to 300 bar. The first expansion reduced the pressure to 70 bar in the HP-T, before entering the nuclear reactor for reheating. In the IP-T, pressure is reduced to 13.9 bar and then sent to the nuclear reactor for reheating. The final pressure out of the LP-T was set to 2.7 bar for maximal electricity generation. The modeling follows the same assumptions for the nuclear reactor, reheaters, and DAC unit as described in the modeling chapter in Section 3.1.2. The flowsheet of the advanced nuclear-powered DAC plant can be seen in Figure 3.5, and the main modeling assumptions are described in Table 3.3.

Table 3.3: Process modelling assumptions for the advanced nuclear-powered DAC plant

Item	Value	Units
Reactor temperature	600	°C
Reactor pressure	300	bar
Pressure out of HP turbine	70	bar
Pressure out of IP turbine	13.9	bar
Pressure out of LP turbine	2.7	bar
Temperature out of DAC unit	99	°C

3.1.4 Direct Air Capture

The DAC unit was assumed to be a black box and was not modeled in UniSim. In UniSim, the DAC unit was modeled as a cooler rejecting heat for DAC purposes. The captured CO₂ was calculated based on waste heat available from the cooler rejecting heat from the nuclear plant and the energy demand required per tonne CO₂. The heat was the limiting factor for DAC from nuclear energy, as described in Section 2.5.3. The amount of captured CO₂ was calculated by dividing the heat available (calculated by UniSim) by the heat required for DAC per kg CO₂. The energy requirements were based on the energy projections in 2030, since the reported values for 2050 was seen as optimistic. The key performance parameters for the DAC technology can be seen in Table 3.4 and were based on Climeworks technology for S-DAC [5].

Table 3.4: DAC key calculation assumptions

Parameter	Value	Unit
Inlet temperature	Ambient	°C
Operating temperature	99	°C
CO ₂ outlet temperature	20	°C
CO ₂ outlet pressure	0.2	bar
Sorbent	Amine-based	-
Thermal energy demand	5.4	MJ _h /kgCO ₂
Electric energy demand	0.91	MJ _e /kgCO ₂

3.1.5 Nuclear Power Plant with CWT

To isolate the nuclear reactor cost for the economic assessment, an original nuclear plant with a cooling tower was simulated to determine the size of the turbines, pumps, HE, and CWT (instead of the DAC unit). The size of the mentioned equipment will be more significant for an original nuclear plant, as they produce more electricity due to the lower outlet temperature out of the last turbine. The reference and advanced nuclear plant was built with a cooling cycle instead of the DAC unit. The cooling cycle consists of a CWT where heat was rejected by the atmosphere, and a water circulation pump adjusts for the pressure drop in the CWT and ensures water flow. The CWT was modeled as a cooler rejecting heat. The modeling assumptions for the CWT for the reference and advanced plant can be found in Table 3.5 and 3.6.

Table 3.5: Cooling water cycle modelling assumptions for the reference plant

Item	Value	Units
Temperature out of cooling cycle	20	°C
Temperature into cooling cycle	29	°C
Temperature into CWT	23	°C
Temperature out of CWT	15	°C
Pressure into HE	0.04	bar
Pressure into CWT	1	bar

Table 3.6: Cooling water cycle modeling assumptions for the advanced plant

Item	Value	Units
Temperature out of cooling cycle	20	°C
Temperature into cooling cycle	48	°C
Temperature into CWT	25	°C
Temperature out of CWT	15	°C
Pressure into HE	0.39	bar
Pressure into CWT	1	bar

A illustration of the cooling cycle can be seen in Figure 3.6. Since this was a minor part of the work, the total flowsheet was not produced in Visio but can be seen in Figure E.3 and E.1 in Appendix E.

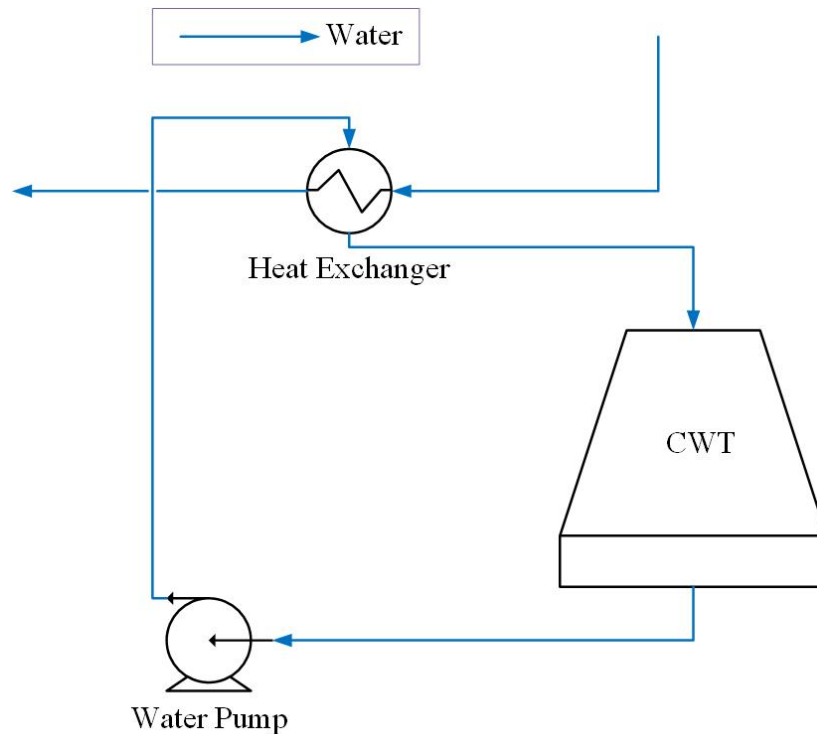


Figure 3.6: Simplified flowsheet of the cooling water cycle.

3.1.6 CO₂ Compression

The compression of CO₂ for storage and transportation purposes was conducted in a multi-stage compression with cooling in between to remove heat generated in the compression steps. The compressors were designed to use the same amount of work for the most energy-efficient compression. Four compressors with a shell-and-tube heat exchanger in between were implemented, with H₂O as the cooling agent. A pump was used to elevate the pressure of the cooling water prior to the HE. The amount of CO₂ for compression was determined based on the DAC capture capacity for both plants. All of the CO₂ from the reference plant was sent to compression. 90.5%

of the CO₂ produced from the advanced plant was sent to compression for storage. The rest of the CO₂ was used for syngas production for the methanol synthesis. The flowsheet of CO₂ compression is presented in Figure 3.7.

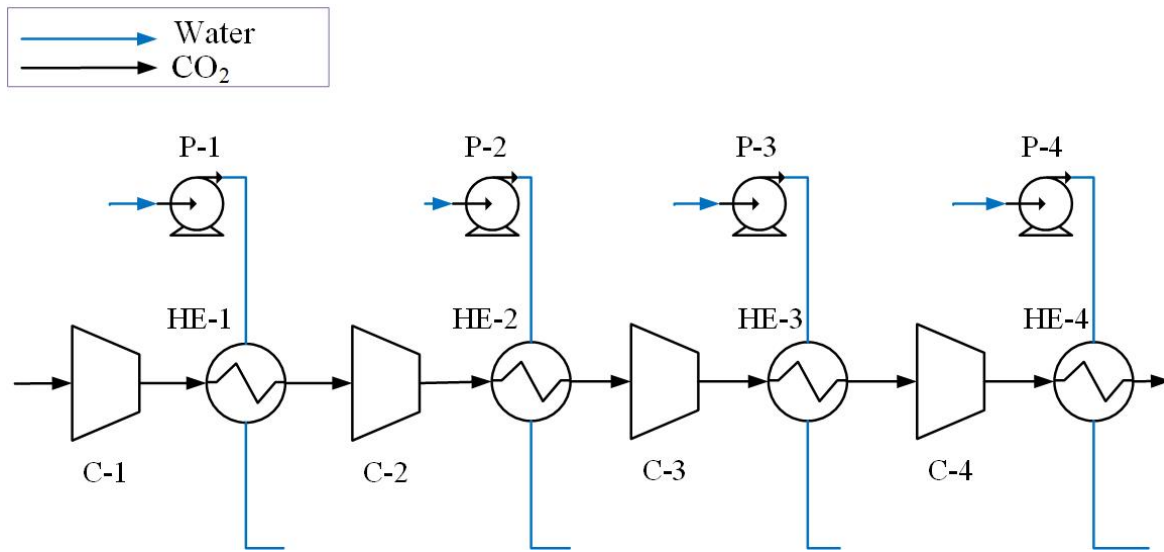


Figure 3.7: Simplified flowsheet of CO₂ compression with cooling.

The main modeling assumptions for the multi-stage CO₂ compression can be located in Table 3.7.

Table 3.7: Compression of CO₂ modeling assumptions

Parameter	Value	Unit
Compressor pressure ratio	4.5	-
CO ₂ temperature inlet	20	°C
CO ₂ pressure inlet	0.2	bar
CO ₂ final pressure	75	bar

3.1.7 PEM Electrolysis Model

After a comprehensive literature study, the PEM electrolysis cell was chosen as the preferred H₂ production method for methanol production. The electrolyzer stack used in this thesis was developed by Arnaiz del Pozo et al. and the paper “Methanol from solid fuels: A cost-effective route to reduced emissions and enhanced energy security” derives and justifies all performance parameters that form the basis for the PEM cell. The equations and relations needed to calculate critical parameters were written in Scilab. Scilab was connected to UniSim with a CAPE-OPEN license to give the streams in Unisim the properties calculated in the Scilab code, considering the PEM performance parameters. Some of the equations forming the base for the Scilab PEM code can be found in Section 2.6.2. Table 3.8 presents the key parameters for the PEM stack using a Nafion membrane.[12]

Table 3.8: Parameters for the PEM cell found in literature for Nafion membranes [12]

Symbol	Parameter	Value	Unit
$j_{0,\text{anode}}$	Anode exchange current density	$5 \cdot 10^{-8}$	A/cm ²
$j_{0,\text{cathode}}$	Cathode exchange current density	$5 \cdot 10^{-8}$	A/cm ²
α_{anode}	Anode charge transfer coefficient	0.8	-
α_{cathode}	Cathode charge transfer coefficient	0.25	-
$E_{\text{act},\text{anode}}$	Anode activation energy	76	kJ/mol
$E_{\text{act},\text{cathode}}$	Cathode activation energy	18	kJ/mol
j_0	Current density cell	1	A/cm ²
-	AC/DC converter	96	%

The modified flowsheet of the PEM electrolyser model is presented in Figure 3.8. Fresh water was fed into the model and cleansed by a deionizer to purify the water for impurities before entering the PEM stack. The purified water was pressurized by a pump to 10 bar. Downstream, the oxygen (O₂) produced at the anode and the H₂ produced at the cathode were sent to a two-phase separator to extract water from the gas. The stream at the anode and cathode did hold a large share of water to ensure that the PEM stack did not overheat. The amount of water needed to remove the waste heat generated by the PEM cell was calculated by UniSim.

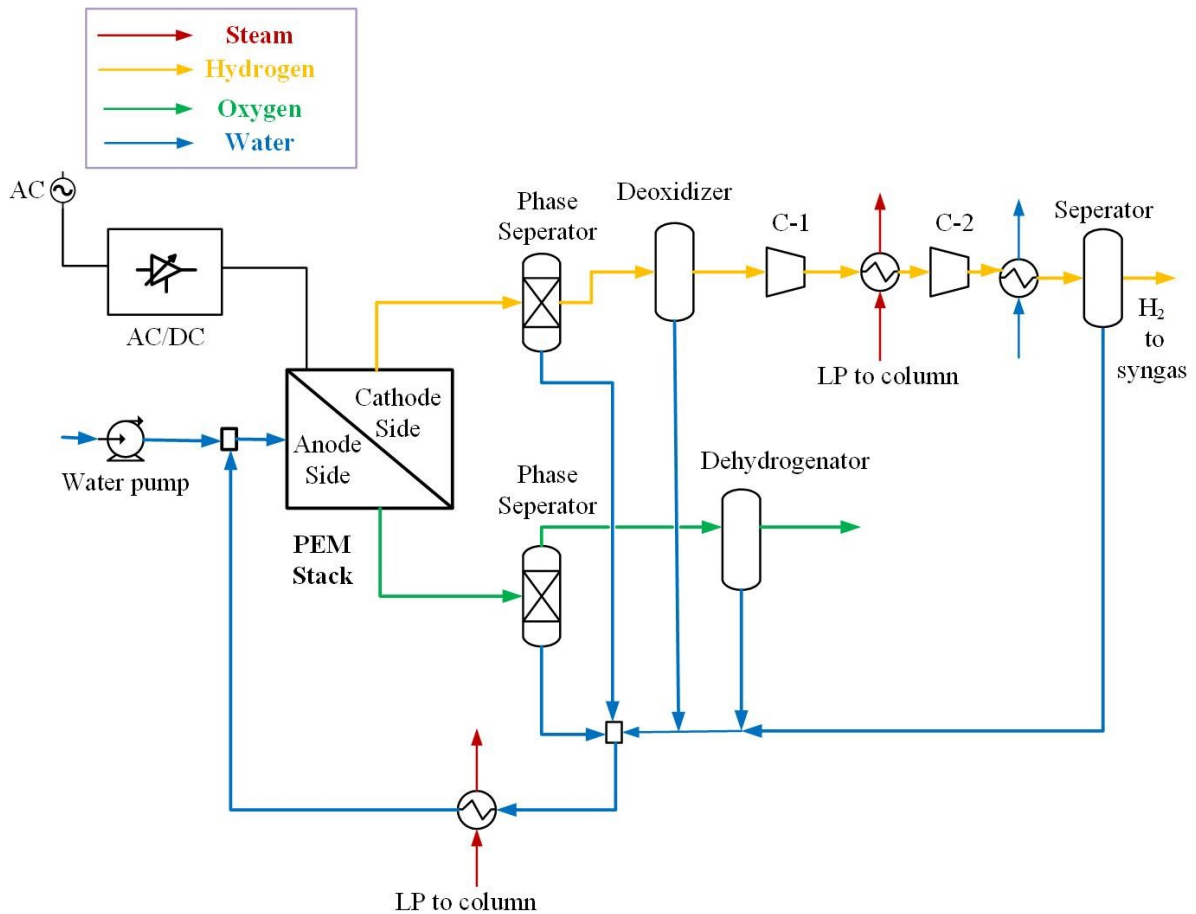


Figure 3.8: Flowsheet of the modified PEM model.

A catalytic recombination induced in a deoxidizer reactor was implemented to purify the stream at the cathode and anode side. The H₂ stream after the filtration and separation steps reached 100% H₂ concentration. A purification step was also implemented for the O₂ stream for safety reasons. The temperature difference between the inlet and outlet of the PEM stack was set to 10 °C. The high-temperature water from the separators and deoxidizers was circulated back to the PEM stack for optimal heat utilization.

The water fed into the electrolyzer model was determined using an adjust-block based on the amount of electricity supplied to the PEM stack. The electricity applied to the PEM stack came from the amount of electricity available from the advanced nuclear plant after electricity from elsewhere in the process was accounted for. Three main changes were made to the original PEM electrolysis model. The first change was the operating temperature of the PEM cell. The waste heat in the PEM model was intended to produce steam for the methanol distillation process and needed temperatures above 115 °C (which was the original outlet temperature of the PEM stack). Therefore, the operational temperature of the cell was elevated by 10 °C. The second change was to circulate all of the water streams in the plant back into the PEM water loop and implement a HE to create steam for the methanol distillation column. The main modeling assumptions for the electrolyzer model are found in Table 3.9.

Table 3.9: PEM model modeling assumptions

Parameter	Value	Unit
Fresh H ₂ O inlet temperature	20	°C
Fresh H ₂ O inlet pressure	1.013	bar
H ₂ O pressure into PEM stack	10	bar
H ₂ O temperature into PEM stack	115	°C
H ₂ O temperature after PEM stack	125	°C
Temperature of recycled H ₂ O after HE	120	°C
C-1 compressor pressure ratio	1.2	-
H ₂ pressure to syngas	30	bar

The last change done to the PEM model was to implement a small compression step at a high-temperature cathodic stream. The heat extracted from the HE placed in the water recycle loop of the PEM cell was not enough to sustain the distillation process of methanol. A HE was implemented after the compressor marked C-1 in Figure 3.8 to create the remaining steam needed for the methanol synthesis. Since the compression of a high-temperature gas is associated with high energy consumption, the compression ratio was carefully designed so that the heat rejected in the HE equaled the amount of the heat deficit in the distillation column.

3.1.8 Synthetic Gas Production

The syngas was produced by mixing and compressing H₂, CO₂, and nitrogen (N₂). The CO₂ stream from DAC had a high level of purity, and a CO₂ concentration of 99.9% was assumed. A 0.01% fraction of N₂ was added to the syngas production to account for the impurities. The

CO₂ and N₂ came directly from the DAC unit at a pressure of 0.2 bar. The hydrogen stream was compressed to 30 bar before entering the syngas production flowsheet, and CO₂ and N₂ were compressed to the level of H₂ in a three-stage inter-cooled process before the substances were mixed together. The compressors were designed to utilize the same amount of energy.

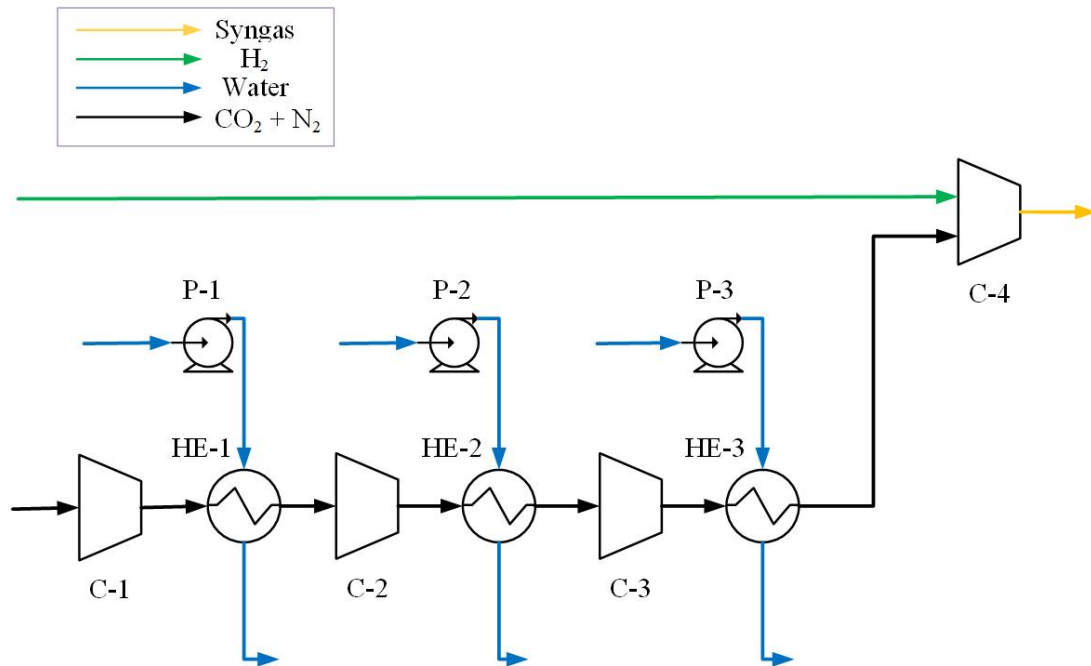


Figure 3.9: Simplified flowsheet of synthetic gas production for methanol synthesis.

The mass flow of CO₂ needed for the syngas production was calculated based on how much H₂ was produced by the electrolyzer cell, where the H₂/CO₂ molar flow should have a ratio of approximately 3 to 1 [12]. In the last step, syngas were compressed to 100 bar to fit the required thermodynamic conditions for the methanol synthesis, as seen in Figure 3.9. No gas cooling was required after the last compression stage since the syngas should enter the methanol synthesis at high temperatures. The main modeling assumptions for the syngas production can be found in Table 3.10.

Table 3.10: Syngas production modeling assumptions

Parameter	Value	Unit
Stream from H ₂ production		
H ₂ fraction	100	%
Pressure	30	bar
Temperature	20	°C
Stream from DAC		
CO ₂ fraction	99.9	%
N ₂ fraction	0.01	%
CO ₂ & N ₂ inlet pressure	0.2	bar
Temperature	20	°C
Final syngas pressure	100	bar

3.1.9 Methanol Synthesis

The methanol synthesis model was developed by Arnaiz del Pozo et al. in UniSim. The plant was modeled to produce 10 000 tMeOH/d with a reactor modeled as an isothermal boiling water reactor with 6000 tubes. The main reactor modeling assumptions for the methanol reactor can be seen in Table 3.11. The conversion of methanol in the reactor was an exothermic process, and heat was transferred across the tube. This heat was used to warm up a separate water stream to produce steam for electricity production in a turbine, as seen in Figure 3.10. Methanol was produced following the principle of CO₂ hydrogenation and the WGS reaction, described in Section 2.8.2. The kinetics used in this model are based on the experimental work conducted by Bussche et al. using a Cu/ZnO/Al₂O₃ commercialized catalyst [90]. The usage of the kinetic model assumed that complete equilibrium was not reached so that the reactor could be sized carefully for more precise capital cost estimation. The plant was designed to produce methanol at <98% purity. The stoichiometric ratio between the reactants fed into the reactor should equal or be as close to 2 as possible [13].

Table 3.11: Reactor modeling assumptions

Item	Value	Units
Shell void	0.5	m
Insulation volume	0.1	m
Tube length (adiabatic section)	1-3	m
Tube length (isothermal section)	9	m
Number of tubes	6000	-
Tube Diameter	0.085	m
Tube wall thickness	0.005	m
Void fraction	0.4	-
Catalyst density	1770	kg/m ³
Catalyst Solid Heat Capacity	5	kJ/kg·°C
Catalyst particle diameter	0.005	m
Catalyst particle sphericity	1	-

As shown in Figure 3.10, syngas was fed to the plant, mixed with recirculated streams of unconverted syngas, and heated in a HE before entering the reactor. The methanol reactor was modeled as two plug-flow reactors: an isothermal reactor and an adiabatic reactor. Since the advanced nuclear plant intended in this work produced a significantly smaller portion of methanol than the original plant, the reactor was scaled down to 2000 tubes, which was the only change made to the reactor design. The number of tubes was chosen based on the convergence of the mole fraction in the second reactor (the second reactor converts almost all of the syngas to methanol). The methanol convergence in the reactor can be seen in Figure E.10 in Appendix E.

The reactor outlet temperature of 260 °C was cooled to ambient temperatures and sent to a high-pressure separator, separating gas and liquids. The vapor product was sent to compression and pre-heating before being recycled to undergo another methanol conversion in the reactor.

The pressure of the liquid stream was reduced to 2 bar before being sent to a low-pressure separator. The unconverted gas follows the same principle as described above for recycling purposes. The liquid fluid was sent to the distillation column, where methanol was extracted, and the unconverted syngas were sent back to the column. The distillation column produced methanol at 60 °C. The methanol modeling assumptions are presented in Table 3.12. The assumptions in Table 3.11 are also employed, only changing the number of tubes.

The water cycle was primarily used to supply the distillation column with low-pressurized steam. The steam was supplied to the HE prior to the distillation column at 1.8 bar and 116.9 degrees C. The amount of heat needed was calculated by UniSim and produced in the PEM model. After the column, the water stream was pressurized to 40 bar. The pressure was reduced to 1.8 bar in the steam turbine for electricity production. The methanol production flowsheet is presented in figure 3.10.

Table 3.12: Methanol synthesis modeling assumptions

Parameter	Value	Unit
Inlet temperature adiabatic reactor	230	°C
Outlet temperature adiabatic reactor	260	°C
Inlet temperature isothermal reactor	260	°C
Outlet temperature isothermal reactor	260	°C
Number of tubes	2000	-
MeOH mole fraction in final product	> 98	%
MeOH temperature in final product	60	°C
Water cycle		
Steam temperature to column	116.9	°C
Steam pressure to column	1.8	bar
Water after pump	40	bar
Pressure after turbine	1.8	bar

A minor simplification was made in calculating the efficiency of the methanol synthesis. Only the electricity for 9.5% of the CO₂ from DAC should be attributed to the total methanol electricity consumption. Therefore, the electricity and the heat needed (divided by 5 to account for the heat/el energy quality ratio) to capture the required CO₂ were converted to electricity and added to the total electricity consumption. This was determined in collaboration with the supervisor, offering a fair representation of the efficiency, including electricity needed for DAC.

3.1.10 Optimization Tool

The optimization tool was not powerful enough to adjust the key energy-demanding factors so that the energy balance would equal to zero [91]. Therefore, the optimizing was conducted by hand, and a small error of <1 MW was considered to be within reasonable limits.

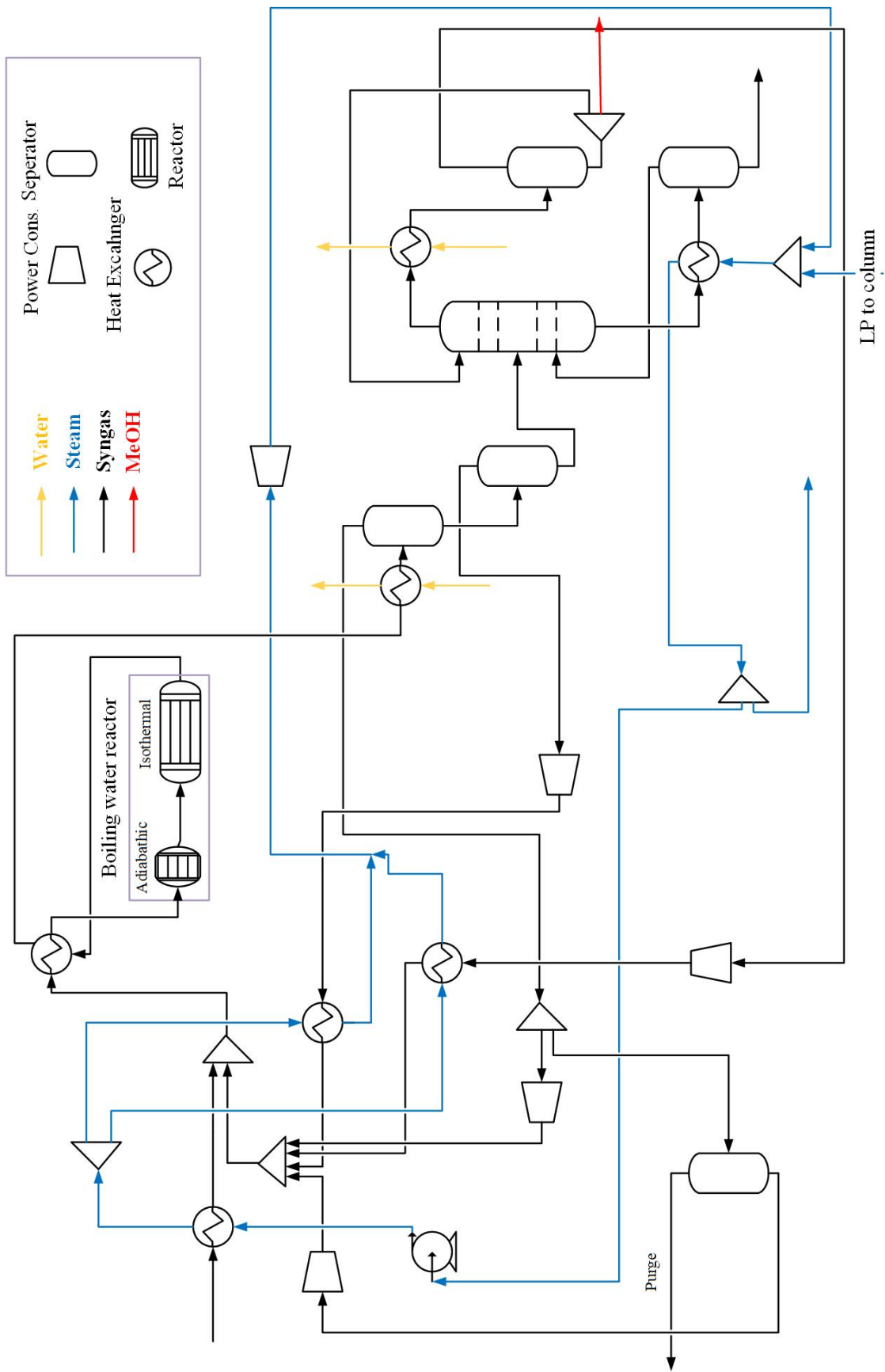


Figure 3.10: Simplified flowsheet of the methanol synthesis.

3.2 Economical Assessment

The technical simulation results served as input parameters for the economic analysis of the plants. Data for each component and the overall plant performance were gathered from the reference and advanced plant. The parameters included choice and size of process equipment, energy balances, make-up water usage, electrolysis water, raw material use, and methanol production capacity. Two different economic analyses were carried out, one for the reference plant and one for the advanced plant, to determine the cost attribution for each plant. Lastly, a comprehensive quantification analysis was carried out. All of the activities were performed in the SEA tool.

As presented in Section 2.4.7 and 2.5.5, nuclear reactors and DAC units are highly capital-intensive components. The cost of DAC and nuclear reactors (especially fourth-generation nuclear reactors) has high uncertainties, and the projected cost in 2050 can only be speculated and relies on findings in the existing literature. The scope of the economic analysis includes the cost of nuclear fuel to the reactor (comprised of the steps in the nuclear fuel cycle). In addition, the economic analysis includes a cost related to the storage of CO₂ onsite. However, an increase in the respective cost, including CO₂ transportation by pipeline, is investigated in the uncertainty quantification. The storage tanks for methanol were sized to store methanol produced for one week. After one week, the methanol was assumed to be collected by a tank truck. The economic analysis does not include costs related to the downstream consumption of CO₂ or methanol after storage purposes. The cost for DAC, nuclear power plant, CO₂ compression, syngas production, methanol production, and distillation was included in the economic analysis and will be described in detail in further sections.

The location and currency that form the basis for the economic evolution are given in Table 3.13. 2020 was chosen as a cost-year basis because the coronavirus pandemic influenced the values from 2020 until today and did not provide a realistic foundation for the assessment.

Table 3.13: Target basis for the economic assessment

Location	China
Cost Year Basis	2020
Currency	\$

3.2.1 SEA Tool

One of the main objectives of the thesis was to give an economical estimation of the reference and advanced plant and to compare the respective plants costs. The SEA tool was developed by the Flow Technology Group from SINTEF Industry and the Department of Energy Engineering from Universidad Politécnica de Madrid in Microsoft Excel. This tool aims to provide a user-friendly methodology for economically analyzing energy and chemical plants. The SEA tool provides cost estimates and has tools comprising sensitivity analysis and uncertainty quantifications. The primary assumptions and mathematic relations for the CAPEX, OPEX, and the cash flow

analysis are presented in Table 3.14. The SEA tool offers two approaches to determine the BEC, the equipment and the scaling approach, which will be described below.[24]

Table 3.14: Cash flow analysis assumptions

Component	Value	Unit
Capital Estimation Methodology		
Bare Erected Cost (BEC)	SEA tool estimate	M\$
Procurement and Engineering Construction (EPC)	10% BEC	M\$
Project Contingency (PT)	20% (BEC + EPC + PC)	M\$
Process Contingency (PC)	0% BEC	M\$
Owners Costs (OC)	15% (BEC + EPC + PT)	M\$
Total Overnight Costs (TOC)	BEC + EPC + PT + OC	M\$
Total Capital Requirement (TCR)	111% TOC	M\$
Operating and Maintenance Cost		
Maintenance	2.5	%TOC
Insurance & Taxes	1.0	%TOC
Labour	60 000	\$/p-y
CO ₂ storage	5 [92]	\$/ton
Nuclear fuel	1 [45–47]	\$/GJ
MeOH price	400 [93]	\$/ton
Sorbent cost	15 [94]	\$/kg
Make up water	0.42 [12]	\$/ton
Electrolyzer water	7.2 [12]	\$/ton
MeOH catalyst	36 [12]	\$/kg
Cash Flow Analysis Assumptions		
Capacity factor first four years	65	%
Capacity factor remaining years	95	%
Discount rate	8	%
Construction period	4	years
Plant lifetime	40	years

Capital Cost Breakdown

The main goal of the SEA tool is to provide a reasonable estimate of the BEC for each component in the plant. The cost correlation references of the source employed depend on the plant's specified location, current, and cost year. The cost of each unit is adjusted to fit the target cost basis using an exchange rate, location factors, and the Chemical Engineering Plant Cost Index (CEPCI). In equation 3.1, the cost estimation in source A is adjusted to the target basis B. E_{AB}

is the current exchange rate from A to B, and F_L is defined as the relative factor for material and labor adjustments for different regions.[24]

$$C_B = C_A \cdot \frac{FL_B}{FL_A} \cdot \frac{CEPCI_B}{CEPCI_A} \cdot E_{AB} \quad (3.1)$$

The BEC for each specific equipment in the plant was based on the correlations from Turton et al. The complete set of equations used for the equipment approach can be further investigated in the “User Guide”. [24]

The SEA tool aims to implement units from an individual equipment list since this approach is the most accurate way to calculate the BEC. However, this approach can not be used in some cases when specialized equipment is used, such as nuclear reactors or DAC units. The scaling method estimates the BEC, calculated by one or more suitable references with cost assessments of the same unit scope. Applying this approach integrates the economic of scale principle. An increase in equipment size could lead to decreased cost per unit capacity depending on the scaling factor. The formula used to calculate the cost for scaled equipment is presented in equation 3.2.[24]

$$C = C_0 \left(\frac{n}{n_0}\right)^e \left(\frac{S_1/n}{S_0/n_0}\right)^f \quad (3.2)$$

C_0 and S_0 represent the reference cost and capacity. S_1 represents the desired scaled-up capacity, while f is the unit exponent (scaling factor), e is the train exponent, and n is the number of trains. The “User Guide” has found that typical values for f are 0.67 and 0.9, depending on the ease of scale-up and commercializing efforts. Lower values for the scaling factor result in lower costs associated with scaling up the component.[24]

Table 3.15: Scaling parameter, reference capacity and -cost, and scaling exponent for different components calculating the BEC following the scaling approach

Component	Scaling parameter	Ref. capacity	Ref. cost [M\$]	Scaling exponent	Ref. literature
Nuclear DAC plant					
CWT	m ³ /s	1	3.17	1	[95]
Nuclear reactor	kW _h	1	1000	1	[37]
DAC	tCO ₂ /y	360000	372	0.9	[5]
Methanol synthesis					
Catalyst	kg	1	32.8	1	[13]
Insulation	m ³	1	1	1	[13]
Storage tank	ton	5000	8.7	1	[96]

Both the scaling and equipment approach were used to determine the economic performance of the reference and advanced plant. The typical equipment, such as pumps, turbines, compressors, separators, and heat exchangers, were implemented and sized based on the input parameters from the Unisim simulation following the equipment approach. The components determined based on the scaling approach with the parameters forming the base for the economic assessment are presented in Table 3.15.

The material for the plant's equipment was determined based on the operative fluid. Components handling non-H₂O or high-pressurized or high-temperature H₂O were implemented as stainless steel (SS) material. Equipment, typically water pumps or heat exchangers for heat rejection at low temperatures, was set to carbon steel (CS) material. The correlations for the different equipment materials have not been included here since this was a minor part of this work.[24]

3.2.2 Reference Nuclear Power Plant

The reference nuclear plant was divided into three components for the economic assessment in the SEA tool: nuclear power plant, DAC unit, and CO₂ compression. A combination of the scaling and equipment approaches was used to determine the cost of the nuclear reactor. The nuclear reactor was implemented using the scaling approach based on the TOC per heat output for a nuclear power plant in China. The price per kW heat was calculated based on the kW of electricity as presented in Section 2.4.7, assuming a 40% efficiency. The cost used for the reactor scaling was based on cost projections for 2030 since the cost estimate for 2050 was considered very optimistic. Since the TOC includes costs for turbines, pumps, HE and a CWT, an original plant was simulated (as described in Section 3.1.5) to determine the size of the turbines, CWT, heat exchanger, and the pump needed for the cooling cycle. The CWT was also determined based on the scaling approach. All of the equipment mentioned above was implemented and subtracted from the nuclear power plant to isolate the cost of the nuclear reactor. Then, the turbines and pump for the nuclear-powered DAC plant were added. The turbines would be smaller and contribute to a lower cost for the nuclear-powered DAC plant than for an original nuclear plant.

The BEC for the DAC unit was calculated using the scaling approach based on the cost per ton CO₂ captured each year. To determine the cost related to the CO₂ compression, the compressors and HE were implemented following the equipment approach. In addition, a small pump was implemented to account for the water circulation needed for the cooling make-up water. A CWT was implemented to account for the cooling make-up water needed to remove the heat in the HE. This cost had a small cost attribute and was added to the cost of CO₂ compression.

The operational cost was divided into fixed operational and maintenance (FOM) cost, varying operational and maintenance (VOM) cost, and nuclear fuel. The VOM comprises make-up water, sorbent material for DAC, and the CO₂ storage cost on-site. The sorbent cost will vary significantly with different technologies, and the value chosen for this project is calculated based on a sorbent study conducted by Azarabadi et al. The calculations are derived in Appendix A [94]. The reference values chosen for each specific cost are represented in Table 3.14. FOM

included the maintenance cost, insurance, and labor work. The number of employees chosen for the reference plant was set to 100 persons.

3.2.3 Advanced Nuclear Power Plant

The advanced nuclear plant was divided into seven components for the economic assessment in the SEA tool: the nuclear power plant, DAC unit, CO₂ compression, PEM electrolyzer model, syngas production, methanol synthesis loop, and storage and distillation of methanol. The nuclear plant, DAC unit, and CO₂ compression follow the same methodology described in the section above. To account for the distinctive features of the advanced reactor, which operates at a much higher temperature and pressure than the reference plant, a 10% increase in the TOC was assumed. The production of syngas was implemented as conventional components consisting of compressors and heat exchangers.

The PEM electrolyzer model was divided into the conventional components following the equipment approach and the PEM stack following the scaling approach. The PEM electrolyzer was scaled based on how much electricity was supplied to the cell and follows the economic setup from Arnaiz del Pozo et al. The PEM stack's components with respective costs can be seen in Table 3.16. The current costs for the PEM electrolyzer were anticipated to decline over the coming decades due to technological development. These reductions were accounted for as the plant's construction was assumed to be at the mid-century, and the cost reductions can be found in the same table.[12]

Table 3.16: Component, cost and cost reduction assumptions for the PEM electrolyzer [12]

Parameter	Value	Unit	Cost reduction
Membrane	347	\$/m ²	10%
PGMs & ionomer	500	\$/m ²	0%
Porous transport layer	650	\$/m ²	20%
Frame	50	\$/m ²	0%
Bipolar plate	300	\$/m ²	50%
Assembly cost	50	\$/m ²	0%
Balance of stack	300	\$/m ²	20%
Power supplies	70	\$/m ²	20%
Stack and power supply installation cost	50% of the total sum		

The equipment and scaling approaches were used to determine the cost for the methanol synthesis model. The compressors, pumps, vessels, reactors, and turbines were determined with the equipment approach. The catalyst used in the methanol synthesis and the insulation of the reactor was determined based on the scaling approach. The reference scaling parameters can be found in Table 3.15. The actual capacity for the catalyst and insulation in this work was calculated based on the parameters forming the base for the reactor, described in the technological analysis methodology in Table 3.11. The setup for the economical calculation of the reactor cost, insulation, and methanol catalyst followed the setup from the SEA tool file of Arnaiz del

Pozo et al.[13] The methanol storage tank cost was calculated following the scaling approach. The tank was scaled with a capacity to store the produced methanol for a week. A pump and a CWT were added to account for the cooling make-up water following the same methodology as described for the reference plant. This has a small cost attribute and was added to the methanol synthesis cost.

The same methodology was followed for the VOM, FOM, and nuclear fuel, as described in Section 3.2.2 for the reference plant. However, some costs were added since the advanced plant had several requirements and components. Electrolytic water and the methanol catalyst were added as a VOM. In addition, methanol was implemented as a product to be sold, lowering the O&M cost. The respective values are described in Table 3.14. The labor was raised to 150 employees due to the increased complexity of the plant.

3.2.4 Uncertainty Quantification

Uncertainty quantification (UQ) is the process of quantifying and analyzing the uncertainty in economic assessments and mathematical models. The Monte Carlo method with Latin Hypercube Sampling was utilized to determine the associated uncertainty and the impact of critical parameters on the LCOC for the reference and advanced plant. The UQ provides multiple possible outcomes and the probability of each outcome from a large pool of random data samples and is integrated into the SEA tool. The values are distributed following a skewed normal distribution determined by three chosen values, a range of low, mid, and high values. The mid value equalizes the median of the normal distribution.

Table 3.17: Values chosen for the uncertainty quantification

Parameter	Unit
DAC cost	\$/ton·y
Nuclear plant cost	\$/kW _h
DAC efficiency	factor
Sorbent cost	\$/kg
Nuclear fuel	\$/GJ
CO ₂ storage	\$/ton
Discount rate	%
Plant lifetime	years
Advanced nuclear plant	factor
Methanol price	\$/ton
Electrolyzer cost	factor

The standard derivation and skewing of the distribution are set to contain 99% of the values ranging from the low to the upper value. Considering the time the SEA tool uses to compile all the different runs and, at the same time, provide a thorough and representative analysis, a set of 1000 runs was chosen. The values chosen for the analysis can be seen in Table 3.17, and the full range following a justification can be seen in Appendix D. The first eight parameters were

included for both plants, and the last three were included for the advanced plant. For each run, all of the influencing values were simultaneously changed, providing the LCOC for the thousand different cases.

The uncertainty range for the UQ was kept the same for the reference and advanced plant. To provide a proper foundation for comparison of the numbers for the different cases, the random numbers chosen had to be the same. Therefore, different parameters for each component were first compiled in one SEA tool file and imported into the other SEA tool file to ensure that the thousand points chosen were the same. Afterward, the data analysis tool pack in Excel was utilized to perform a regression analysis to determine the parameter's impact on the LCOP. The impact was determined by multiplying the coefficient from the regression analysis with half of the uncertainty range chosen for the individual parameter.

The histogram feature from the Excel data analysis tool pack was used to determine how many of the thousand cases fell within a specific range with respect to the LCOC. A suitable range for the bins was determined. The same approach was followed to calculate how often the reference plant would be cheaper to build compared to the advanced plant in the 1000 cases. In addition, an if-statement was implemented in Excel to evaluate when the reference plant would be less expensive to produce than the advanced plant.

The energy balance in the reference and advanced plant would be affected when the DAC efficiency factor was adjusted in the UQ. As described in Section 3.1.10, each plant's energy balance was carefully designed. Compiling the UniSim simulation for each of the thousand cases to develop the energy balance correctly was not considered beneficial. Therefore, the energy consumption in the UQ for the CO₂ compression was kept constant for all the thousand trials, equaling the electrical consumption calculated in the base case. The captured CO₂ was divided by the DAC efficiency factor, meaning that if the efficiency of DAC is less than 1, more CO₂ will be captured. The fixed value for CO₂ compression was multiplied by the factor of the new CO₂ capture rate and the CO₂ capture rate from the base case, hence increasing the CO₂ compression with increasing CO₂ capture. The energy usage of DAC was set to consume the amount of electricity required for a net zero energy balance. After discussing this with the supervisor, it was considered a reasonable assumption, providing fair results.

4 Results and Discussion

This chapter will present the most important results, with accompanying discussion. The reference plant and the advanced plant will be analyzed individually and compared. First, the technical results present the energy balance and the overall plant performance. Then, the economic results present the LCOC, capital-, and operational expenditures. A comprehensive uncertainty quantification analysis was performed to quantify the degree of uncertainty in the assessment and determine the parameters that influence the LCOC the most.

4.1 Energy Distribution and Environmental Performance

The energy balance and plant performance can be seen in Table 4.1 for the reference and advanced plant. The amount of fuel needed for the thermal energy supplied to the boiler and reheater(s) is 2897 MW_h of heat for the reference plant and 4084 MW_h of heat for the advanced plant, respectively. The DAC units are approximately the same size, and since the electricity produced by the advanced plant is about three times larger, more fuel needs to be supplied to the advanced plant to deliver the same amount of heat. One of the main obstacles to overcome with fourth-generation reactors is the high fuel consumption. However, fast breeder reactors offer a solution to this problem, which is discussed further in the chapter.

Table 4.1: Energy breakdown and plant performance for reference plant and advanced plant

	Ref. Plant	Adv. Plant	Unit
Fuel	2897	4084	MW _h
Steam turbine	560.1	1653	MW _e
Pump	10.9	40.8	MW _e
CO ₂ compression	197.0	188.9	MW _e
DAC process	352.0	370.8	MW _e
Net power	0.2	1052.5	MW _e
$\eta_{\text{NuclearPlant}}$	19.0	39.5	%
Heat to DAC	2401	2472	MW _h
CO ₂ captured	444.7	457.8	kg/s
Power to H ₂ and MeOH production	-	1052.5	MW _e
Water circulation pumps	-	1.2	MW _e
Steam turbine MeOH	-	10.1	MW _e
Recycle compression	-	6.4	MW _e
H ₂ and syngas compression	-	50.9	MW _e
Power to PEM electrolyzer	-	1004	MW _e
Net power	-	0.1	MW _e
H ₂ produced	-	5.99	kg/s
$\eta_{\text{PEMelectrolyzer}}$	-	71.6	%
CO ₂ needed from DAC	-	43.6	kg/s
MeOH produced	-	31.66	kg/s
η_{MeOH}	-	54.3	%

The reference plant produces 560.1 MW_e of electricity from both turbines, and the electricity consumption for DAC, compression, and pumps is 559.9 MW_e. The plant was designed to achieve full electrical self-sufficiency for DAC and CO₂ compression, equaling a net balance of 0.2 MW_e. DAC consumes roughly 4-5 times as much heat as electricity, and the power cycle was adjusted accordingly. Enhancing heat within the plant indicates a trade-off in how much electricity the plant produces, resulting in decreased thermal efficiency, as described in Section 2.4.6. The reference plant achieved a thermal efficiency with a total of 19%. The efficiency is almost half the efficiency of an original nuclear plant, which has an efficiency of around 33%.

The advanced plant produces 1653 MW_e of electricity from the three turbines. This facility was engineered to optimize electricity generation so that the hydrogen production from the electrolyzer was maximized. The water pumps, CO₂ compressors, and DAC process consume 600.7 MW_e of electricity. The net power from the advanced nuclear power plant is 1052.5 MW_e, resulting in a high thermal efficiency of 39.5%. However, advanced nuclear power plants constructed for power generation could approach 45-50% efficiencies. The (up to) 10% and 14% decrease in efficiency for the advanced and reference plant is due to heat being rejected at 100 °C for DAC instead of ambient temperature for standard cooling towers.

The heat extracted from the nuclear power plant to DAC for both the reference and advanced plant is 2401 MW_h and 2472 MW_h, respectively. The CO₂ captured from the plants is calculated based on the amount of heat available and the amount of heat required per kg of CO₂, which is kept constant for both plants. This results in a CO₂ capture rate of 444.7 kg/s for the reference plant and 457.8 kg/s for the advanced plant.

The hydrogen production is 5.99 kg/s with an efficiency based on the LHV of 71.6%. The methanol produced from the advanced plant is 31.66 kg/s, corresponding to 2735 t/d. This production rate equals a large methanol facility today. Including the energy required by DAC to capture the amount of CO₂ needed in the methanol synthesis, the overall efficiency for the methanol loop is 54.3% and was calculated with the relation presented in Section 2.8.3. Today, the range typically lies between 50-60% for green methanol production from electricity and DAC. One of the main reasons for the efficiency not to be higher is due to the energy needed in the compression of the high-temperature gas stream to provide enough heat to the distillation column, as described below.

Table 4.2: Heat demand and production of waste heat to distillation column

	Adv. Plant	Unit
Heat needed to column	87.8	MW _h
WH from PEM	25.6	MW _h
WH from HT comp.	9.8	MW _h
WH from deox.	26.4	MW _h
WH from dehydr.	27.0	MW _h
Net WH	1	MW _h

As presented in the Section 3.1.7, the electrolyzer loop was modified to provide enough heat for the distillation column. As seen in Table 4.2, UniSim calculated that 87.8 MW_h of low-pressurized steam was needed. It was assumed that the waste heat (WH) released from the hydrogen oxidation reactions in the dehydrogenator and deoxygenator could be utilized, contributing with 26.4 MW_h and 27 MW_h respectively. Excess water was fed through the PEM cell, ensuring that the cell did not overheat. This heat was rejected in a HE and evaporated water to steam for the column, creating 25.6 MW_h of heat. The remaining amount of heat was collected in the compression step of the high-temperature (HT) cathodic hydrogen stream, producing 9.8 MW_h. The heat needed for the column corresponded to 2.77 MW_h/kgMeOH, which is slightly above the range of heat typically supplied of 2.4-2.6 MW_h/kgMeOH [12].

4.2 Capital Expenditures

Figure 4.1 presents the capital expenditures for the two plants. The figure presents the TOC for each ton CO₂ produced per day for the reference and advanced plant. The main findings were that the DAC unit contributes the highest cost and that the nuclear reactor would have a more significant cost contribution for the advanced plant than the reference plant. The reference plant has a total cost of 203.6 k\$/tonCO₂, and the largest share of the cost comes from the DAC unit, with a cost of 139.1 k\$/tonCO₂ per day. The nuclear plant accounts for 29.3% of the cost with 59.6 k\$/tonCO₂. The nuclear reactor accounts for 95% of the cost share related to the costs of the nuclear power plant, the remainder being the Rankine power cycle. A minor cost share came from the CO₂ compression activity, with 4.9 k\$/tonCO₂.

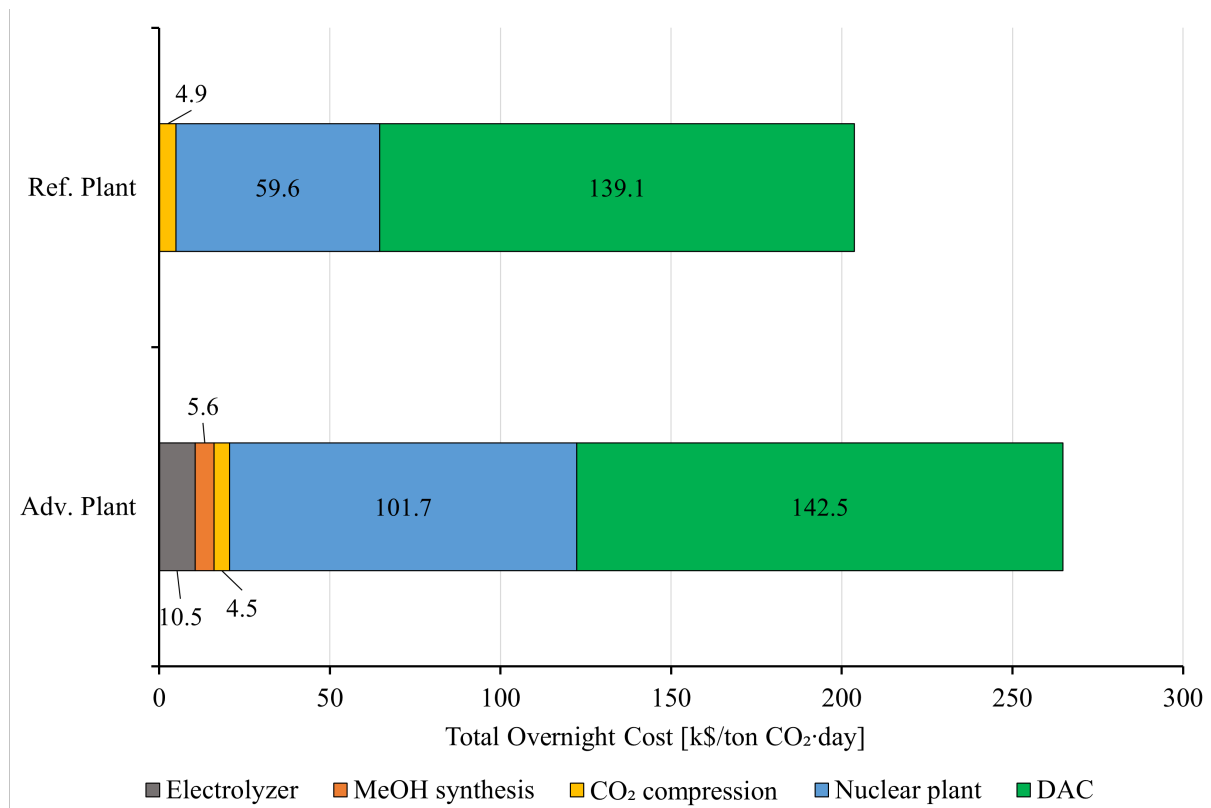


Figure 4.1: Total overnight cost expressed as k\$/tonCO₂ for the reference and advanced plant.

The advanced plant has a greater TOC for each ton CO₂ produced per day with a total of 264.8 k\$/tonCO₂. A large share of the cost came from the DAC unit with 142.5 k\$/tonCO₂. This only differs with 3.4 k\$/tonCO₂ from the reference plant because both plants almost have the same capture capacity as seen in Table 4.1, which forms the base for the economical scaling for the DAC unit. The second-highest cost share is related to the nuclear plant with 101.7 k\$/tonCO₂ accounting for 38.4% of the total capital cost. The nuclear reactor accounts for 92.3% of the share related to the costs of the nuclear power plant. This percentage is smaller compared to the reference plant since the equipment needed for the Rankine power cycle is larger, and an extra intermediate-pressure turbine was used, raising the capital cost for the advanced plant. A smaller share of the capital cost is related to hydrogen production and methanol synthesis, only accounting for 7.8% of the total capital cost.

The cost for the electrolyzer was 10.5 k\$/tonCO₂. Today, the cost related to the electrolyzer would be higher than what was calculated in this thesis. Since the projects described in this thesis were assumed to be built on a future time scale, a cost reduction in the PEM electrolyzer cell was assumed. The IEA has recognized hydrogen as an essential energy source for the NZE by 2050 scenario, driving development and cost reduction for the PEM technology. The assumptions made in the cost reduction for the PEM electrolyzer cell are described in Section 3.2.3. Regarding capital expenditures, the investment needed for green methanol equipment synthesis from H₂ and CO₂ has been reported to equal the cost of MeOH production equipment for fossil fuels, resulting in the absence of additional expenses for the downstream process of green methanol synthesis compared to the convenient methanol production [84].

There are two main reasons why the nuclear power plant was considerably more expensive for the advanced plant than the reference plant. The first reason was the size of the nuclear reactor in terms of scale. The advanced nuclear reactor consumes slightly above 1/3 more nuclear fuel and produces almost three times as much electricity compared to the reference plant. This, in turn, leads to a larger nuclear plant concerning equipment, causing a rise in capital costs. The second reason is that the cost basis for the advanced nuclear reactor is assumed to cost 10% more than a conventional third-generation reactor because it operates at a much higher temperature. As of today, there are no commercially available advanced nuclear reactors. Therefore, the nuclear reactor's cost is unpredictable and remains one of the most uncertain factors, next to the DAC cost, in this work. A comprehensive uncertainty quantification was carried out, and the possible outcomes of different costs for the advanced nuclear reactor will be discussed at a later point.

4.3 Operational Expenditures

The O&M costs for the reference and advanced plant are presented in Figure 4.2. Considering the capital-intensive nature of nuclear and DAC facilities, the O&M costs make a comparatively minor contribution. The reference plant has an O&M cost of 43.7 \$/tonCO₂. FOM cost holds the largest share of the cost, with 20.5 \$/tonCO₂, followed by the VOM at 10.6 \$/tonCO₂. The main contributor to the VOM for the reference plant is cost related to CO₂ storage. As seen in the figure, the sorbent used in the DAC unit and the nuclear fuel spent in the reactor account for 13.5% and 15.3% of the O&M cost, respectively.

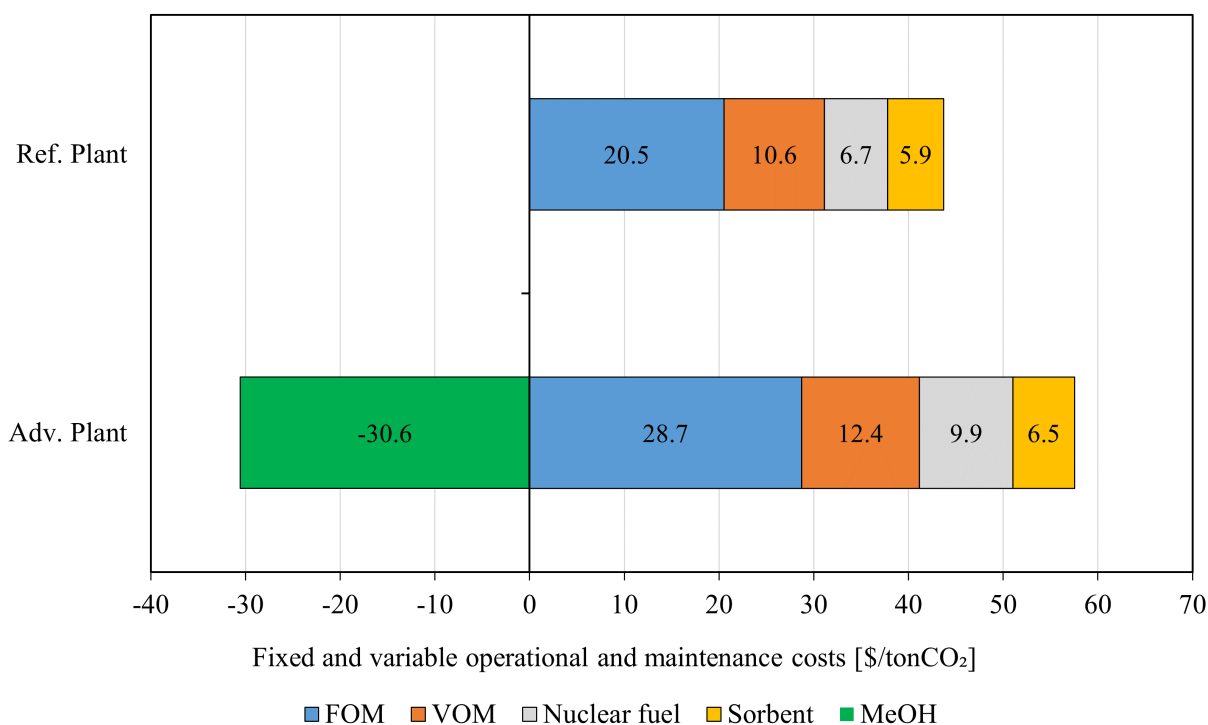


Figure 4.2: Fixed and variable operational and maintenance (FOM & VOM) cost as cost contributor for each ton CO₂ produced for the reference and advanced plant.

For the advanced plant, the total O&M cost is 57.5 \$/tonCO₂, as seen in Figure 4.2. Including the negative cost from methanol sold at 400 \$/kg, the net O&M cost was drastically reduced to 26.9 \$/tonCO₂. The main cost contributor is the FOM with 28.7 \$/tonCO₂. The main reason for the FOM to be higher for the advanced plant compared to the reference plant is the higher cost of insurance and maintenance. Also, more employees are required for the advanced plant, raising labor costs. The nuclear fuel cost is constant for each plant, and the fuel cost related to the advanced plant was 3.2 \$/ton CO₂ more costly than the reference plant due to the higher amount of heat supplied to the advanced nuclear. The main reason for the higher VOM cost for the advanced plant is the electrolysis water needed for hydrogen production and the methanol catalyst present in the methanol synthesis.

One of the main uncertainties related to the operating cost is the amount and price of the sorbent material needed in the DAC process. Currently, this price is relatively high (up to 100 \$/kg), and the price chosen for this experiment is one of the lowest found in the literature (15 \$/kg). This assumption was considered a reasonable estimate, considering the construction of the plant in a future scenario benefitting from technological development. Even though the DAC technology is striving under constant initiatives and economic subsidies, it is not confident that this cost will be reduced as much as projected. Several unknown factors are linked to the sorbent's performance, such as lifetime, working capacity, and cyclic time, which will vary greatly. The sorbent has been included in the uncertainty quantification carried out in this thesis, and its respective effect on the economic assessment will be discussed at a later stage.

4.4 Levelized Cost of CO₂

The LCOC for the reference and advanced plant can be seen in Figure 4.3. The LCOC for the reference plant was 98.3 \$/ton. The figure shows that the largest share of the cost came from capital expenditures, accounting for 59.5% of the total cost. FOM, which is primarily related to the capital expenditure of the plant, contributes another 22.5%, indicating the capital-intensive nature of these facilities. For the advanced plant, LCOC was calculated to be 104.9 \$/ton. The capital cost for the advanced plant is 23.2 \$/ton more than the capital cost for the reference plant, mainly due to the larger, more advanced nuclear reactor and additional process units required for methanol synthesis. This results in a higher FOM cost for the advanced plant, accounting for 29.5% of the LCOC. These extra costs are balanced by the revenues from selling the produced green methanol, which is shown as a negative cost in Figure 4.3. At a methanol price of 400 \$/kg, the profit from the sale of methanol lowered the LCOC by 22.6%. The price at which methanol is sold extensively affects the LCOC, where a higher methanol price could significantly reduce the LCOC.

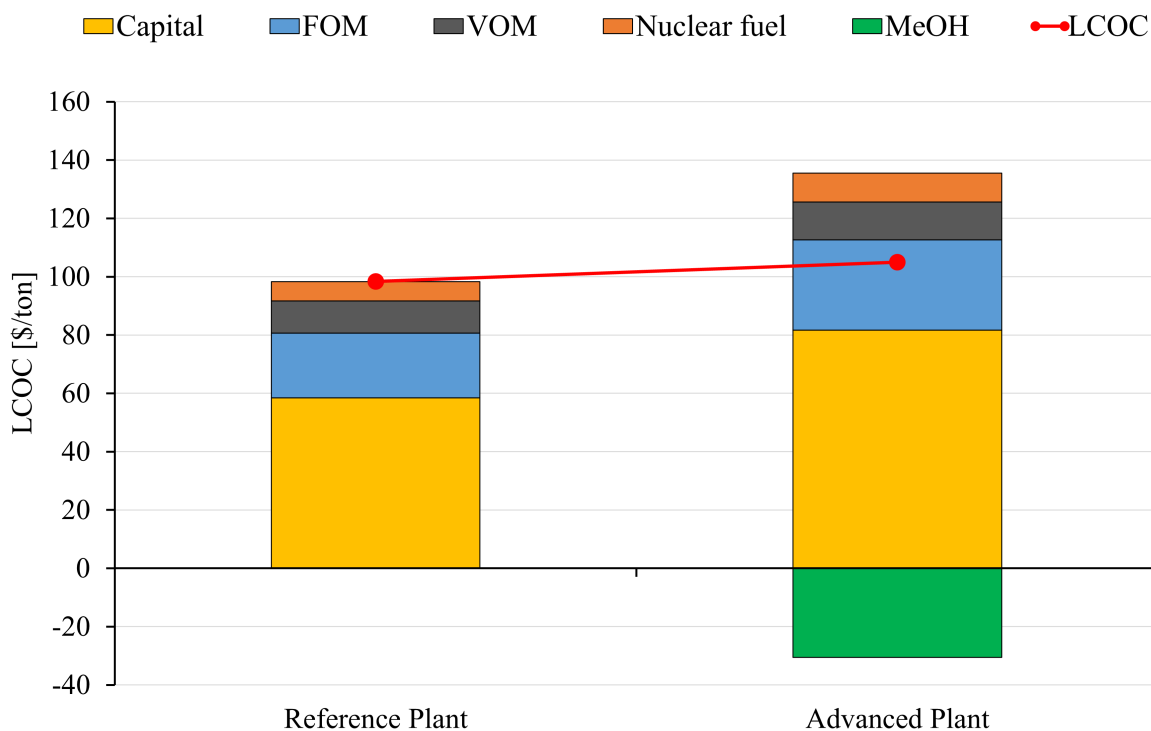


Figure 4.3: LCOC for the reference and advanced plant.

The numbers for the LCOC ranging from slightly under to slightly above 100 \$/ton for the reference and advanced plant are attractively low for DAC technology. Aside from the large DAC cost reductions assumed for the mid-century timeframe of this study, the main reason for both plants reaching low levels is the low TOC of the nuclear power plant. As presented in Section 2.4.7, the cost varies enormously between regions. The main reason this plant was built in China was the low TOC at 2500 \$/kW_e. China is the second largest nuclear-producing nation (after the U.S.) and has wide knowledge within the technological domain of nuclear

energy. Several studies have found that the prices for building nuclear technology were lowered with a high level of experience. The LCOC for the plant would be significantly higher if the plant were to be built in other parts of the world, for example in Norway, which has little or no experience with large commercialized nuclear power plants. However, a large benefit of the proposed nuclear-DAC facilities is that they can be constructed in regions with low cost and public resistance related to nuclear power plants, and will be discussed further in Section 4.6.

4.5 Uncertainty Quantification

The UQ investigates some of the most uncertain factors that impact the economic assessment. One thousand cases with randomly generated parameters within the chosen range were compiled, building on the Monte Carlo simulation principle. The factors chosen for the nuclear-powered DAC plant are DAC unit cost, nuclear plant cost, DAC efficiency (energy usage per ton CO₂ captured), sorbent cost, nuclear fuel cost, CO₂ storage cost, discount rate, and plant lifetime. The electrolyzer cost, methanol price, and additional cost for an advanced nuclear reactor were included on top of the aforementioned parameters for the advanced plant.

4.5.1 Influencing Parameters of the LCOC

The linear regression model for the UQ is a good fit ($R^2 > 0.97$), indicating that the uncertain parameters essentially had linear effects on the LCOC. The regression analysis determined which parameter exhibited the greatest potential to impact the LCOC and can be seen in Figure 4.4. The main observation was that both plants have high sensitivity to a high DAC unit capital cost and nuclear reactor price. The additional cost of an advanced nuclear reactor can potentially make the advanced plant very costly. The influencing factors will be discussed in depth below.

DAC capital cost (250-700 \$/tonCO₂-year) is associated with a high level of uncertainty providing this technology with a particular cost range since it remains at its early stages, and this study targets a future scenario where DAC is available at scale. A very high cost is currently associated with the capital investment due to scaling up not being easily achievable. However, modular improvements are expected to make DAC units easier to mass-produce, hence lowering the cost in the future. The advanced plant is slightly more sensitive to this parameter than the reference plant because a fraction of the captured CO₂ is used for methanol production instead of being stored and sold.

Nuclear power cost (650-2100 \$/kW_h corresponding to 1625-5250 \$/kW_e) is one of the most critical factors, including a wide cost range justifying the uncertainty associated with nuclear power projects. Factors such as the nuclear reactor design, plant location, nuclear fuel consumption, unforeseen factors, and employee experience level will significantly influence the total nuclear plant cost. If the lower end of the range for nuclear power cost could be reached, a high degree of standardization and a rise in the social acceptance of nuclear energy would be required. However, a nuclear project's projected lifetime and costs tend to overrun their estimate, often resulting in a higher final cost. Despite technological development, due to severe incidents and social resistance, there is continuous work on improving the reactor's safety, which can cause the capital cost for nuclear power to increase in the future. The advanced plant is much more

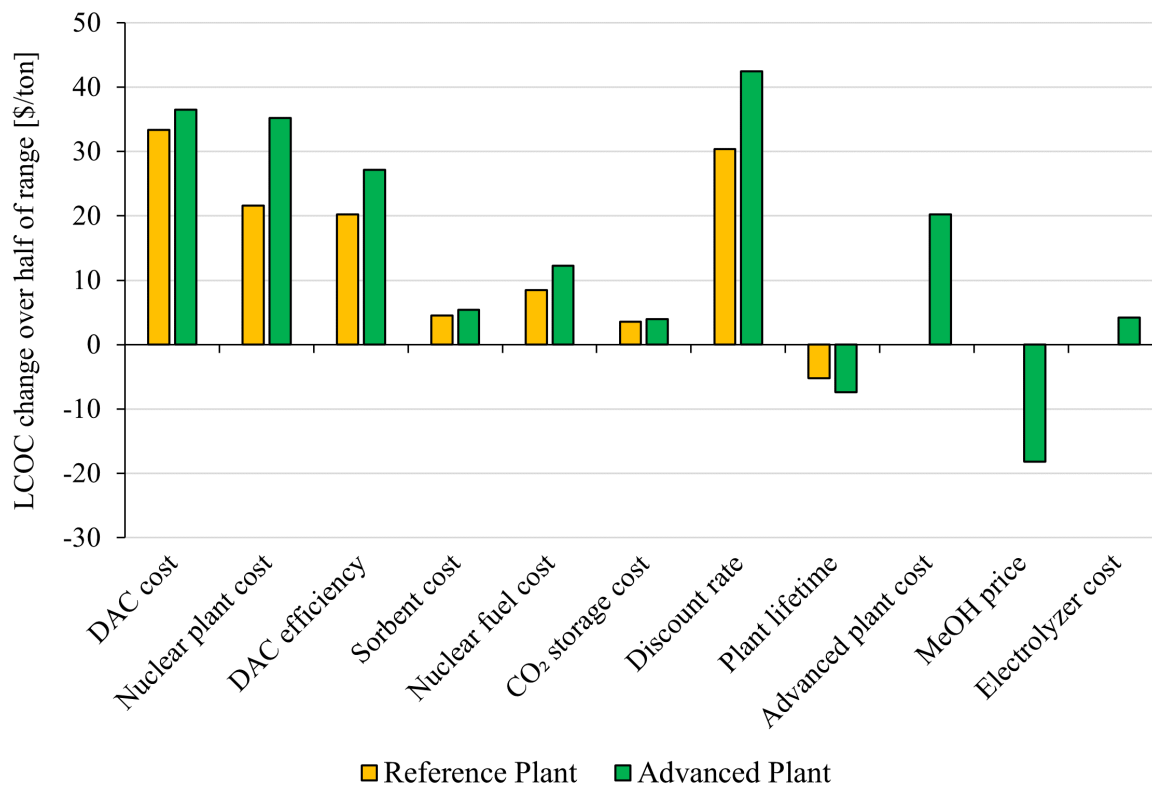


Figure 4.4: The change in LCOC across half of the parameters uncertainty range.

sensitive to the nuclear power plant cost because of the much larger plant required to produce the extra electricity for methanol synthesis.

DAC efficiency (0.5-1.5) could have a large effect on the rise of the LCOC. The efficiency factor was multiplied by the energy usage required to capture a ton of CO₂, which means that the CO₂ capture capacity would be significantly reduced with a higher energy demand to capture a ton of CO₂. In the worst-case scenario, the LCOC could rise by 20 and 27 \$/ton for the reference and advanced plant. As seen in the figure, the advanced plant is more sensitive to a change in energy efficiency for DAC. This is mainly because this plant is selling less CO₂ as a product since 9.5% of the captured CO₂ is needed for the methanol synthesis. A techno-economic study by Fashihi et al. assumed a fixed development rate of DAC and found that the energy heat consumption in 2050 could be reduced with 39% of today's energy requirement for S-DAC [5]. However, these estimates are viewed as optimistic.

Discount rate (4-12%) significantly impacts both facilities because both projects are highly capital-intensive. A high discount rate is typically set for projects with many uncertainties, and a well-known technology could achieve lower rates. Initially, the reference and the advanced plant would likely end up in the upper range due to the complexity and non-commercial nuclear plants working with a DAC unit. However, a successful large-scale rollout of the technology, as assumed in this work, should bring financing costs down. Also, the DAC technology has still to prove gigascale CO₂ removal and to operate for the total lifespan (≈ 20 years). In addition, market factors could cause the interest rate to vary strongly over time and between regions, making it important to construct these plants in regions and periods with low borrowing costs.

Advanced reactor cost (0.7-1.6) can potentially affect and raise the LCOC to a large extent. No commercialized fourth-generation reactors have been built today, and the chosen range for the uncertainty quantification can only be speculated and determined based on information in literature discussing future and pilot projects. Due to the low maturity and standardization for scale-up of the technology, the price today would often be higher than for commercial third-generation reactors. Several initiatives are developing and driving the price of the fourth-generation reactor down. As presented in Section 2.4.3, fourth-generation designs are planned to be ready for commercialization in 2030. In addition, a set of Japanese researchers has claimed that they were able to produce an advanced nuclear reactor with an efficiency of 40% with a 30% cost reduction compared to a standard third-generation pressurized boiler reactor. Developers and companies keep their economic estimates private but have said that the advanced design could significantly revolutionize nuclear reactors and reduce the up-front capital cost.

Methanol price (200-650 \$/ton) has a significant potential to lower the LCOC for the advanced plant. If the methanol were to reach costs in the upper range, the LCOC could be lowered as much as 18.2 \$/ton. Some have speculated that the price of methanol will surge, driven by the demand from end-user industries. However, the price of grey methanol could fall below 290 \$/ton for different regions [97]. This would make it challenging for green methanol to compete with methanol produced from fossil fuels (methanol produced from fossil fuels accounts for 99% of global methanol production) if the cost of green methanol reaches the higher end of the specified range. Subsidies and comprehensive deployment of a CO₂ tax could make green methanol competitive and will be discussed in detail in Section 4.6.

Lifetime (20-60 years) would not have a remarkable impact on the LCOC. If the plants were to reach the likely lifetime above 50 years, this could lower the LCOC by 5 \$/ton and 7 \$/ton. This small impact is due to the effect of the discount rate, which strongly diminishes the effect of the latter years of plant operation on the LCOC. This analysis does not include the impact for an operational lifetime under 20 years, assuming a high possibility that the plant operates above 20 years based on historical data [27, 30, 31]. However, if this were not the case, a lifespan of 10 and 5 years for the advanced plant would equal an LCOC of 178.4 \$/ton and 288.1 \$/ton. Indicating that if the highly capital-intensive plant were to be shut down before 20 years of operation, this would have a catastrophic impact on the economic investment. In the later years, nuclear technology has proven to have a stable operation built to withstand natural disasters and an extremely low probability of technological failure. On the other hand, since nuclear energy is considered a controversial energy source, it may suffer from early decommissioning from political pressure, demonstrations, or terrorism in a worst-case scenario. Such plants would therefore be situated in stable regions where the likelihood of such early decommissioning is extremely low.

Nuclear fuel (0.3-2.8 \$/GJ) has a relatively low impact on the LCOC, compared to other parameters. However, it can affect the LCOC with a rise up to 8.4 \$/ton and 12.2 \$/ton for the reference and advanced plant. Costs are considerably higher for the advanced plant due to the additional fuel consumed to generate surplus electricity for H₂ and methanol production. One of the significant obstacles to overcome with some of the fourth-generation reactors is the high fuel consumption. However, future fourth-generation reactors investigated with a fast-breeder design show that the reactor can generate more fissile material than it consumes. This could

lower fuel consumption close to zero, offering a solution to the intricate nuclear waste handling problem.

Electrolyser cost (0.5-2) has a small impact on the LCOC for the advanced plant. This is mainly due to other parts of the plant being highly capital-intensive and only a moderate fraction of the consumed nuclear fuel being used for H₂ production (the majority is still used for DAC). In addition, the cost for the PEM cell calculated in this work is relatively low due to the assumed cost reduction for PEM electrolyzers in the future. The cost would be more prominent if the electrolyzer were powered by renewable energy, which would need equipment oversizing to handle the fluctuating supply of electricity.

Sorbent cost (7-30 \$/kg) was considered a moderate uncertainty factor but is found not to have a large impact on the LCOC from the uncertainty quantification. As previously stated, the range provided is relatively low and is based on a massive scale-up in production and improvement of the chemical technology of the sorbent. **CO₂ storage cost** (3-9 \$/ton) has a minor influence of the LCOC. This is mainly due to the plant being constructed relatively close to a storage reservoir, excluding the need for extensive CO₂ transportation equipment.

4.5.2 Comparison of LCOC

A histogram was created for both cases to get an overview of the 1000 random cases compiled for both plants. The plot in Figure 4.5 shows how many cases fell within the same range (bin) of the LCOC for the reference and advanced plants. 713 of the cases for the reference plant fall within the range with an LCOC between 90-120 \$/ton. 543 of the cases for the advanced plant fall within the same range. This means that the advanced plant has a larger range of possible outcomes, especially to the upper end of the LCOC as observed from the figure.

As the reference plant has a relatively stable distribution, the advanced plant can be cheaper often when multiple parameters fall to the low end of the range. At the same time, the plot indicates that the advanced plant is also more likely to have a higher total cost than the reference plant. The main reason for the bounds to be wider for the advanced plant is due to having more uncertainty parameters and generally showing a larger sensitivity to the shared parameters. The extensive range between the upper and lower bounds for the advanced plant implies substantial uncertainty in the central case estimates presented in earlier sections. Still, the more expensive cases could be affordable in the future, whereas the less expensive cases will be highly attractive economically. The “World Energy Outlook” has projected CO₂ prices for the APS for Organization for Economic Cooperation and Development countries (excluded Mexico) to be at 135 \$/ton in 2030, 175 \$/ton in 2040, and 200 \$/ton in 2050. In the NZE scenario, the CO₂ price is assumed to be 250 \$/ton in 2050, making all the cases for the advanced plant highly profitable.

The difference in LCOC was calculated for the reference and advanced plant, resulting in the distribution shown in Figure 4.6. In 58.8% of the 1000 cases, the reference plant would be the cheapest option compared to the LCOC of the advanced plant. The median and 90% confidence interval for the reference plant is 100.5 (76.1-141.3) \$/ton. For the advanced plant, the median and 90% confidence interval is 109 (72.9-161.9) \$/ton. This indicates that there is a

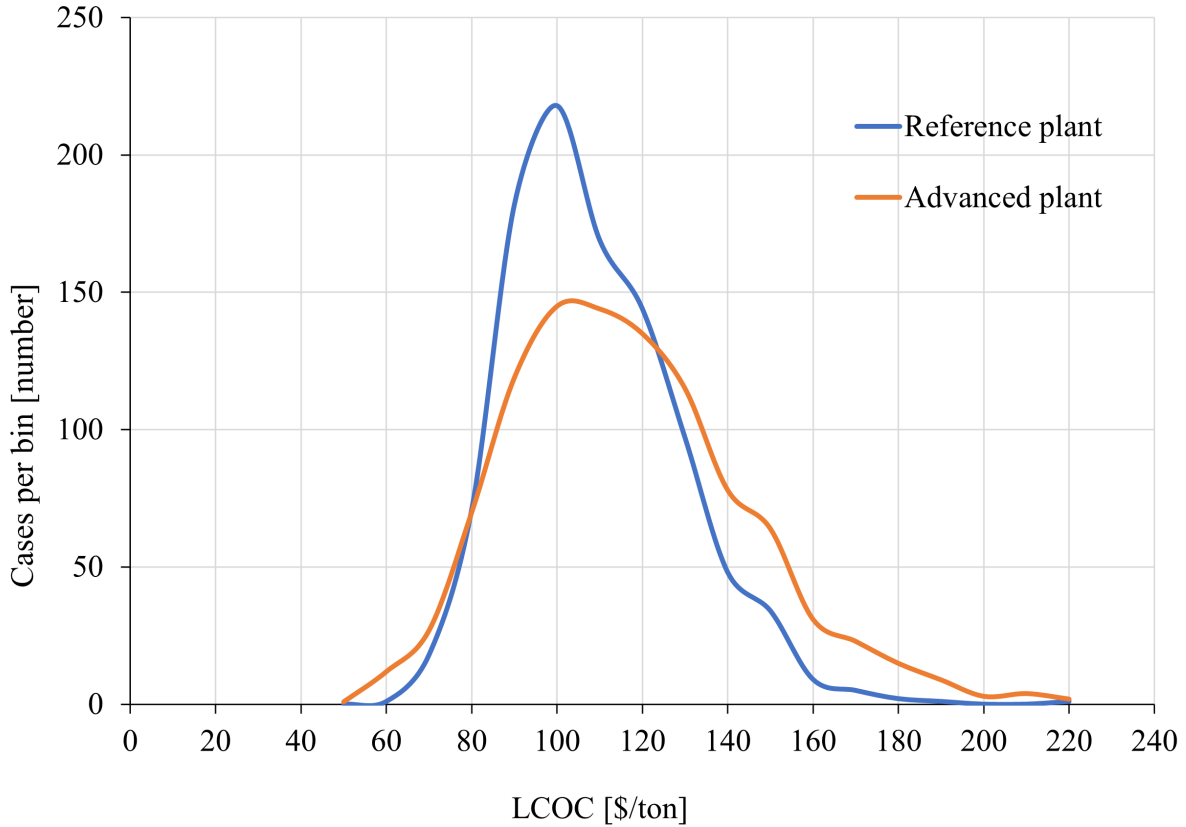


Figure 4.5: LCOC for all 1000 points in the uncertainty quantification for the reference and advanced plant.

90% possibility that the LCOC of the reference plant ranges between 76.1-141.3 \$/ton and the advanced plant ranges between 72.9-161.9 \$/ton. On average, the reference plant is 8.5 \$/ton cheaper than the advanced plant. The reason can be clarified with the same explanation given in the previous paragraph.

One simplification has been made regarding the energy balance producing the uncertainty quantification. Since the energy balance is carefully designed and highly dependent on several components and factors from the UniSim file, it was not feasible to do the UniSim simulation 1000 times. When looking at the DAC energy efficiency, this affects how much CO₂ it is possible to capture, as well as the electricity usage for CO₂ compression and DAC. However, the methodology chosen for this problem, is presented in Section 3.2.4, and would most likely not have a high impact on the results obtained from the uncertainty quantification.

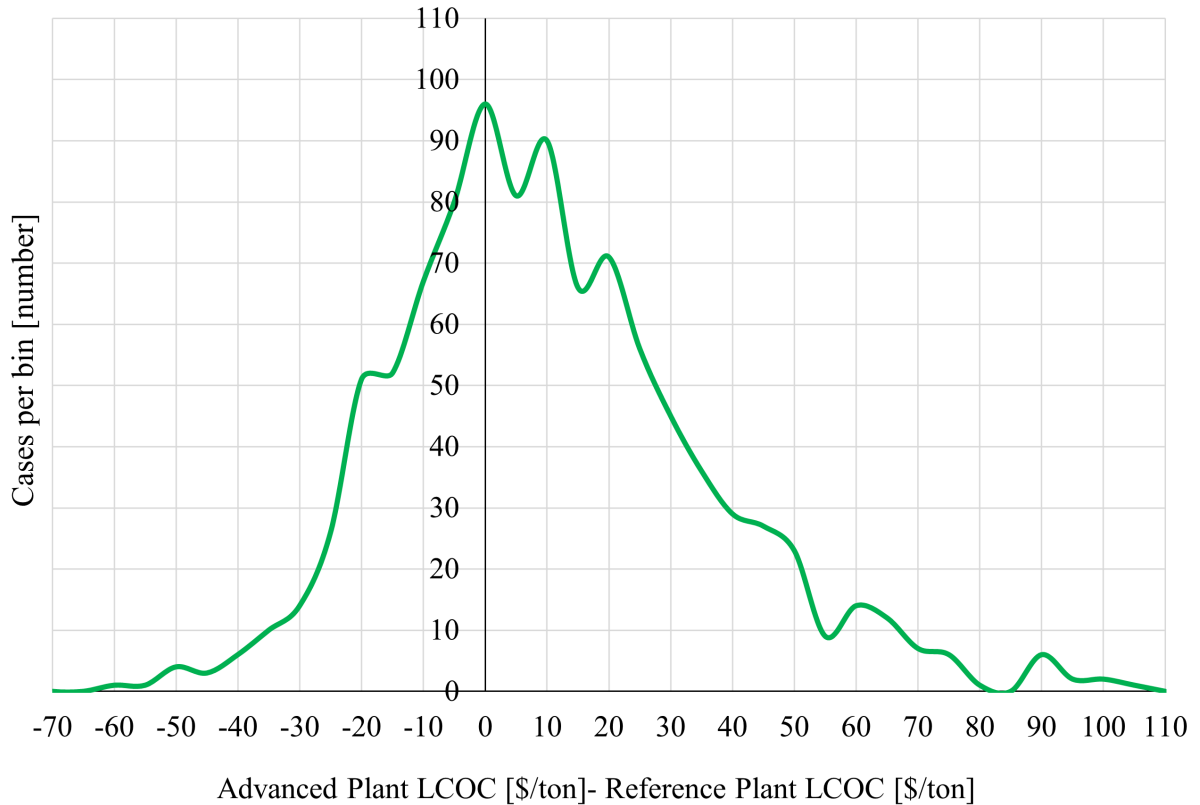


Figure 4.6: A representation of the 1000 cases in the UQ. For a negative x-value, the LCOC for the advanced plant will be lower than the reference plant. For a positive x-value, the LCOC for the reference plant will be lower than for the advanced plant.

4.5.3 Advanced Nuclear Reactor and Methanol Cost Sensitivity

An additional sensitivity analysis was carried out since the advanced nuclear reactor was one of the components associated with the highest cost uncertainty. Figure 4.7 shows the price methanol needs to be sold at with increasing nuclear reactor cost factor to break even with the LCOC for the reference plant. The base case scenario for the advanced nuclear reactor was set to a factor of 1.1, corresponding to a 10% (expressed per kW of heat produced) cost increase compared to the reference nuclear reactor.

For the most optimistic scenarios with a reactor cost factor of 0.7, the methanol can be sold at 258 \$/ton to make the advanced plant competitive. On the other hand, if the advanced nuclear reactor was constructed at a cost factor of 1.6, the methanol price needs to reach 771 \$/ton to break even with the LCOC for the reference plant. If the latter becomes the case, an advanced plant with hydrogen and methanol production will not be economically compatible with today's methanol production. For comparison, as of January 2020, the global average methanol price was about 290 \$/ton [98]. However, the methanol price has increased to around 350-450 \$/ton up until June 2022 [99]. If a CO₂ tax of 100 \$/ton was implemented, this would benefit green methanol since the usage of grey methanol would increase by 138 \$/ton (calculated based on molecular weight for methanol and CO₂).

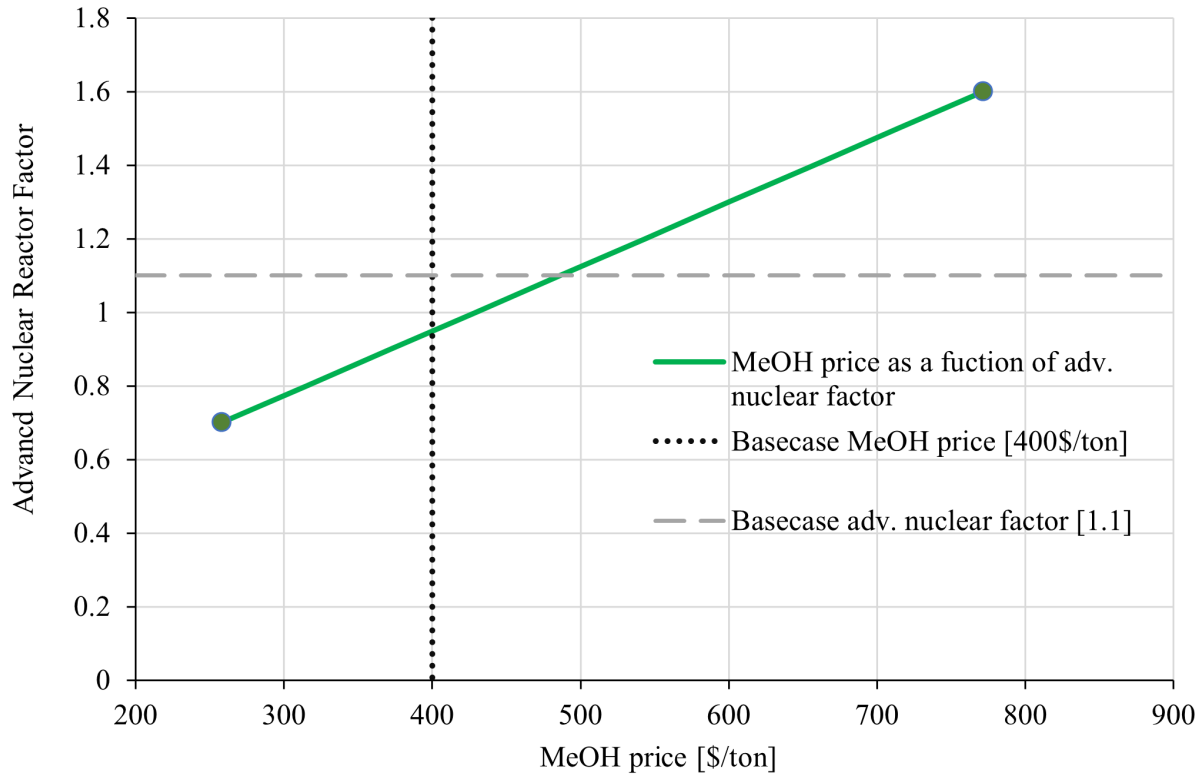


Figure 4.7: The correlation between MeOH sale price and advanced nuclear reactor factor to make the advanced plant break even with the reference plant. Factor 1 corresponds to 1000 $\$/\text{kW}_h$.

Some of the advanced reactors use other working fluids than water. Several fourth-generation reactors utilize working fluids such as molten salt, helium, lead, and sodium. This would increase the cost due to a more exotic working fluid than water. The advanced reactor cost would also be increased due to the higher reactor temperature. Third-generation nuclear reactors typically range from 290-400 °C, while fourth-generation reactors range from 480-1000 °C, resulting in a possible temperature increase of over 700 °C [37]. Meanwhile, some advanced reactor features readily increase the cost they could become cheaper due to lower operating pressures and possibly some inherent safety features. LucidCatalyst is an international company that specializes in techno-economic projects. They carried out a study on behalf of a modeling-enhanced innovations trailblazing nuclear energy reinvigoration program, aiming to determine the highest allowable capital cost for advanced reactors by mid-2030 in the U.S (the U.S accounts for 30% of worldwide nuclear generation). They concluded that advanced nuclear reactors need to reach a cost of less than 3000 $\$/\text{kW}_e$ to be attractive to investors and owners. The same study reveals that advanced nuclear reactors can deliver a large amount of dispatchable power without increasing the total cost of electricity [100].

4.6 Future Outlook: Green Methanol from Nuclear Power Plants

There is no way around that low-carbon electricity generation, negative emission technologies, low-carbon hydrogen, and hydrogen derivatives will play an essential role in meeting global energy needs and decarbonizing our industries, driven by ambitious climate targets. The following paragraphs will discuss crucial future aspects of nuclear energy, DAC scale-up, green methanol production, how the deployment of a carbon tax could influence the big picture, and methanol as a fuel.

Nuclear Power

Nuclear power has been identified as an important energy source, nearly doubling the nuclear power capacity by mid-century in IEA's updated roadmap for NZE by 2050. Despite its ability to generate low-emission electricity, nuclear power faces a divergent future. Due to high up-front costs and long construction times with a poor record of projects delivered on time, nuclear power encounters challenges in some jurisdictions compared to other alternatives, such as natural gas and renewables. In addition, nuclear power plants have to overcome an obstacle in terms of public opposition in several regions. The premature closure of nuclear power plants, whether due to social and political pressure, as observed in Germany, or any other reason before the minimal standard operational lifespan of approximately 20 years, would have a catastrophic impact on the LCOE. Another challenge to overcome is the costly and time-consuming process of safely disposing of spent nuclear fuel. In addition, if nuclear energy were to be massively scaled up, uranium extraction from the earth's crust would be massively enlarged [37].

The nuclear power sector is increasingly worried about the fuel supplies due to Russia's invasion of Ukraine. Russia plays a crucial role in uranium fuel production, representing 38% of global uranium fuel production and over 45% of the fuel enrichment capacity (as of 2020) [7]. This could be a problem if Russia were to stop the export of uranium fuel. However, several other operators have claimed they can deliver uranium fuel if this happens. On the other hand, the Russian invasion of Ukraine has forced nations to rethink their energy security strategies. This has sparked a new initiative for nuclear energy as the government aims to reduce its dependence on energy from other nations, looking at nuclear energy with new eyes. As presented in Section 2.4.10, Sweden decided to phase out nuclear energy in 1980 but has found new interest with plans for new nuclear plants in the coming years, with two reactors operating by 2035, and up to ten new large-scale reactors coming online by 2045 [101].

Considering nuclear as an energy source for driving DAC, as done in the present work, holds the major advantage of allowing the plant to be sited where it is most likely to be constructed at a low cost on time and within budget. The plants could also be placed far from civilization to avoid the challenges of public resistance. Since the electricity produced is utilized on-site, there is no need for transmission infrastructure to a demand center. These factors will have a large positive influence on minimizing costs and maximizing the operational lifetime of nuclear plants. If the electricity or heat from nuclear plants is intended for hydrogen production, the associated cost would be lowered if the hydrogen user was co-located with the nuclear plant, reducing the cost of hydrogen transportation. Therefore, a combination of a nuclear-powered DAC and a

green methanol production plant at the exact location would be a good fit. Even though the plant is located far from civilization, methanol is cheap to transport over long distances, not causing a large increase in operational expenditures.

One concern with the massive scale-up of nuclear-powered DAC plants is the increased fuel consumption and waste handling. According to the IEA, it is 413 GW_e of nuclear capacity today, requiring 1251 GW_h of heat (based on a 33% efficiency for nuclear energy) [7]. If the nuclear-powered DAC plants were to be scaled up, capturing 6 Gt of GHG emissions corresponding to 10% of the world's global GHG emissions, the nuclear fuel consumption as of today would need to be doubled. Since the capacity of electricity from nuclear energy is projected to nearly double in NZE by 2050, the demand for nuclear fuel would be nearly tripled, assuming that the nuclear-fueled DAC plants would be built. This would require a scale-up of uranium mining and new ways to handle nuclear waste. As mentioned earlier, using breeder reactors could ease this problem, reducing the time- and cost-intensive process related to the nuclear fuel cycle.

Nuclear-powered DAC (potentially combined with green methanol production) also makes sense from an efficiency perspective. Today, around 66% of the heat created in nuclear power plants is rejected to the atmosphere in large cooling towers. Suppose the electricity produced in nuclear power plants is used to produce green methanol at 55% efficiency. In that case, only 18% of the original energy in the nuclear fuel ends up in the final methanol product, making it even more important to find a productive use for all the otherwise rejected energy. A study by Wesley Cole et al. in 2023 highlighted five factors that could make nuclear energy more competitive and attractive. One of the listed factors described the attractiveness of utilizing nuclear energy for carbon capture and producing low-carbon hydrogen [102].

Regarding CO₂ avoidance potential, it can be speculated that building nuclear plants producing electricity displacing coal-fired plants would be better than utilizing it for DAC. For example, a 1 GW_e nuclear power plant would produce approximately 8 TWh_e of electricity each year. In comparison, an equally sized coal-fired power plant would produce roughly 8 MtCO₂/y. If the nuclear plant were to replace the coal-fired plant, this would avoid 8 MtCO₂/y. Since the CO₂ removal of the reference plant comes to about 14 MtCO₂/year, this configuration allows us to maximize the climate benefits of nuclear power, even though the cost of CO₂ avoidance will most likely be higher than replacing the coal-fired plant. However, this comparison is not highly relevant for the mid-century timeframes because most of the coal-fired power plants are anticipated to be retired at that point. Since the CO₂ removal of the reference plant comes to about 14 MtCO₂/year, this configuration allows us to maximize the climate benefits of nuclear power, even though the cost of CO₂ avoidance will most likely be higher than replacing the coal-fired plant. However, this comparison is not highly relevant for the mid-century timeframes because most of the coal-fired power plants are anticipated to be retired at that point.

Direct Air Capture

Meeting the Paris Agreement goals will require CO₂ removal from the atmosphere at a gigaton scale. DAC is one promising way to capture CO₂ from the atmosphere, both as a key CDR approach and providing climate-neutral CO₂ needed to produce synthetic fuels. DAC is predicted

to become prominent in the coming decade for the NZE scenario, as highlighted in Figure 4.8. The price of DAC needs to achieve giga scale removal at 100 \$/tonCO₂ according to the IEA to have a meaningful impact in reducing global warming [6]. Currently, this number is 2-7 times higher, addressing the need for innovation across the DAC value chain, hence improving the technology and overcoming the critical bottleneck of lowering DAC system cost. Also, extensive subsidies are needed to lower the price. Currently, DAC is thriving by subsidies by public and private investors, and in 2022, Climeworks raised the largest ever DAC investment of 650 M\$.

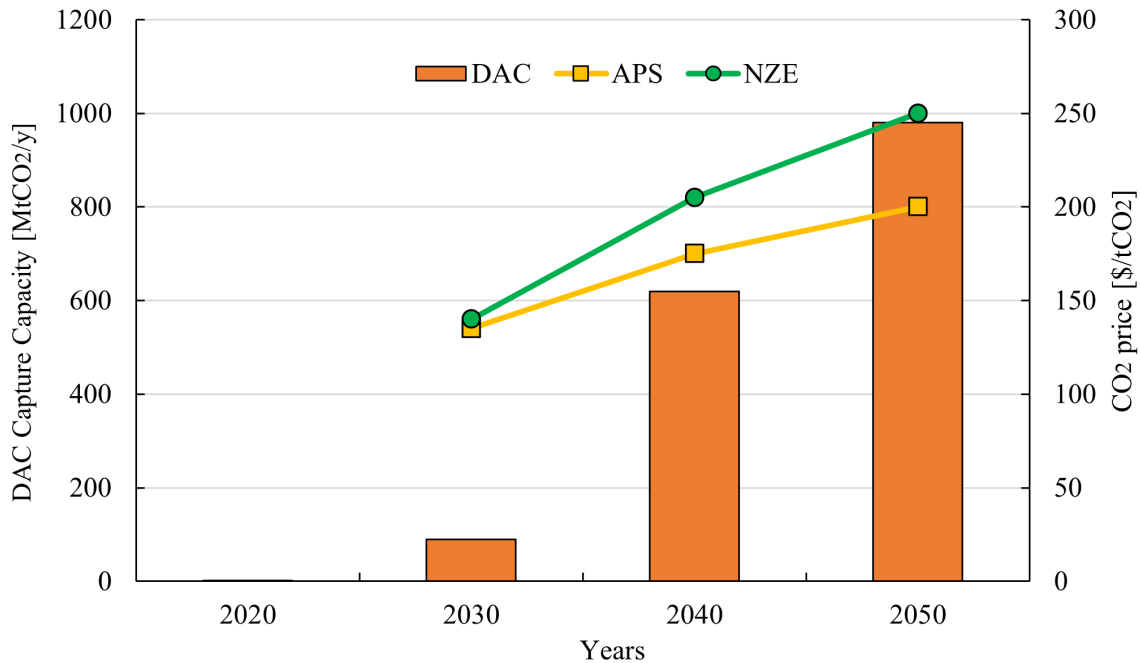


Figure 4.8: Future projections for DAC scale-up capacities to reach NZE by 2050, and projected CO₂ prices for the APS and NZE scenario [6, 62].

Since the CO₂ concentration in the air is much more dilute than the flue gas from a fossil-fueled power plant, DAC requires a significantly higher share of energy to capture CO₂ than other point-source capture methods. The energy provided for DAC must come from low or non-carbon sources to ensure net CO₂ removal. Today, the largest operating DAC facility is powered by geothermal energy in Iceland, with a capture capacity of 4 000 tCO₂/y. Several low-carbon energy sources could power DAC, and the IEA estimates that DAC would have the best chances to become prominent in areas with abundant cheap renewable energy - for example, next to a giant desert solar farm or large wind parks. DAC can also be powered by nuclear energy, which is a good fit since it generates large amounts of heat and electricity. The abovementioned energy sources could power S-DAC. However, challenges remain in how to power L-DAC from low-carbon sources, which operate at high temperatures at 900 °C (600 °C over S-DAC). If this challenge were successfully addressed, studies have shown that L-DAC could perform large-scale CO₂ removal at a lower cost than S-DAC [11]. Accelerating the commercial availability of fully electric L-DAC will be crucial to make L-DAC competitive.

The advanced plants' CO₂ capture rate was calculated to be 457.8 kgCO₂/s, which equals 14.4 MtCO₂/yr. As presented in Section 2.5, the total capture from DAC as of 2023 was 0.1 MtCO₂/yr. The plant would capture 144 times as much CO₂ as the global DAC CO₂ capture capacity. This number may sound unreasonable high. However, as of June 2023, there were only 27 operating facilities with relatively low capacity, and several 1 MtCO₂/yr plants have begun construction. The IEA has predicted that to reach NZE, DAC must capture 980 MtCO₂/year in 2050, requiring a significant and accelerated scale-up. To reach the NZE by 2050 goal, 68 plants of the advanced plant (assuming no CO₂ for methanol synthesis) and 72 of the reference plants need to be built. To put these numbers in perspective, DAC needs to reach a capture rate of 90 MtCO₂/yr in 2030, which only accounts for around 0.3% of the world's annual CO₂ emissions (based on CO₂ emissions from 2022). This implies that the effort to mitigate global warming relies not only on the importance of NET but also on a broad portfolio of other emissions reduction technologies and a substantial shift in human behavior and the habits contributing to the rise of CO₂ concentration in the atmosphere

Implementation of a CO₂ Tax

The CO₂ tax could contribute to making DAC viable at scale. As presented in Section 2.5.5, IEA identified that with a carbon tax of 130 \$/tCO₂ in 2030, all of the regions in the respective study would reach gigaton capture cost under 100 \$/tCO₂ [6]. If this tax was combined with the value of the captured CO₂, the process could be economically profitable in the future. Ideally, there would be a fixed global international CO₂ tax, where NET would receive the tax from the government for each ton of CO₂ withdrawn from the atmosphere. However, in the real world, this would likely be more complex. As mentioned above, DAC needs to be placed in areas where construction and energy prices are low, and the world must somehow pay these countries to combat the world's problem of climate change. This is a complex issue, and it is impossible to predict with certainty what such agreements might look like.

The implementation of a CO₂ tax would also contribute to lowering the cost of electrolytic hydrogen production. The rapid expansion of low-emissions hydrogen is a key pillar of the NZE scenario, with related investment rising from near zero today to 80 \$billion per year by 2040. To get on track with the NZE scenario, more than 550 GW of electrolyzers will be installed globally by 2030, indicating an increase between 1.5 and 3 times the capacity of all announcements today. Indications from the Chinese market show a trend of building larger electrolysis projects in the hundreds of MW scale [72]. Green hydrogen production will have a hard time becoming cost-competitive with blue or grey hydrogen production unless a tax on emitting CO₂ into the atmosphere is widely enforced.

As seen in Figure 4.8, the CO₂ price is expected to reach levels of 200 \$/tonCO₂ by the mid-century for the APS and NZE scenario. This is much higher than the LCOC calculated in this thesis at approximately 100 \$/tonCO₂. If the CO₂ tax is implemented as predicted and nuclear DAC plants can be built at a price estimated in this work, nuclear DAC facilities would become enormously attractive for investors, triggering a massive rollout of these facilities. As the amount of CO₂ removed from the atmosphere increases, climate targets will be more easily met, and the CO₂ price will fall. This could lead to an equilibrium of the CO₂ price, stabilizing right above

the price of nuclear DAC technology. This would make it hard for other CDR technologies with LCOC above 100 \$/ton to compete economically. From an economic point of view, it would be more suitable for some hard-to-abate sectors, like aviation, to keep emitting CO₂ and then capture it with DAC from the atmosphere

Green Methanol

Currently, the cost of green methanol is significantly higher compared to methanol from fossil fuels and depends to a large extent on the cost of hydrogen and CO₂. Even though the TRL for green methanol production is high, carbon accounting and availability are major obstacles to its widespread adoption and cost reduction. The majority of the literature found in this work identifies the deployment of a carbon tax as a critical path for making green methanol competitive. CO₂ derived liquid fuels, such as methanol, will continue to be uncompetitive in the absence of a strict CO₂ policy compared to the cost of diesel, oil, or gasoline. IRENAs future outlook for methanol innovation found that even though the cost of green methanol is high and production volumes low, it could become cost competitive by 2050 or earlier, indicating that renewable methanol could be widely adopted on a future time scale [9].

A techno-economic study conducted by Sollia et al. investigated the production of green methanol with hydrogen production from a PEM electrolyzer and CO₂ from a point source. The study showed that the levelized cost of methanol (LCOM) was 960 €/t, over double the price that green methanol is currently sold at. However, the same study found that the respective technology can become economically profitable as early as 2030-2035. This is due to the combined effect mainly from the increase in green methanol sale price, reduction of the capital cost and increase of commercial maturity for electrolyzers, lowered price of renewable electricity, and the expected employment and increase in CO₂ tax price.[83]

The limiting factors in terms of scaling up a green methanol plant are highly dependent on the availability and price of hydrogen, CO₂, and the source of electricity [84]. In addition, the production of green methanol needs substantial subsidies to drive projects and development in the right direction. Furthermore, it requires a shift in our approach to economic profitability. Achieving progress in green innovation projects needs to take a step away from the anticipation of significant financial returns on these kinds of projects. A fundamental shift in human behavior is imperative to render this sustainable in the long term. Also, a change in green innovation and economic thinking needs to change, and the investment in clean energy needs to more than triple by 2030 to around 4 \$trillion to reach NZE [3].

Even though green methanol is expensive to produce, it is interesting to compare it to an everyday life product. The average petrol price in Norway in 2023 was 2.1 \$/l (21.5 NOK/l). The LHV of petrol is approximately 32 MJ/l, corresponding to a petrol cost of 65.9 \$/GJ. Assuming a price of 400 \$/ton of methanol and that the LHV for methanol is 19.7 GJ/ton, results in 20.3 \$/GJ. This is less than 1/3 of the price Norwegians pay for petrol. The reason why Norwegian petrol is so expensive is the massive taxation. However, this shows that green fuels can be affordable even though they are more expensive to produce.

Green Methanol From Different Energy Sources

Several parties have investigated green methanol production from renewable energy sources. Methanol synthesis requires a steady flow of synthetic gas into the facility. Considering the lack of constant wind and solar power availability with low capacity factors, some storage devices need to be implemented. If hydrogen was produced with water electrolysis, hydrogen would need to be compressed and stored due to the fluctuating electricity production from renewables. Pressurization of hydrogen for storage requires a fair share of energy, and hydrogen gas is highly flammable and can easily escape containment. The need for proper and safe equipment would increase capital and maintenance costs for the plant.

Using nuclear energy could avoid the additional storage equipment due to the stable electricity and heat production. Nuclear energy has a high capacity factor with an average of 92% compared to 10-25% for solar and 30-45% for wind, which could make nuclear energy an attractive alternative for green methanol production. Stable electricity and heat production from nuclear energy present new opportunities for the production of green hydrogen, which is crucial for green methanol production. On the other hand, as presented in Section 2.6.4, a study conducted by the IEA for hydrogen production shows that in almost all cases, hydrogen from renewables would be cheaper than hydrogen from nuclear energy. In some cases, when nuclear power reaches total overnight costs of less than 2000 \$/kW_e, H₂ from nuclear production could compete with H₂ produced by renewables. According to the same study, renewables and nuclear energy for H₂ production are currently much more expensive than H₂ from coal and natural gas, emphasizing the need of a CO₂ tax [6].

A study by Arnaiz del Pozo et al. compared the LCOM for different ways to produce 10 000 tMeOH/d. One of the production methods was to utilize wind and solar power for hydrogen production and the waste heat generated in the PEM model for DAC purposes. The cost assumptions for DAC were set to 2050 predictions. Even though a 100 €/ton CO₂ credit was included, the cost of renewable methanol production continued to be significantly higher than the natural gas-based alternatives. The study also found that the overall cost was significantly lower using CO₂ from pipelines. For methanol production using CO₂ from pipelines and DAC CO₂ to break even with the conventional natural gas routes, a CO₂ credit of 121.3–146.7 €/ton and 300 €/ton was needed [13]. Since the DAC unit is the largest contributor to the capital cost in this thesis, using CO₂ imported from pipelines could potentially lower the LCOC, although this strategy is questionable from a climate perspective if the pipeline CO₂ is from fossil origin. However, it is essential to consider that CO₂ transportation suffers from a lack of pipeline infrastructure connecting industrial sites to CO₂ capture facilities.

Methanol as a Transportation Fuel

Methanol as a fuel has the potential to substantially reduce GHG emissions compared to traditional fossil fuels. Using methanol in a spark-ignition engine can actively contribute to sustainable development and circumstantially reduce the carbon footprint in the transportation sector. Also, the engine can deliver more power at a higher efficiency due to methanol's high octane number, allowing a higher compression ratio. A pivotal reason to further investigate methanol

as a transportation fuel is the easy upscaling of production. Methanol synthesis is a well-known, straightforward process that can employ a relatively wide range of raw material feedstocks. The chemical properties of methanol make the fuel easier and less expensive to store than hydrogen. However, methanol as a fuel has several challenges that must be addressed.

One major drawback of methanol is the low energy density as described in Section 2.7.2. This means that methanol almost weighs the same as diesel but holds slightly less than half of the energy. In addition, methanol has about half the volumetric density as diesel and gasoline. This means that the fuel tanks need to be adjusted to store the same amount of energy. This could significantly affect transportation units like ships and flights with limited space for fuel storage. However, methanol has a higher energy density than other alternative shipping fuels, including LNG, ammonia, and hydrogen, favoring methanol over the aforementioned fuels.

Another critical challenge to overcome is the accessibility and availability of methanol. Since methanol has different properties compared to the most used fuels, some changes to the infrastructure may be needed. To ensure a transition to methanol as a substitute for gasoline, significant capital and comprehensive planning are needed to facilitate progress in infrastructure development. Also, there will be a need to build multiple fuelling stations for methanol. Currently, there is a long distance between fuelling stations, especially in remote areas. Even though there is a lack of infrastructure and methanol fuelling stations, this problem could be avoided by rolling out methanol for the shipping industry. Ships could sail in and tank from the cost line if the plant producing green methanol is located close to the sea or by transporting methanol at low cost to a filling station near shore. Methanol as fuel has been identified as a path to reduce emissions in the shipping industry, with world-leading companies investing in methanol vessels. Maersk has set a net zero greenhouse gas emissions target for 2040 and has ordered 18 methanol vessels with plans for more [103].

Producing methanol as a renewable synthetic fuel is highly cost-intensive. Over time, production costs of CO₂-derived fuels are expected to come down, mainly due to capital cost reductions, availability of low-cost renewable electricity and feedstock CO₂, and economic subsidies. Several initiatives and plans have been announced to implement subsidies for synthetic fuels, primarily hydrogen and hydrogen-derived products, as a part of the energy transition away from fossil fuels. These subsidies include incentives facilitating the development and deployment of synthetic fuels. There is also substantial economic support for carbon tax initiatives and grants for pilot projects. Enrolling subsidies could introduce methanol as a fuel at a large scale for industrialized countries. However, an important challenge that needs to be addressed is how to raise enough finances required to adopt methanol or other synthetic fuels in developing countries.

The transformation from conventional gasoline and diesel to pure methanol can prove challenging. Today, few machines operate with pure methanol as fuel. This causes a causality dilemma. Large quantities of affordable methanol are needed before these machines will be developed and produced at scale to consume the methanol fuel. At the same time, a large methanol demand is needed before new sustainable methanol production processes can be scaled up to drive down costs. One solution could be to blend methanol into conventional fuels. However, comprehensive testing is needed to determine how much methanol could be blended into diesel or gasoline and

how much modification the engine needs for a higher methanol percentage blend. Hassan et al. carried out a study of a methanol blend in an internal combustion diesel engine. A methanol volume blend of up to 14% improved the performance of the fuel. A further increase of the blending ratio resulted in faulty ignition quality [104].

5 Conclusion

Governments worldwide have set ambitious goals and strategies to achieve NZE, reducing the negative consequences of climate change. One critical pathway for achieving NZE is to reduce accumulated CO₂ in the atmosphere and to recycle CO₂ in a closed-loop principle. In addition, synthetic fuels produced using recycled CO₂ have received increased interest in decarbonizing hard-to-abate sectors such as heavy transport, aviation, and shipping.

This thesis compares two plants intended to be constructed in the mid-century that use nuclear power for DAC: the reference plant, which utilizes a third-generation nuclear reactor for CO₂ capture, and the advanced plant, which employs a fourth-generation nuclear reactor, using excess electricity after DAC for hydrogen production by PEM electrolyzer combined with DAC CO₂ for green methanol production. Nuclear combined with DAC was assumed to be a good fit given the substantial heat required in the DAC process and the large amount of waste heat generated in nuclear power plants. First, a comprehensive technical simulation of both plants was conducted in UniSim Design R492 before an in-depth economic assessment, including an uncertainty quantification, was conducted with the SEA tool.

This work indicates that the reference plant is marginally more economically favorable to build than the advanced plant under central assumptions. The LCOC for the reference plant was 98.3 \$/ton and 104.9 \$/ton for the advanced plant. This increase is due to capital expenditures linked to a larger nuclear plant, a fourth-generation nuclear reactor, and additional costs for methanol synthesis, not being fully recuperated by the assumed methanol sales price of 400 \$/ton. The plants could be highly economically feasible if the CO₂ price is rolled out and implemented globally following projections reaching 200 \$/ton or more by mid-century. If the nuclear DAC plants were largely enforced in the future, this could eventually put a cap on the CO₂ price, reaching an equilibrium just above the LCOC for the plants. However, constraints such as the availability of nuclear fuel and, more importantly, the complex waste handling need to be addressed. If the reference plant were massively employed to capture 10% of the global GHG emissions, fuel consumption would nearly be doubled, representing a significant increase in nuclear waste. The breeder nuclear reactor produces more fissionable material than it consumes and presents a solution to this problem.

The CO₂ captured by the reference plant was 14 MtCO₂/y and 14.4 MtCO₂/y for the advanced plant. If this technology was scaled up for mass production, this could contribute to reaching the DAC targets outlined in the NZE scenario. Furthermore, the captured CO₂ breakdown for the advanced plant shows that 90.5% of the CO₂ was sent to compression and storage, with the remaining 9.5% utilized for green methanol production. The production of the methanol plant was 2 735 tMeOH/d, equaling a large facility with an efficiency of 54.3%. Two central factors in the choice between the reference and the advanced plants are the methanol sales price and the rise in cost for fourth-generation nuclear reactors. If the advanced reactor can be constructed at the exact cost (per unit heat output) as current reactors, the methanol price must be 429 \$/ton to break even. However, if the advanced reactor were 50% more expensive than the current reactors, the breakeven price would rise to 714 \$/ton.

The uncertainty quantification showed that in 58.8% of the 1000 instances examined, the reference plant would result in a lower LCOC than the advanced plant. The median and 90% confidence interval for the reference and advanced plants were 100.5 (76.1-141.3) \$/ton and 109.0 (72.9-161.9) \$/ton, respectively. This means that both plants are highly likely to become economically profitable if the CO₂ price reaches the projected values of 200 \$/ton in the APS and 250 \$/ton in the NZE scenario by 2050. The two main uncertainty factors of the respective plants are the expenditures associated with nuclear reactors and DAC units. Nuclear uncertainty is mainly linked to the reactor cost, augmented by uncertainties about next-generation technology costs for the advanced plant. DAC uncertainty is related to capital costs and energy efficiency. These factors are found by the results from the uncertainty quantification and confirmed in the existing literature. This work has assumed a significant cost reduction for DAC units, and innovation is needed across the DAC value chain to lower the respective cost. Also, rapid scale-up and commercializing of DAC and fourth-generation nuclear reactors are needed to determine and drive costs down.

Even though the IEA estimates that hydrogen and hydrogen-based fuels, such as methanol, could potentially provide a quarter of the energy needed by 2050 in the NZE scenario, it is hard to predict the exact role of the respective energy carriers [10]. The high production cost is the major challenge to overcome in adapting green methanol as a liquid fuel today. The role of methanol will depend on several factors, such as policy decisions, technological developments, and economic conditions. CO₂-derived methanol could emerge as a competitive option in some regions depending on the local methanol price and the implementation of a CO₂ price. However, the widespread adoption of pure methanol is far ahead on a time scale. One strategic approach to facilitate a gradual transition from fossil fuels to pure methanol is blending conventional fuels with methanol, which has demonstrated positive effects in pilot projects.

5.1 Future Work

This study indicates that nuclear-fueled DAC and nuclear-fueled DAC combined with green methanol production could become economically beneficial by mid-century. However, several aspects need to be addressed before, such as researching and optimizing nuclear reactor designs, especially emphasizing the importance of breeder reactors to enable massive scaling of this technology without concerns about fuel supply and waste disposal. Furthermore, governments worldwide should undertake initiatives to improve the public perception of nuclear energy.

Further work should be directed to the exploration and development of DAC technology, which is crucial to lowering the significant related cost and ensuring rapid scale-up. In addition, L-DAC could be prominent in removing CO₂ from the atmosphere at a large scale. However, the technology needs further development to become fully electrified to ensure net CO₂ removal. Developing a policy that employs a CO₂ tax globally is essential to make green initiatives and innovation more competitive. The provision of an international CO₂ credit for NET will be essential for nuclear DAC plants that will be concentrated in countries capable of constructing nuclear reactors at the lowest cost. Finally, more research is needed to explore the viability of blending methanol into fossil fuels to ensure a transition from fossil-based fuels within a reasonable timeframe.

References

- [1] European Parliament. *COP28 climate talks agree on transitioning away from fossil fuels*. Dec. 13, 2023. URL: <https://www.europarl.europa.eu/news/en/press-room/20231205IPR15686/cop28-climate-talks-agree-on-transitioning-away-from-fossil-fuels> (visited on 12/28/2023).
- [2] Rebecca Lindsey. *Climate Change: Atmospheric Carbon Dioxide*. May 12, 2023. URL: <http://www.climate.gov/news-features/understanding-climate/climate-change-atmospheric-carbon-dioxide> (visited on 05/27/2023).
- [3] IEA. *Net Zero by 2050 – Analysis*. IEA. May 2021. URL: <https://www.iea.org/reports/net-zero-by-2050> (visited on 12/05/2023).
- [4] IPCC. *Sixth Assessment Report — IPCC*. Apr. 2022. URL: <https://www.ipcc.ch/assessment-report/ar6/> (visited on 11/19/2023).
- [5] Mahdi Fasihi, Olga Efimova, and Christian Breyer. “Techno-economic assessment of CO2 direct air capture plants”. In: (July 1, 2019). URL: <https://www.sciencedirect.com/science/article/pii/S0959652619307772> (visited on 11/10/2023).
- [6] International Energy Agency. *Direct Air Capture: A key technology for net zero*. Apr. 20, 2022. URL: https://read.oecd-ilibrary.org/energy/direct-air-capture_bbd20707-en (visited on 11/16/2023).
- [7] IEA. *Nuclear Power and Secure Energy Transitions*. IEA. June 2022. URL: <https://www.iea.org/energy-system/electricity/nuclear-power> (visited on 12/04/2023).
- [8] IEA. “Pathway for liquid fuels”. In: *World Energy Outlook 2022* (Sept. 2022). (Visited on 09/13/2023).
- [9] IRENA. *Innovation Outlook: Renewable Methanol*. Jan. 27, 2021. URL: <https://www.irena.org/publications/2021/Jan/Innovation-Outlook-Renewable-Methanol> (visited on 11/23/2023).
- [10] IEA. *Executive summary – Global Hydrogen Review 2021 – Analysis*. 2021. URL: <https://www.iea.org/reports/global-hydrogen-review-2021/executive-summary> (visited on 11/29/2023).
- [11] Nicolas E. Stauff, Mann W. Neal et al. *Assessment of Nuclear Energy to Support Negative Emission Technologies*. Sept. 7, 2023. URL: chrome-extension://efaidnbmnnnibpcjppcgklcfindmkaj/https://fuelcycleoptions.inl.gov/SiteAssets/SitePages/Home/Nuclear_to_support_NET_final.pdf (visited on 10/11/2023).
- [12] Carlos Arnaiz del Pozo, Ángel Jiménez Álvaro, and Schalk Cloete. “Methanol from solid fuels: A cost-effective route to reduced emissions and enhanced energy security”. In: (Oct. 15, 2022). URL: <https://www.sciencedirect.com/science/article/pii/S0196890422010494> (visited on 09/21/2023).
- [13] Carlos Arnaiz del Pozo, Schalk Cloete, and Ángel Jiménez Álvaro. “Techno-economic assessment of long-term methanol production from natural gas and renewables”. In: (Aug. 15, 2022). URL: <https://www.sciencedirect.com/science/article/pii/S0196890422005817> (visited on 09/21/2023).
- [14] IEA. “Global Energy and Climate Model”. In: (Oct. 2023). URL: <https://www.iea.org/reports/global-energy-and-climate-model> (visited on 12/13/2023).

- [15] Andrew Rex. *Mere Thermodynamics*. 2009. URL: https://web.p.ebscohost.com/ehost/ebookviewer/ebook/bmx1YmtfXzMwMzg3N19fQU41?sid=1bb79dc5-e48f-46b4-9f2a-60f49e443b78@redis&vid=0&format=EB&lpid=lp_45&rid=0 (visited on 12/28/2023).
- [16] Claire Yu Yan. “2.3 Phase diagrams”. In: *Book Title: Introduction to Engineering Thermodynamics*. Sept. 1, 2022. URL: <https://pressbooks.bccampus.ca/thermo1/chapter/phase-diagrams/> (visited on 11/15/2023).
- [17] Dheeraj Shankarrao Bhiogade. “Ultra supercritical thermal power plant material advancements: A review”. In: (Sept. 1, 2023). URL: <https://www.sciencedirect.com/science/article/pii/S294991782300024X> (visited on 12/28/2023).
- [18] G. Lucacci. “7 - Steels and alloys for turbine blades in ultra-supercritical power plants”. In: *Materials for Ultra-Supercritical and Advanced Ultra-Supercritical Power Plants*. Jan. 1, 2017, pp. 175–196. URL: <https://www.sciencedirect.com/science/article/abs/pii/B9780081005521000075> (visited on 11/15/2023).
- [19] Modeste Tchakoua Tchouaso, Tariq Rizvi Alam, and Mark Antonio Prelas. “Chapter Seventeen - Space nuclear power: Radioisotopes, technologies, and the future”. In: *Photovoltaics for Space*. Jan. 1, 2023, pp. 443–488. URL: <https://www.sciencedirect.com/science/article/pii/B9780128233009000145> (visited on 11/15/2023).
- [20] Knut Hofstad. *Rankine-syklus*. In: *Store norske leksikon*. Jan. 25, 2023. URL: <https://snl.no/Rankine-syklus> (visited on 11/15/2023).
- [21] Hsihsa Otham. “Vapor Power Cycles”. In: (2023). URL: https://www.academia.edu/29319692/Vapor_Power_Cycles (visited on 11/15/2023).
- [22] Buck Feng. *Power Plant Efficiency: Coal, Natural Gas, Nuclear, and More*. Apr. 17, 2023. URL: <https://www.pcienergysolutions.com/2023/04/17/power-plant-efficiency-coal-natural-gas-nuclear-and-more/> (visited on 11/15/2023).
- [23] Ibrahim Dincer and Calin Zamfirescu. “Chapter 5 - Conventional Power Generating Systems”. In: *Advanced Power Generation Systems*. Jan. 1, 2014. URL: <https://www.sciencedirect.com/book/9780123838605/advanced-power-generation-systems>.
- [24] Carlos Arnaiz del Pozo, Schalk Cloete, and Ángel Jiménez Álvaro. *SEA Tool User Guide*. 2020. URL: <https://github.com/SINTEF/Scale-Coupled-Open-Innovation-Network/blob/main/Economics/SEA%20Tool%20-%20User%20Guide.docx> (visited on 11/15/2023).
- [25] Caesar Wu and Rajkumar Buyya. “Chapter 14 - Cost Modeling: Terms and Definitions”. In: *Cloud Data Centers and Cost Modeling*. Jan. 1, 2015. URL: <https://www.sciencedirect.com/book/9780128014134/cloud-data-centers-and-cost-modeling> (visited on 11/15/2023).
- [26] Raymond L. Murray and Keith E. Holbert. “Part 1: Basic concepts”. In: *Nuclear Energy (Seventh Edition)*. Jan. 1, 2015, pp. 515–522. URL: <https://www.sciencedirect.com/science/article/pii/B9780124166547099895> (visited on 09/15/2023).
- [27] Raymond L. Murray and Keith E. Holbert. “Chapter 18 - Nuclear power plants”. In: *Nuclear Energy (Seventh Edition)*. Jan. 1, 2015, pp. 291–313. URL: <https://www.sciencedirect.com/book/9780124166547/nuclear-energy> (visited on 11/24/2023).
- [28] World Nuclear Association. *Nuclear Power Today | Nuclear Energy - World Nuclear Association*. Aug. 2023. URL: <https://world-nuclear.org/information-library/cu>

- urrent-and-future-generation/nuclear-power-in-the-world-today.aspx (visited on 11/24/2023).
- [29] International Atomic Energy Agency. *Small Modular Reactor (SMR) Regulators' Forum*. Jan. 18, 2018. URL: <https://www.iaea.org/topics/small-modular-reactors/smr-regulators-forum> (visited on 01/12/2024).
- [30] Office of Nuclear Energy. *What's the Lifespan for a Nuclear Reactor? Much Longer Than You Might Think*. July 2022. URL: <https://www.energy.gov/ne/articles/whats-lifespan-nuclear-reactor-much-longer-you-might-think> (visited on 11/24/2023).
- [31] World Nuclear Association. *Nuclear Decommissioning: Decommission nuclear facilities - World Nuclear Association*. May 2022. URL: <https://world-nuclear.org/information-library/nuclear-fuel-cycle/nuclear-wastes/decommissioning-nuclear-facilities.aspx> (visited on 11/25/2023).
- [32] US department of nuclear energy. *NUCLEAR 101: How Does a Nuclear Reactor Work?* Mar. 29, 2021. URL: <https://www.energy.gov/ne/articles/nuclear-101-how-does-nuclear-reactor-work> (visited on 04/12/2023).
- [33] Nasser Awwad, ed. *Nuclear Power Plants : The Processes from the Cradle to the Grave*. 2021. URL: <https://directory.doabooks.org/handle/20.500.12854/67874> (visited on 11/24/2023).
- [34] World Nuclear Association. *Uranium Supplies: Supply of Uranium - World Nuclear Association*. Aug. 2023. URL: <https://world-nuclear.org/information-library/nuclear-fuel-cycle/uranium-resources/supply-of-uranium.aspx> (visited on 12/29/2023).
- [35] Office of Nuclear Energy. *NUCLEAR 101: How Does a Nuclear Reactor Work?* Energy.gov. Aug. 2, 2023. URL: <https://www.energy.gov/ne/articles/nuclear-101-how-does-nuclear-reactor-work> (visited on 11/24/2023).
- [36] World Nuclear Association. *Safety of Nuclear Reactors - World Nuclear Association*. Mar. 2022. URL: <https://world-nuclear.org/information-library/safety-and-security/safety-of-plants/safety-of-nuclear-power-reactors.aspx> (visited on 12/04/2023).
- [37] World Nuclear Association. *Generation IV Nuclear Reactors: WNA - World Nuclear Association*. Dec. 2020. URL: <https://world-nuclear.org/information-library/nuclear-fuel-cycle/nuclear-power-reactors/generation-iv-nuclear-reactors.aspx> (visited on 11/25/2023).
- [38] GIF. *Home - Generation IV Systems*. Sept. 2013. URL: https://www.gen-4.org/gif/jcms/c_59461/generation-iv-systems (visited on 11/23/2023).
- [39] World Nuclear Association. *Nuclear Process Heat - World Nuclear Association*. Sept. 2021. URL: <https://world-nuclear.org/information-library/non-power-nuclear-applications/industry/nuclear-process-heat-for-industry.aspx> (visited on 11/23/2023).
- [40] World Nuclear Association. *Nuclear Power Reactors | How does a nuclear reactor work? - World Nuclear Association*. May 2023. URL: <https://world-nuclear.org/information-library/nuclear-fuel-cycle/nuclear-power-reactors/nuclear-power-reactors.aspx> (visited on 11/23/2023).

- [41] Energy Education. *Breeder reactor*. June 19, 2015. URL: https://energyeducation.ca/encyclopedia/Breeder_reactor (visited on 01/10/2024).
- [42] John van Zalk and Paul Behrens. “The spatial extent of renewable and non-renewable power generation.” In: (Dec. 1, 2018). URL: <https://www.sciencedirect.com/science/article/pii/S0301421518305512> (visited on 05/01/2023).
- [43] World Nuclear Association. *Nuclear Power Economics*. Aug. 2022. URL: <https://world-nuclear.org/information-library/economic-aspects/economics-of-nuclear-power.aspx> (visited on 05/08/2023).
- [44] IEA. *Projected Costs of Generating Electricity*. 2020. URL: <https://www.iea.org/reports/projected-costs-of-generating-electricity-2020> (visited on 12/01/2023).
- [45] ACIL. *Projected energy prices in selected world regions*. May 2008. URL: chrome-extension://efaidnbmnnnibpcajpcgglefindmkaj/https://treasury.gov.au/sites/default/files/2019-07/low-pollution-future_ACIL-Tasman.pdf (visited on 12/04/2023).
- [46] Javier Palacios et al. “Levelized Costs for Nuclear, Gas and Coal for Electricity, under the Mexican Scenario”. In: (Oct. 6, 2004). URL: <chrome-extension://efaidnbmnnnibpcajpcgglefindmkaj/https://www.osti.gov/servlets/purl/840500> (visited on 05/10/2023).
- [47] Rod Adams. *Nuclear Energy Is Cheap and Disruptive; Controlling the Initial Cost of Nuclear Power Plants is a Solvable Problem - Atomic Insights*. Feb. 6, 2010. URL: <https://atomicinsights.com/nuclear-energy-is-cheap-and-disruptive-controlling-the-initial-cost-of-nuclear-power-plants-is-a-solvable-problem/> (visited on 05/04/2023).
- [48] Daniel Weisser. “A guide to life-cycle greenhouse gas (GHG) emissions from electric supply technologies”. In: (Sept. 1, 2007). URL: <https://www.sciencedirect.com/science/article/pii/S036054420700028X> (visited on 05/26/2023).
- [49] Jie Yang et al. “How Social Impressions Affect Public Acceptance of Nuclear Energy: A Case Study in China”. In: 18 (Jan. 2022). URL: <https://www.mdpi.com/2071-1050/14/18/11190> (visited on 11/25/2023).
- [50] World Nuclear Association. *Plans for New Nuclear Reactors Worldwide*. Aug. 2023. URL: <https://world-nuclear.org/information-library/current-and-future-generation/plans-for-new-reactors-worldwide.aspx> (visited on 09/15/2023).
- [51] World Nuclear Association. *Nuclear Power in Germany*. Apr. 2023. URL: <https://world-nuclear.org/information-library/country-profiles/countries-g-n/germany.aspx> (visited on 01/17/2024).
- [52] Euronews. “Finland grows more and more open to nuclear energy”. In: (Dec. 8, 2022). URL: <https://www.euronews.com/2022/12/08/iran-executes-its-first-prisoner-convicted-for-participating-in-nationwide-protests> (visited on 05/26/2023).
- [53] World Nuclear Association. *Nuclear Energy in Sweden*. Dec. 2023. URL: <https://world-nuclear.org/information-library/country-profiles/countries-o-s/sweden.aspx> (visited on 01/02/2024).

- [54] Global CCS Institute. » 3. *Global Status of CCS*. 2022. URL: <https://status22.globalccsinstitute.com/2022-status-report/global-status-of-ccs/> (visited on 05/15/2023).
- [55] IEA. *Tracking Clean Energy Progress 2023 – Analysis*. IEA. July 2023. URL: <https://www.iea.org/reports/tracking-clean-energy-progress-2023> (visited on 12/05/2023).
- [56] Steve Rackley. “Chapter 7 - CO2 absorption”. In: *Negative Emissions Technologies for Climate Change Mitigation*. Jan. 1, 2023, pp. 109–132. URL: <https://www.everand.com/book/659695247/Negative-Emissions-Technologies-for-Climate-Change-Mitigation> (visited on 11/17/2023).
- [57] Steve Rackley. “Chapter 13 - Direct Air Capture”. In: *Negative Emissions Technologies for Climate Change Mitigation*. Jan. 1, 2023, pp. 292–306. URL: <https://www.everand.com/book/659695247/Negative-Emissions-Technologies-for-Climate-Change-Mitigation> (visited on 11/17/2023).
- [58] Keju An et al. “A comprehensive review on regeneration strategies for direct air capture”. In: (Oct. 1, 2023). URL: <https://www.sciencedirect.com/science/article/pii/S2212982023001981> (visited on 12/05/2023).
- [59] Mihrimah Ozkan et al. “Current status and pillars of direct air capture technologies”. In: (Apr. 15, 2022). URL: <https://www.sciencedirect.com/science/article/pii/S2589004222002607> (visited on 12/12/2023).
- [60] Steve Rackley. “Chapter 2 - Overview of negative emissions technologies”. In: *Negative Emissions Technologies for Climate Change Mitigation*. Jan. 1, 2023, pp. 19–39. URL: <https://www.everand.com/book/659695247/Negative-Emissions-Technologies-for-Climate-Change-Mitigation> (visited on 11/17/2023).
- [61] David Izikowitz. “Carbon Purchase Agreements, Dactories, and Supply-Chain Innovation: What Will It Take to Scale-Up Modular Direct Air Capture Technology to a Gigatonne Scale”. In: (Apr. 1, 2021). URL: https://www.researchgate.net/publication/350690343_Carbon_Purchase_Agreements_Dactories_and_Supply-Chain_Innovation_What_Will_It_Take_to_Scale-Up_Modular_Direct_Air_Capture_Technology_to_a_Gigatonne_Scale.
- [62] IEA. *World Energy Outlook 2022*. Oct. 2022. URL: <https://www.iea.org/reports/world-energy-outlook-2022> (visited on 01/10/2024).
- [63] Steve Rackley. “Chapter 17 - Carbon Dioxide Utilization”. In: *Negative Emissions Technologies for Climate Change Mitigation*. Jan. 1, 2023, pp. 391–411. URL: <https://www.everand.com/book/659695247/Negative-Emissions-Technologies-for-Climate-Change-Mitigation> (visited on 11/17/2023).
- [64] IEA. *Putting CO2 to Use*. Sept. 2019. URL: <https://www.iea.org/reports/putting-co2-to-use> (visited on 09/21/2023).
- [65] Wan Yun Hong. “A techno-economic review on carbon capture, utilisation and storage systems for achieving a net-zero CO2 emissions future”. In: (June 1, 2022). URL: <https://www.sciencedirect.com/science/article/pii/S277265682200015X> (visited on 01/12/2024).
- [66] US department of nuclear energy. *NuDACCS – Nuclear Direct Air Capture with Carbon Storage*. Aug. 19, 2022. URL: <chrome-extension://efaidnbmnnnibpcajpcglclefindmk>

- aj/https://netl.doe.gov/sites/default/files/netl-file/22CM_CDR17_Webster.pdf (visited on 05/09/2023).
- [67] COP28. *COP28 Declaration Of Intent - Hydrogen*. Dec. 2023. URL: <https://www.cop28.com/en/cop28-uae-declaration-on-hydrogen-and-derivatives> (visited on 01/16/2024).
- [68] Vishal Ram and Surender Reddy Salkuti. “An Overview of Major Synthetic Fuels”. In: (Jan. 2023). URL: <https://www.mdpi.com/1996-1073/16/6/2834> (visited on 11/19/2023).
- [69] M. J. Bos, S. R. A. Kersten, and D. W. F. Brilman. “Wind power to methanol: Renewable methanol production using electricity, electrolysis of water and CO₂ air capture”. In: (Apr. 15, 2020). URL: <https://www.sciencedirect.com/science/article/pii/S0306261920301847> (visited on 11/29/2023).
- [70] S. Shiva Kumar and V. Himabindu. “Hydrogen production by PEM water electrolysis – A review”. In: (Dec. 1, 2019), pp. 442–454. URL: <https://www.sciencedirect.com/science/article/pii/S2589299119300035> (visited on 09/22/2023).
- [71] Office of Energy Efficiency & Renewable Energy. *Hydrogen Production: Electrolysis*. 2023. URL: <https://www.energy.gov/eere/fuelcells/hydrogen-production-electrolysis> (visited on 11/29/2023).
- [72] IEA. *Electrolysers - Energy System*. IEA. July 10, 2023. URL: <https://www.iea.org/energy-system/low-emission-fuels/electrolysers> (visited on 11/29/2023).
- [73] S. Toghyani et al. “Thermal and electrochemical performance assessment of a high temperature PEM electrolyzer”. In: (June 1, 2018). URL: <https://www.sciencedirect.com/science/article/pii/S0360544218305498> (visited on 12/21/2023).
- [74] Norsk E-fuel. *Press Release: Partnership with Norwegian*. Apr. 24, 2023. URL: https://www.norsk-e-fuel.com/articles/partnership_with_norwegian (visited on 11/23/2023).
- [75] Jacob Trumpy. *Norwegian satser 50–60 mill. på norsk fabrikk for bærekraftig drivstoff*. Apr. 24, 2023. URL: <https://www.dn.no/luftfart/norwegian/geir-karlsen/norwegian-satser-5060-mill-pa-norsk-fabrikk-for-barekraftig-drivstoff/2-1-1439349> (visited on 01/05/2024).
- [76] Outi Mäyrä and Kauko Leiviskä. “Chapter 17 - Modeling in Methanol Synthesis”. In: *Methanol*. Jan. 1, 2018, pp. 475–492. URL: <https://www.sciencedirect.com/science/article/abs/pii/B9780444639035000170> (visited on 11/16/2023).
- [77] Francesco Dalena et al. “Chapter 1 - Methanol Production and Applications: An Overview”. In: *Methanol*. Jan. 1, 2018, pp. 3–28. URL: <https://www.sciencedirect.com/science/article/abs/pii/B9780444639035000017> (visited on 11/16/2023).
- [78] Hubert Stokowski. *Is Hydrogen a Sustainable Fuel for Green Transport?* Nov. 6, 2020. URL: <http://large.stanford.edu/courses/2020/ph240/stokowski1/> (visited on 01/10/2024).
- [79] Methanol Institute. *Marine Methanol: Future-Proof Shipping Fuel*. May 27, 2023. URL: <https://www.methanol.org/marine/> (visited on 01/05/2024).
- [80] Jonas Martin, Anne Neumann, and Anders Ødegård. “Renewable hydrogen and synthetic fuels versus fossil fuels for trucking, shipping and aviation: A holistic cost model”. In:

- (Oct. 1, 2023). URL: <https://www.sciencedirect.com/science/article/pii/S136403212300494X> (visited on 01/05/2024).
- [81] Pattabh Raman Narayanan. *Methanol from CO₂: a technology and outlook overview*. In: Apr. 2023. URL: <https://www.digitalrefining.com/article/1002891/methanol-from-co2-a-technology-and-outlook-overview> (visited on 10/17/2023).
- [82] Methanol Institute. *Renewable Methanol*. Apr. 6, 2021. URL: <https://www.methanol.org/renewable/> (visited on 01/10/2024).
- [83] Stefano Sollai et al. “Renewable methanol production from green hydrogen and captured CO₂: A techno-economic assessment”. In: (Feb. 1, 2023). URL: <https://www.sciencedirect.com/science/article/pii/S2212982022004644> (visited on 09/21/2023).
- [84] A. Hankin and N. Shah. “Process exploration and assessment for the production of methanol and dimethyl ether from carbon dioxide and water”. In: (Aug. 22, 2017). URL: <https://pubs.rsc.org/en/content/articlelanding/2017/se/c7se00206h> (visited on 12/13/2023).
- [85] CRI. *World’s largest CO₂-to-methanol plant starts production*. Oct. 26, 2022. URL: <https://www.carbonrecycling.is/news-media/worlds-largest-co2-to-methanol-plant-starts-production> (visited on 11/17/2023).
- [86] Innovasjon Norge. *Gir 100 millioner til Finnfjord*. Sept. 20, 2022. URL: <https://www.innovasjon Norge.no/nyhetsartikkel/gir-100-millioner-til-finnfjord> (visited on 12/13/2023).
- [87] Ali Al-Matar. *Selecting Fluid Packages (Thermodynamic Model) for HYSYS/ Aspen Plus/ ChemCAD Process Simulators*. Oct. 27, 2015. URL: https://researchgate.net/publication/283259774_Selecting_Fluid_Packages_Thermodynamic_Model_for_HYSYS_Aspen_Plus_ChemCAD_Process_Simulators.
- [88] Honeywell Forge. *Honeywell UniSim Design Suite*. Nov. 2023. URL: <https://www.honeywellforge.ai/us/en/products/industrial-operations/honeywell-unisim-design-suite> (visited on 11/23/2023).
- [89] Rice University Department of Chemical Engineering. *Logical Unit Operations*. 2015. URL: <https://www.owl.net.rice.edu/~ceng403/hysys/logicals.html> (visited on 11/30/2023).
- [90] K. M. Vanden Bussche and G. F. Froment. “A Steady-State Kinetic Model for Methanol Synthesis and the Water Gas Shift Reaction on a Commercial Cu/ZnO/Al₂O₃Catalyst”. In: (June 1, 1996). URL: <https://www.sciencedirect.com/science/article/abs/pii/S0021951796901566> (visited on 11/30/2023).
- [91] UniSim Support. *Unisim calculations*. E-mail. Nov. 9, 2023. (Visited on 11/09/2023).
- [92] Global CCS Institute. *The costs of CO₂ storage: post-demonstration CCS in the EU*. July 15, 2011. URL: <https://www.globalccsinstitute.com/resources/publications-reports-research/the-costs-of-co2-storage-post-demonstration-ccs-in-the-eu/> (visited on 12/04/2023).
- [93] Felix Schorn et al. “Methanol as a renewable energy carrier: An assessment of production and transportation costs for selected global locations”. In: (Aug. 25, 2021). URL: <https://www.sciencedirect.com/science/article/pii/S2666792421000421> (visited on 01/16/2024).

- [94] Habib Azarabadi and Klaus S. Lackner. “A sorbent-focused techno-economic analysis of direct air capture”. In: (Sept. 15, 2019). URL: <https://www.sciencedirect.com/science/article/abs/pii/S0306261919306385> (visited on 11/11/2023).
- [95] Ryan D. *How Much Does a Cooling Tower Water Treatment System Cost?* May 13, 2016. URL: <https://samcotech.com/cost-cooling-tower-water-treatment-system/> (visited on 12/01/2023).
- [96] Guido Collodi et al. “Demonstrating Large Scale Industrial CCS through CCU – A Case Study for Methanol Production”. In: (July 1, 2017). URL: <https://www.sciencedirect.com/science/article/pii/S1876610217313280> (visited on 12/01/2023).
- [97] IndexBox. *Green Methanol Price*. Dec. 1, 2023. URL: <https://www.indexbox.io/search/green-methanol-price/> (visited on 12/04/2023).
- [98] IndexBox. *World - Methanol (Methyl Alcohol) - Market Analysis, Forecast, Size, Trends And Insights*. Jan. 1, 2024. URL: <https://www.indexbox.io/search/methanol-price-per-ton-2020/> (visited on 01/09/2024).
- [99] Statista. *Monthly methanol spot prices by region*. Mar. 24, 2023. URL: <https://www.statista.com/statistics/1323381/monthly-methanol-spot-prices-worldwide-by-region/> (visited on 01/20/2024).
- [100] Lucid Catalyst. *Cost and Performance Requirements for Flexible Advanced Nuclear Plants in Future U.S Power Markets*. July 2020. URL: <https://www.lucidcatalyst.com/arpa-e-report-nuclear-costs> (visited on 12/07/2023).
- [101] Simon Johnson. “Sweden plans new nuclear reactors by 2035, will share costs”. In: (Nov. 16, 2023). URL: <https://www.reuters.com/business/energy/sweden-plans-new-nuclear-reactors-by-2035-can-take-costs-2023-11-16/> (visited on 01/11/2024).
- [102] Wesley Cole et al. “The potential role for new nuclear in the U.S. power system: A view from electricity system modelers”. In: (Mar. 1, 2023). URL: <https://www.sciencedirect.com/science/article/pii/S1040619023000179> (visited on 01/11/2024).
- [103] Maersk. *Maersk to deploy first large methanol-enabled vessel on Asia - Europe trade lane*. Dec. 7, 2023. URL: <https://www.maersk.com/news/articles/2023/12/07/maersk-to-deploy-first-large-methanol-enabled-vessel-on-asia-europe-trade-lane> (visited on 01/10/2024).
- [104] Qais Hussein Hassan et al. “The impact of Methanol-Diesel compound on the performance of a Four-Stroke CI engine”. In: (Jan. 1, 2021). URL: <https://www.sciencedirect.com/science/article/pii/S2214785320399326> (visited on 01/10/2024).

A DAC Sorbent Calculations

Table A.1: The parameters and calculations of the sorbent [94]

	Activity	Value	Unit
A	Sorbent cost	15 (range: 7-30)	\$/kg
B	Cycle time	49	min
C	Working capacity	1	mol/kg
D	CO ₂ capture rate	487,7	kg/s
E	CO ₂ captured pr cycle ($D/0,044 * B * 60$)	26599733,6	mol
F	Sorbent capacity needed (E/C)	26599733,6	kg
G	Sorbent capital cost (F/A)	398996003,9	\$
H	Sorbent lifetime	2	years
I	Sorbent replacement cost (F/H)	199498002	\$/year
J	Capacaty factor	95	%
K	CO ₂ capture per year ($D/1000 * 3600 * 8766 * J$)	14619963,7	ton/year
L	Sorbent replacement cost (I/K)	13,64	\$/ton CO ₂

B Future Levelized Cost of DAC With and Without Carbon Tax

Levelised cost of capturing carbon by DACS technology for selected regions, 2030 and 2050

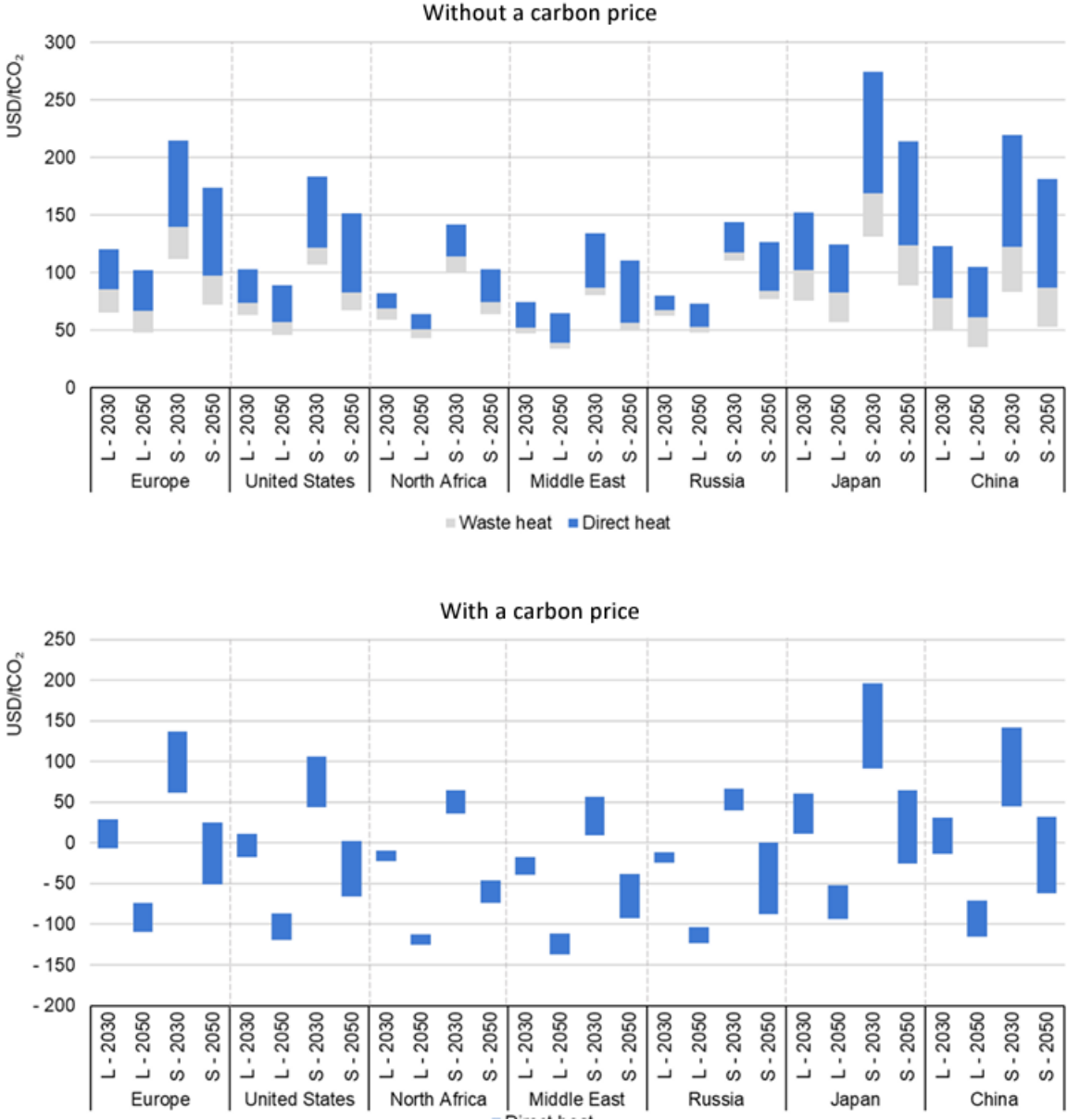


Figure B.1: Levelized cost for DAC with and without carbon tax for different regions for years 2030 and 2050 [6].

C Total Overnight Cost for Nuclear Generating Technologies

Table 3.4a: Nuclear generating technologies – New build						
Country	Technology	Net capacity (MWe)	Overnight costs (USD/kWe)	Investment costs (USD/kWe)		
				3%	7%	10%
France	EPR	1 650	4 013	4 459	5 132	5 705
Japan	ALWR	1 152	3 963	4 402	5 068	5 633
Korea	ALWR	1 377	2 157	2 396	2 759	3 066
Russia	VVER	1 122	2 271	2 523	2 904	3 228
Slovak Republic	Other nuclear	1 004	6 920	7 688	8 850	9 837
United States	LWR	1 100	4 250	4 721	5 435	6 041
Non-OECD countries						
China	LWR	950	2 500	2 777	3 197	3 554
India	LWR	950	2 778	3 086	3 552	3 949

Figure C.1: Total overnight cost for nuclear generating technologies [44].

D Justification for the Uncertainty Quantification

Table D.1: Justification for the uncertainty quantification

Component	Values Assumed	Justification
Discount rate	Low: 4	Long-term future scenario with low risk
	Med: 8	Standard discount rate for chemical plants
	High: 12	Near-term scenario with high capital demand and risks
Plant lifetime	Low: 20	Early decommissioning due to technical challenges, accidents or political decisions
	Med: 40	Based on average lifetime for nuclear plants
	High: 60	Based on literature stating that newer plants could operate for 60 years or even longer
Advanced Nuclear Reactor	Low: 0.7	Assuming that the more advanced nuclear reactor could lower the cost of today's nuclear reactors
	Med: 1.1	Assuming a slight cost increase from today's nuclear reactors
	High: 1.6	Assuming that the more advanced nuclear reactor design would result in a significant cost increase
Electrolyzer Cost	Low: 0.5	The low end of the range provided for long term projections for electrolyzer cost
	Med: 1	The average range provided for long term projections for electrolyzer cost
	High: 2	The high end of the range provided for long term projections for electrolyzer cost
MeOH price	Low: 200	Based on the lowest ranges found in literature
	Med: 400	Based on average cost found in literature
	High: 600	Based on a high range found in literature
CO ₂ storage	Low: 2	The lowest number for on-site storage
	Med: 5	The average cost for on-site storage
	High: 9	The average cost assuming some transportation by pipeline

Table D.2: Justification for the uncertainty quantification

Component	Values Assumed	Justification
DAC capital cost	Low: 250	Based on a high development and rapid scale up of DAC units
	Med: 372	Chosen based on the projected cost for DAC. Price chosen for 2030 since the projections for 2050 are recognized as optimistic
	High: 700	Based on a low development and slowscale up of DAC units
Nuclear plant cost	Low: 650	Based on development and cost reductions
	Med: 1000	Based on historical data for TOC for nuclear energy in China
	High: 2100	Based on typically cost overruns and that the technology is higher for other countries
DAC efficiency	Low: 0.5	Based on data found in literature in the low range
	Med: 1	Chosen based on the projected energy usage for DAC. Value chosen for 2030 since the projections for 2050 are recognized as optimistic
	High: 1.5	Based on data found in literature in the upper range
Sorbent cost	Low: 7	Based on the lower ranges found in literature and large cost reductions due to high development
	Med: 15	Based on findings in literature and normal cost reduction and development
	High: 30	Based on upper ranges in literature assuming low development and cost reductions
Nuclear fuel	Low: 0.27	Low ranges found in literature
	Med: 1	Most of the ranges is slightly above or less than 1
	High: 2.8	Higher ranges found in literature

E UniSim Flowsheets

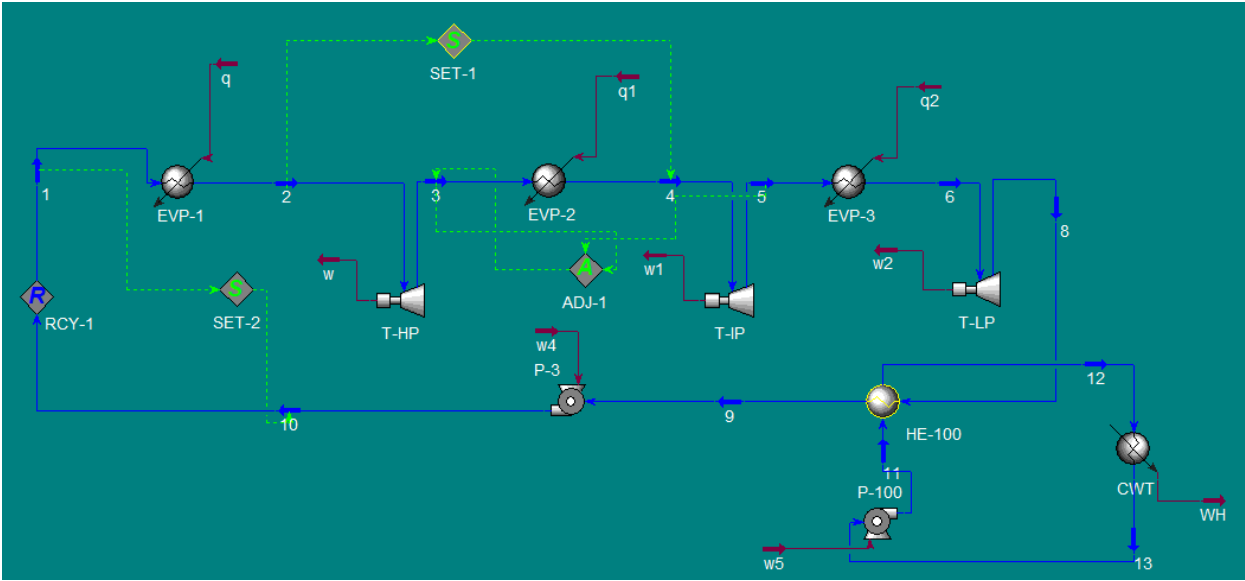


Figure E.1: Advanced nuclear plant with CWT.

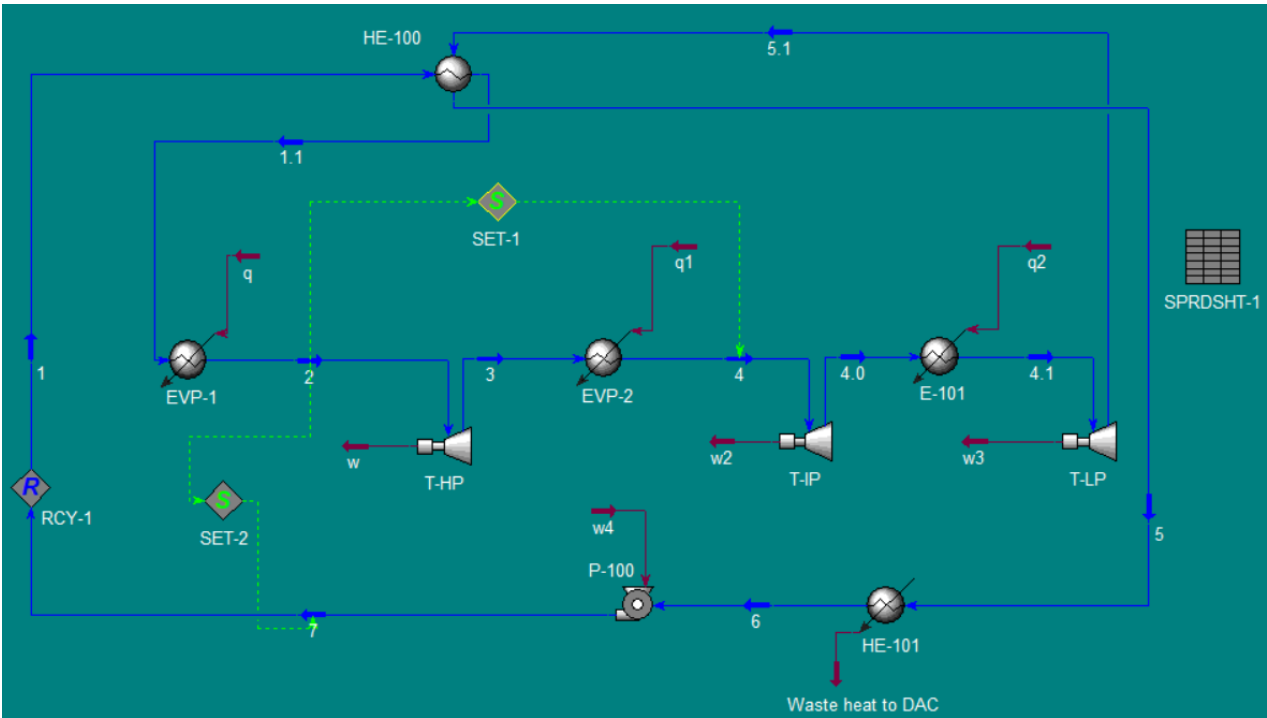


Figure E.2: Advanced nuclear plant with DAC.

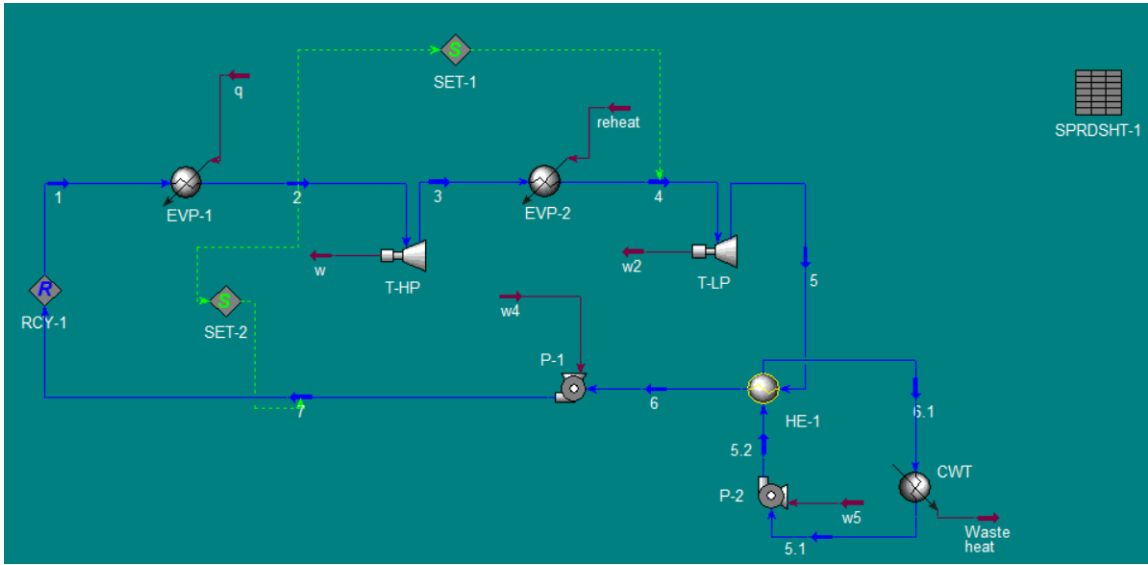


Figure E.3: Reference nuclear plant with CWT.

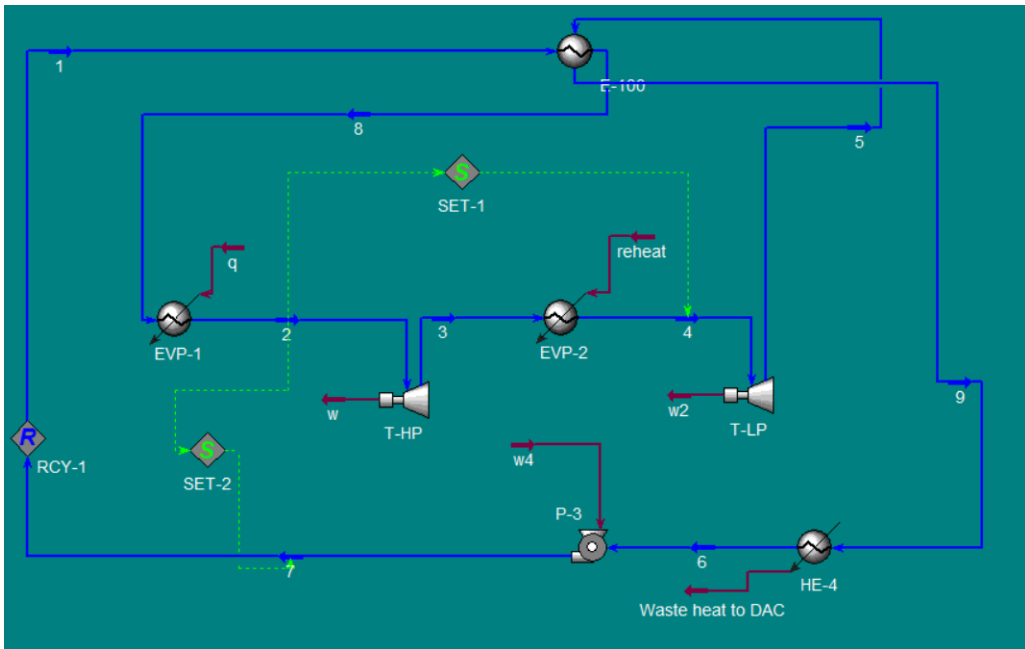


Figure E.4: Reference nuclear plant with DAC.

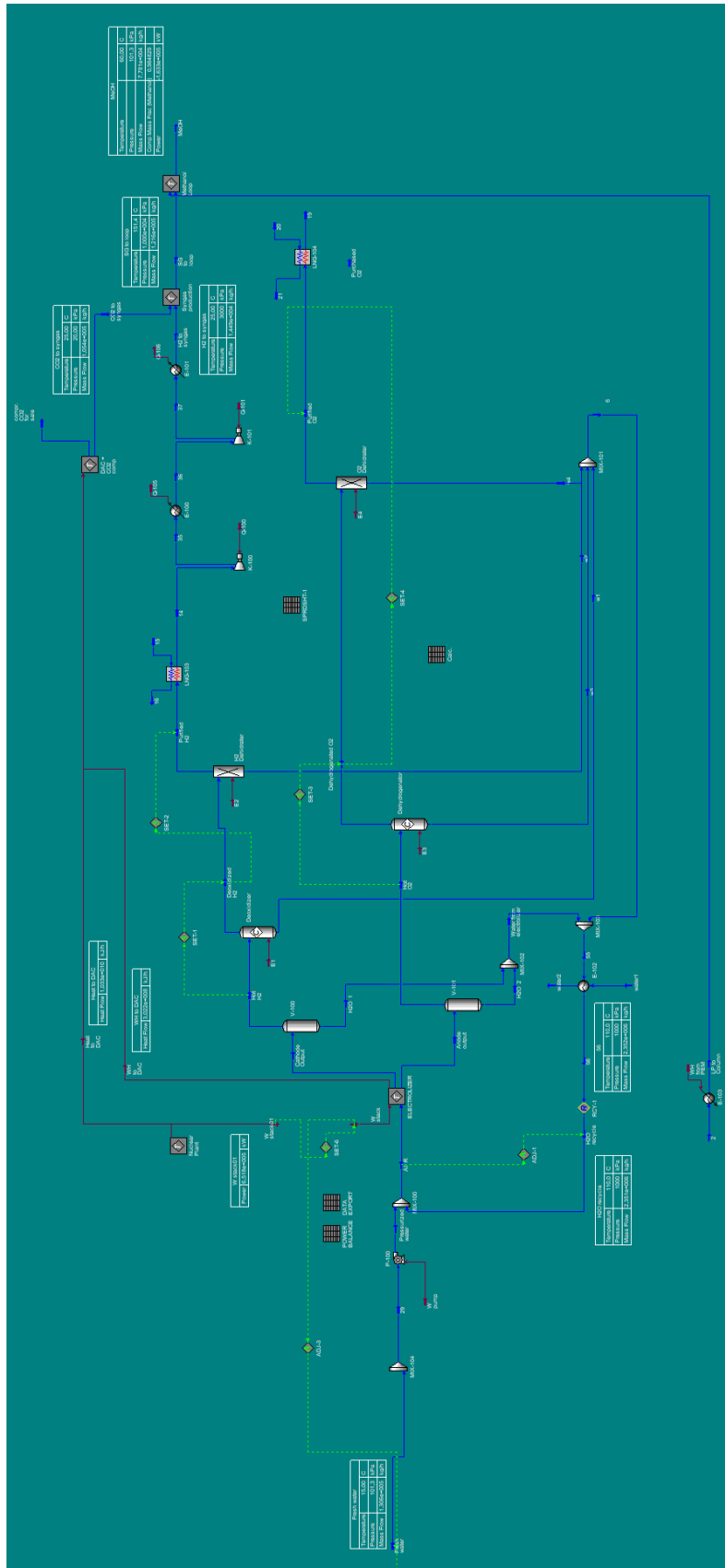


Figure E.5: A flowsheet comprising all the simulated sub-processes represented as a sub-flowsheet, including the nuclear power plant, CO₂ compression, PEM electrolyzer, syngas production, and methanol synthesis.

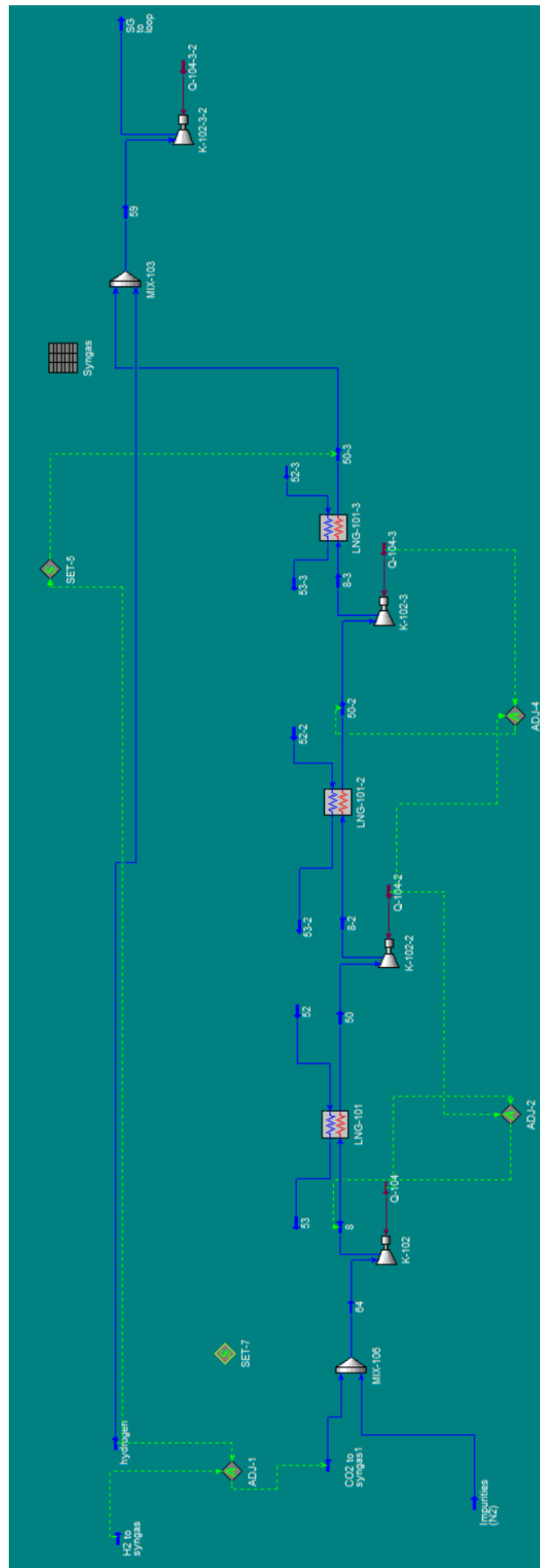


Figure E.6: Flowsheet of the syngas production.

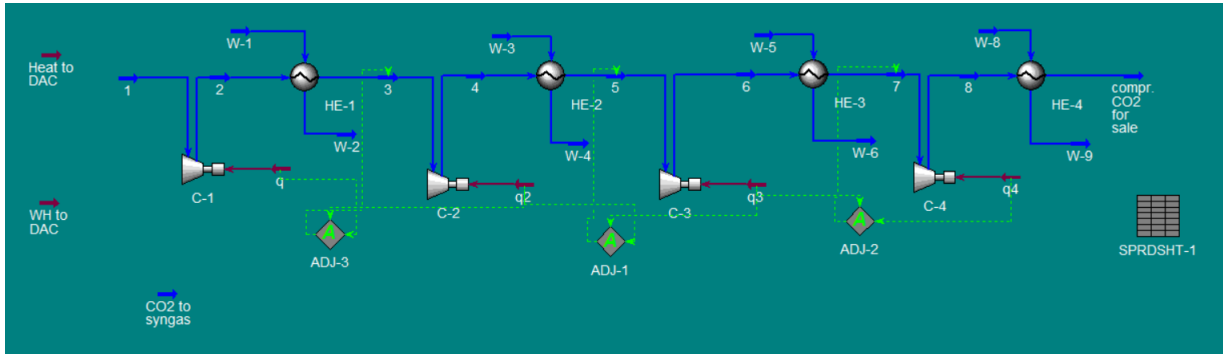


Figure E.7: Flowsheet of CO₂ compression.

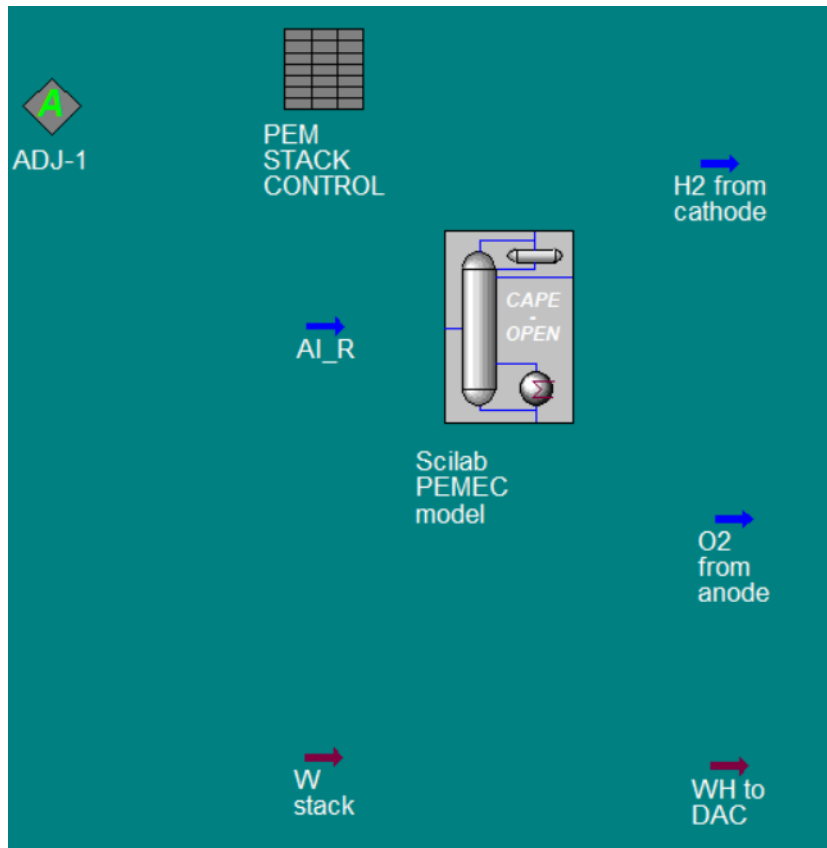


Figure E.8: Flowsheet of the PEM electrolyzer model.

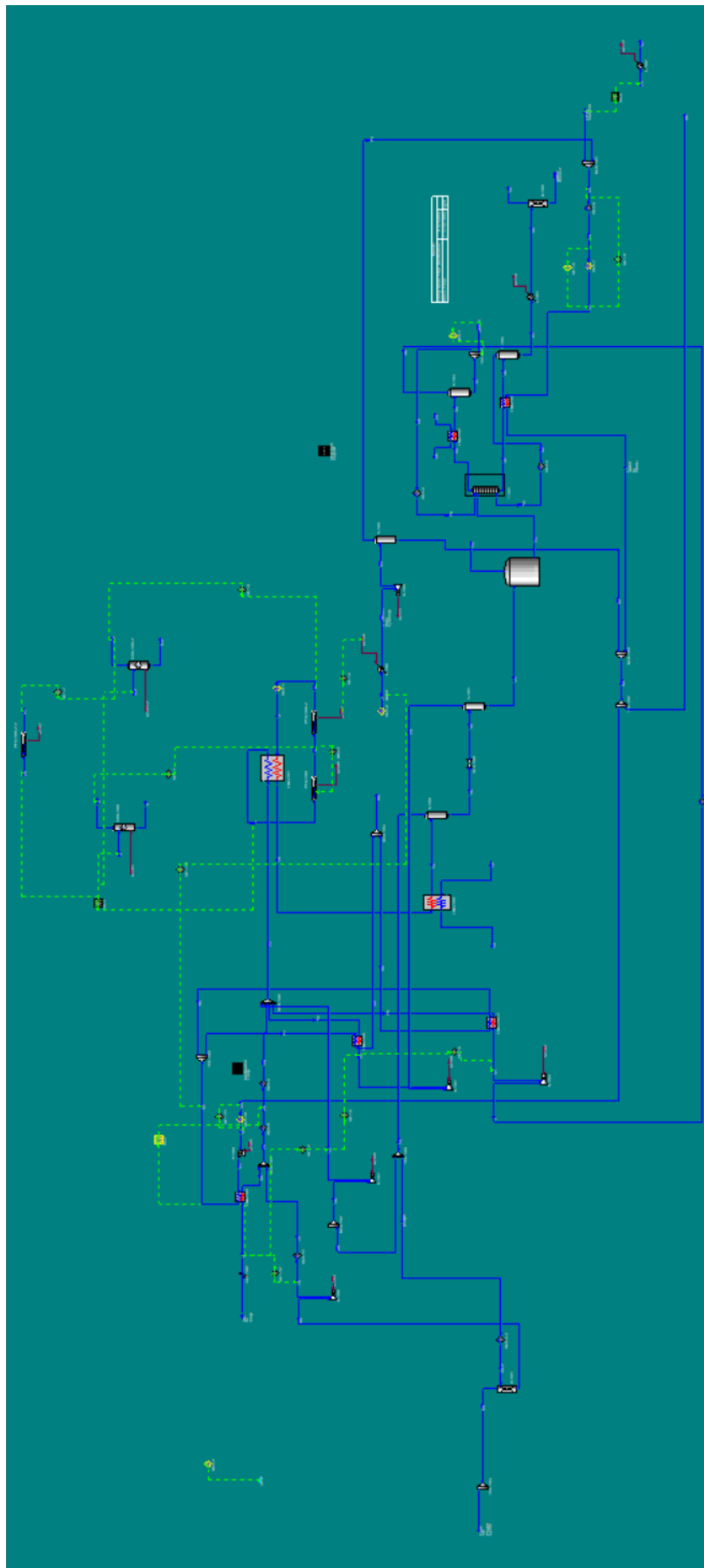


Figure E.9: Flowsheet of the methanol synthesis.

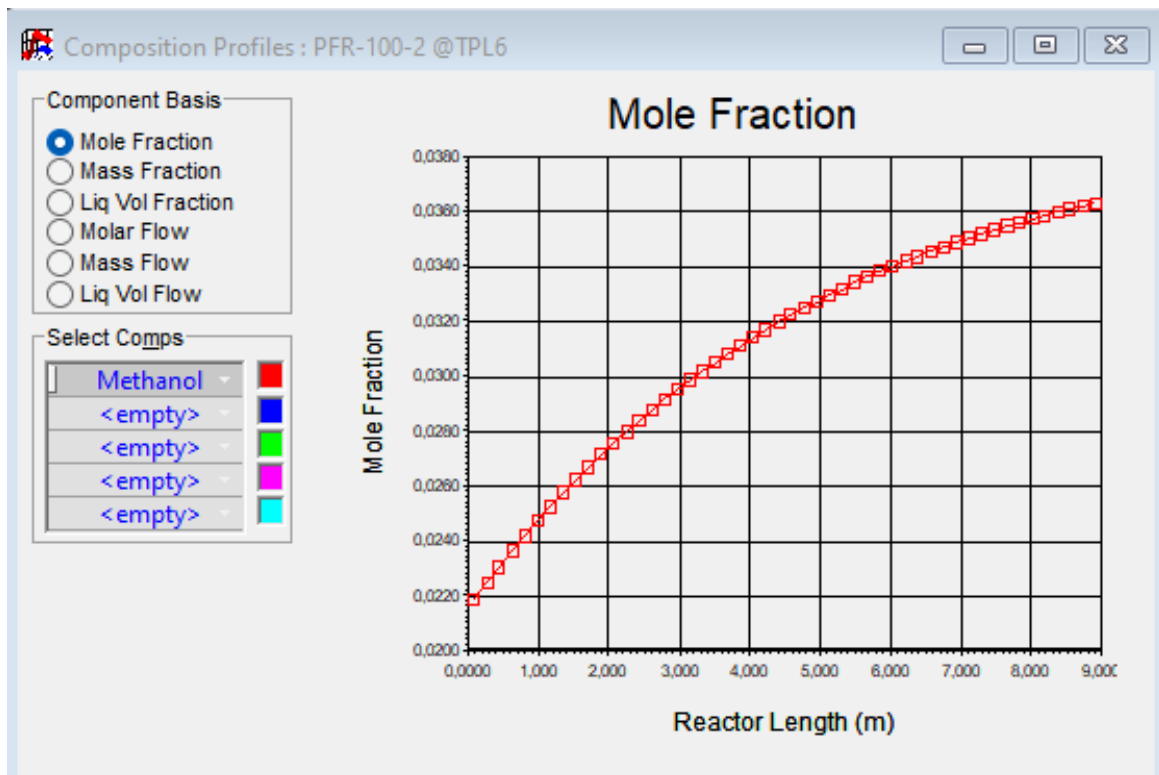
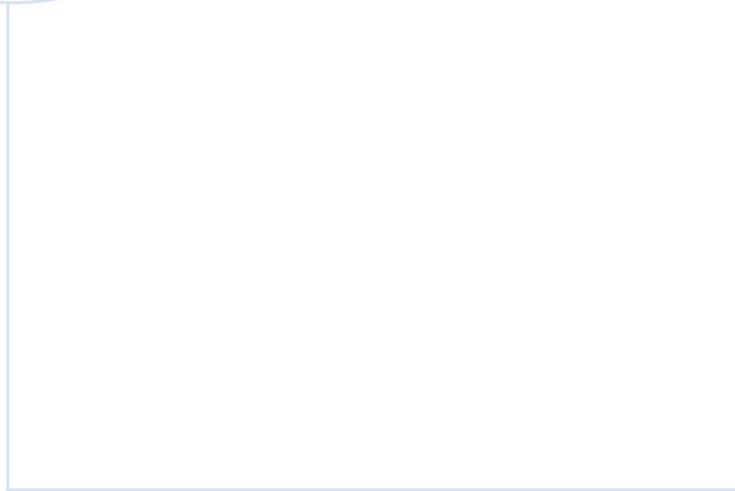


Figure E.10: A plot of the methanol mole fraction as a function of reactor length.



 **NTNU**

Norwegian University of
Science and Technology